Phylogeny and biogeography of the pantropical whip spider family Charinidae (Arachnida: Amblypygi)

GUSTAVO SILVA DE MIRANDA^{1,2*,o}, ALESSANDRO P. L. GIUPPONI³, NIKOLAJ SCHARFF^{2,4} and LORENZO PRENDINI⁵

¹Center for Macroecology, Evolution and Climate, Natural History Museum of Denmark (Zoological Museum), University of Copenhagen, Denmark

²Entomology Department, National Museum of Natural History, Smithsonian Institution, Washington, DC 20560, USA

³Laboratório de Referência Nacional em Vetores das Riquetsioses, LIRN-FIOCRUZ, Rio de Janeiro, RJ, Brazil ⁴Zoology Section, Natural History Museum of Denmark, University of Copenhagen, Denmark

⁵Division of Invertebrate Zoology, American Museum of Natural History, New York, NY 10024-5192, USA

Received 11 November 2019; revised 3 July 2020; accepted for publication 1 August 2020

The present contribution addresses the phylogeny and biogeography of the pantropical whip spider family Charinidae Quintero, 1986, the most species-rich in the arachnid order Amblypygi Thorell, 1883, based on morphology and multilocus DNA sequences, analysed simultaneously using parsimony, maximum likelihood and Bayesian inference. The morphological matrix comprises 138 characters, scored for four outgroup taxa and 103 ingroup terminals representing all genera and 64% of the species of Charinidae. The multilocus dataset comprises sequences from two nuclear and three mitochondrial gene loci for four outgroup taxa and 48 ingroup representing 30 (23%) taxa of Charinidae. Charinidae are monophyletic, with Weygoldtia Miranda et al., 2018 sister to a monophyletic group comprising Charinus Simon, 1892 and Sarax Simon, 1892, neither of which are reciprocally monophyletic. Charinidae diverged from other amblypygid families in the Late Carboniferous, c. 318 Mya, on the supercontinent Pangaea. Weygoldtia diverged from the common ancestor of Charinus and Sarax during the Late Permian, c. 257 Mya, when changes in climate reduced tropical forests. The divergence of Charinus and Sarax coincides with the fragmentation of Pangaea, c. 216 Mya. Sarax colonized South-East Asia via Australia. The charinid fauna of New Caledonia originated before the Oligocene, when the island separated from Australia, c. 80 Mya.

ADDITIONAL KEYWORDS: phylogenetic systematics – morphological systematics – biogeography – molecular phylogeny – zoological nomenclature.

INTRODUCTION

Whip spiders, order Amblypygi Thorell, 1883, are exquisite arachnids with a dorsoventrally compressed body, robust, spinose pedipalps and a long whip-like first pair of antenniform legs (Weygoldt, 2000). All known species are nocturnal predators that vary in size from relatively small (c. 1 cm in total body length) to large (c. 5 cm). The order comprises five families of which the pantropical Charinidae Quintero, 1986, with 129 described species (Fig. 1), is the most speciose and has the broadest geographical distribution, inhabiting

the intertropical zone on all continents (Fig. 2; Miranda

The family Charinidae was first created as part of a revised classification of Pulvillata Quintero, 1986, a paraphyletic suborder of Amblypygi comprising eight genera with pulvilli (or arolia), soft, cushionlike lobes or pads between the claws of the telotarsi

et al., 2018a). A Gondwanan distribution pattern was previously suggested for Charinidae, according to which the early lineages diverged prior to the breakup of the supercontinent, during the Cretaceous (Weygoldt, 2000). However, neither the phylogeny of the family nor the processes of divergence and diversification that lead to its current disjunct distribution have ever been investigated.

 $[*] Corresponding \ author. \ E-mail: {\bf smiranda.gustavo@gmail.com}$



Figure 1. Selected Brazilian species of the whip spider genus *Charinus* Simon, 1892, habitus in life. A, *Charinus ricardoi* Giupponi & Miranda, 2016, Amazonas. B, *Charinus jibaossu* Vasconcelos, Giupponi & Ferreira, 2014, Minas Gerais. C, *Charinus vulgaris* Miranda & Giupponi, 2011, Rondônia. D. *Charinus potiguar* Vasconcelos *et al.*, 2013, Rio Grande do Norte. E, *Charinus magalhaesi* Miranda *et al.*, 2021, Amazonas. F, *Charinus cearensis* Miranda *et al.*, 2021, Ceará. G, *Charinus eleonorae* Baptista & Giupponi, 2003, Minas Gerais. H, *Charinus asturius* Pinto-da-Rocha, Machado & Weygoldt, 2002, São Paulo. Photos by L. Sousa de Carvalho (A, F), R. Ferreira (B, D, G, H) and A.P.L. Giupponi (C, E).

with an adhesive function (Quintero, 1986; Weygoldt, 1996; Wolff et al., 2015a, b). Quintero (1986) assigned Catageus Thorell, 1899, Charinides Gravely, 1911, Charinus Simon, 1892, Phrynichosarax Gravely, 1915, Sarax Simon, 1892 and Tricharinus Quintero, 1986 to Charinidae, and Charon Karsch, 1879 and Stygophrynus Kraepelin, 1895 to Charontidae Simon, 1892. Quintero's (1986) classification was based on a manual (pre-computer) phylogenetic analysis of 17 characters, polarized a priori as synapomorphic or plesiomorphic, and scored for supraspecific terminals representing genera, the monophyly of which was assumed (three of these genera were subsequently synonymized). Despite these limitations, most of Quintero's (1986) characters remain informative for phylogenetic analysis and classification to this day.

A subsequent phylogenetic analysis of all genera of Amblypygi by Weygoldt (1996), based on 29 morphological characters, upheld Charinidae and its component genera, but rejected the sister-group relationship with Charontidae. Whereas Charinidae remained within Euamblypygi Weygoldt, 1996 and sister to Neoamblypygi Weygoldt, 1996, Charontidae was placed sister to all other families, within Neoamblypygi. As with Quintero (1986), a manual cladistic analysis was presented by Weygoldt (1996), in which each character was polarized a priori and scored for supraspecific terminals representing genera, the monophyly of which was assumed. Weygoldt (1996) also tested the result using the parsimony program, Hennig86 (Farris, 1989). Despite its limitations, Weygoldt's (1996) phylogenetic hypothesis was influential and the characters were incorporated and built upon by subsequent authors investigating the phylogeny and systematics of extant and fossil Amblypygi at various taxonomic levels (Prendini *et al.*, 2005; Garwood *et al.*, 2017; Miranda *et al.*, 2018b). Miranda *et al.* (2018b) further refined the characters previously used by Quintero (1986) and Weygoldt (1996), and added many new ones.

Whereas the monophyly and generic content of Charinidae have been tested over the course of several morphological phylogenetic analyses, its component genera have not received similar scrutiny. Previous authors initially separated the charinid genera according to the presence or absence of ventral sacs on the opisthosoma. Species with ventral sacs were placed in Catageus, Phrynichosarax or Sarax, whereas species without ventral sacs were placed in Charinides, Charinus or Tricharinus. Subsequently, the species of Phrynichosarax were transferred to Sarax, one species of Sarax was transferred to the recently described genus Weygoldtia Miranda et al., 2018 and Catageus, demonstrated to be a senior synonym of Stygophrynus, was transferred to Charontidae (Harvey, 2003; Miranda et al., 2018a). Consequently, only two genera, Sarax and Weygoldtia, presently accommodate species with ventral sacs in Charinidae.

Charinides, Charinus and Tricharinus were originally separated according to the number of articles on the basitibia of leg IV: species with three articles were accommodated in Charinides, species with four in Charinus, and species with two in Tricharinus (Gravely, 1911, 1915). Delle Cave (1986) considered this classification inconsistent. Weygoldt (2000) demonstrated that the number of articles decreases when the legs are regenerated. Charinides and Tricharinus were ultimately synonymized with

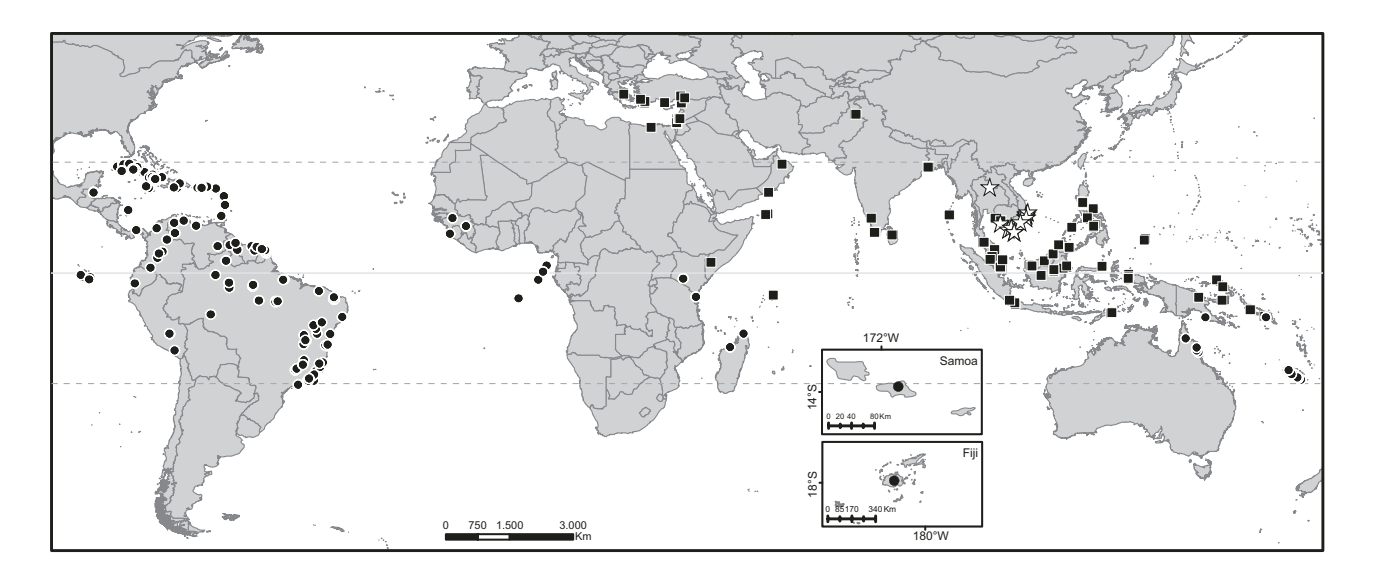


Figure 2. Distributions of the three whip spider genera of Charinidae Quintero, 1986: Charinus Simon, 1892 (circles); Sarax Simon, 1872 (squares); Weygoldtia Miranda et al., 2018 (stars).

Charinus (Delle Cave, 1986; Weygoldt, 2000), regardless of the number of articles on basitibia IV.

In an attempt to better classify the species of *Charinus*, Weygoldt (2005) proposed three species groups based on the morphology of the female genitalia, a system followed until recently, although not tested phylogenetically. Species with a cushion-like surface on the gonopods were assigned to the *australianus* group; species with a finger-like gonopod, to the *bengalensis* group; and species with a sucker-like female gonopod, to the *brasilianus* group.

Many new species of Charinidae have been described in recent years (e.g. Armas et al., 2016; Giupponi & Miranda, 2016: Miranda et al., 2016a, b, c, 2018a: Teruel. 2016; Vasconcelos & Ferreira, 2016, 2017; Vasconcelos et al., 2016; Harms, 2018; Seiter et al., 2018). These species are currently accommodated in three genera: Weygoldtia with two species restricted to Cambodia, Laos and Vietnam, Sarax Simon, 1872 with 36 species distributed from East Africa and the Arabian Peninsula to South-East Asia, and *Charinus* with 94 species widespread in the Americas, Africa and Oceania (Miranda et al., 2021). However, the internal classification has remained uncertain, as neither the monophyly of the genera or species groups of *Charinus*, nor the phylogenetic relationships among them have ever been tested in a quantitative phylogenetic analysis. The timing and processes that resulted in the current distribution of taxa in the family have likewise never been investigated.

The present contribution addresses the phylogeny and biogeography of Charinidae for the first time, based on comprehensive datasets of morphological characters and multilocus DNA sequences, analysed simultaneously using Bayesian inference (BI), maximum likelihood (ML) and parsimony. A dated molecular phylogeny provides insight into the divergence and diversification of the family in the context of major geological and climatic events in Earth history. Weygoldt's (2006) hypothesis of a Gondwana origin of Charinidae is tested, and new evidence provided for the presence of relictual lineages of Charinidae in New Caledonia.

MATERIAL AND METHODS

TAXON SAMPLING

The matrix included four outgroup taxa, a schizomid, thelyphonid and exemplar species of two amblypygid genera representing Phrynidae Blanchard, 1852 and Phrynichidae Simon, 1872 (Table 1; Appendix 1; Supporting Information, Appendix S1). The taxonomy of Charinidae follows Miranda *et al.* (2021).

The ingroup comprised 92 (71%) species of Charinidae (in addition to four undescribed morphospecies), i.e. 65 (70%) species of *Charinus*, 25 (69%) species of *Sarax* and both species of *Weygoldtia*, and covered almost the entire geographical distribution of the family, including all continents on which charinids occur. Up to six conspecific terminals (individuals) represented each ingroup species, when available. Morphological data were replicated for conspecific terminals in order to minimize ambiguous optimizations due to missing entries (Grant *et al.*, 2006).

Ten ingroup taxa in the morphological matrix were ultimately omitted from the analyses due to the large number of missing entries caused by missing parts of specimens, the absence of one sex and/or an abundance of troglobiotic characters: Charinus brescoviti Giupponi & Miranda, 2016; C. carajas Giupponi & Miranda, 2016; C. fagei Weygoldt, 1972; C. loko Miranda et al., 2021, C. longipes Weygoldt, 2006; C. madagascariensis Fage, 1954; C. milloti Fage, 1939; C. orientalis Giupponi & Miranda, 2016; C. susuwa Miranda et al., 2021, C. troglobius Baptista & Giupponi, 2002. The final morphological matrix comprises 82 ingroup species represented by 103 terminal taxa (Table 1).

A simultaneous analysis with the morphological matrix pruned to contain only the taxa represented by molecular and morphological data was also constructed and comprised the same outgroups and 30 ingroup taxa (15 species of *Charinus*, 13 species of *Sarax* and both species of *Weygoldtia*) represented by 48 terminal taxa (Table 1; Fig. S1).

Table 1. Counts and percentages of described species, undescribed morphospecies and terminal taxa per genus included in matrices used for simultaneous phylogenetic analysis of the whip spider family Charinidae Quintero, 1986. First count gives initial sample, second count after omitting ten ingroup taxa from the morphological matrix, and third count after pruning to contain only the taxa represented by molecular and morphological data

	Total species	Species %	Morphospecies	Terminal taxa
Outgroup	4/4/4			4/4/4
Ingroup	92/82/30	71/64/23	4/4/4	113/103/48
Charinus	65/55/15	70/59/16	1/1/1	71/61/21
Sarax	25/25/13	69/69/36	3/3/3	39/39/24
Weygoldtia	2/2/2	100/100/100		3/3/3

TISSUE SAMPLES AND MATERIAL EXAMINED

Field-collected specimens were preserved in 95% ethanol at ambient temperature and subsequently frozen at -20 °C. Tissue samples used for DNA extraction are stored in the Ambrose Monell Collection for Molecular and Microbial Research at the American Museum of Natural History, New York (AMNH). Voucher specimens are deposited in the collections of the AMNH, the Coleção de História Natural da Universidade Federal do Piauí, Floriano, Brazil (CNHUFPI), the Hebrew University of Jerusalem, Israel (HUJ), the Museum of Comparative Zoology, Cambridge, USA (MCZ), the Museu Nacional, Rio despace heJaneiro, Brazil (MNRJ), and the Zoological Museum, University of Copenhagen, Denmark (ZMUC). Tissue samples, vouchers and material examined for scoring the morphological matrix are listed in the Supporting Information, Appendix S1.

MORPHOLOGICAL DATA

A morphological data matrix comprising 138 characters (Appendices 1 and 2; Figs 7–14, 18–21), scored for 92 ingroup taxa represented by 113 terminals (*Charinus* sp., a morphospecies from Grenada, is a juvenile and was not coded in the matrix) and four outgroup taxa, was prepared in MESQUITE v.3.2 (Maddison & Maddison, 2017) by direct examination of specimens. The matrix is deposited in Morphobank, project number 3538. Twenty-nine characters from Weygoldt (1996) were included unmodified or redefined when necessary. Characters from Quintero (1986) were also incorporated, as well as additions and modifications of characters published by Garwood *et al.* (2017) and Miranda *et al.* (2018b).

The logical character structure proposed by Sereno (2007) was followed in developing characters with care taken to observe logical and biological independence of characters (Wilkinson, 1995). No a priori assumptions were made concerning character transformation; 46 multistate characters were treated as unordered/non-additive (Fitch, 1971). Character-state reconstruction was performed on the preferred tree (below; Figs 3 and 6) using parsimony in MESQUITE.

Morphological terminology follows Harvey & West (1998), Weygoldt (2000) and Giupponi & Kury (2013). Most homology hypotheses for characters shared by Amblypygi and Uropygi Thorell, 1883 (the monophyletic group comprising Schizomida Petrunkevitch, 1945 and Thelyphonida Latreille, 1804) follow Shultz (2007). Due to the marked differences between the three orders, 80 characters were inapplicable to the schizomid, Stenochrus sbordonii (Brignoli, 1973) and 57 to the thelyphonid, Mastigoproctus aff. giganteus.

MICROSCOPY, IMAGING AND MAPPING

Morphological characters were observed and scored with a Leica M205AC stereomicroscope. Digital images were prepared with a BK plus Imaging System from Visionary Digital (Palmyra, PA, USA; http://www.visionarydigital.com) equipped with a Canon 7D digital camera at the ZMUC. Image stacks were combined using Zerene Stacker (Zerene Systems LLC; http://zerenesystems.com/cms/stacker) and processed in Photoshop CS6 (Adobe, San Jose, CA, USA) to adjust for colour, brightness and contrast. Plates were prepared with Adobe InDesign.

Specimens for scanning electron microscopy were dehydrated in a series of ethanol concentrations from 75% to 100% with 10% differences between consecutive concentrations for 20-30 min each and stored overnight in 100% ethanol. Specimens were subsequently cleaned ultrasonically for 30 s using a Branson 200 sonicator (Danbury, CT, USA). Parts to be mounted were then critical point dried using a Baltec CPD-030 critical point drier (Balzers, Liechtenstein) and attached to round-headed rivets using aluminium tape with conductive adhesive and coated with platinum-palladium in a JEOL JFC-2300HR highresolution coater (Tokyo, Japan). Scanning electron micrographs were taken with JEOL JSM-6335F and JEOL JSM-6390LV scanning electron microscopes at the ZMUC and the Fundação Oswaldo Cruz, Rio de Janeiro, Brazil, respectively.

Distribution maps were created with ArcMap v.10.2 (ESRI, Redlands, CA, USA) using vector layers for countries obtained from Natural Earth <naturalearthdata.com>.

DNA ISOLATION, AMPLIFICATION AND SEQUENCING

Genomic DNA was isolated from leg muscle tissue dissected from specimens fixed in 95–100% ethanol, amplified and sequenced using standard protocols (Nishiguchi et al., 2002; Prendini et al., 2005) at the AMNH Sackler Institute of Comparative Genomics. Primers used for the polymerase chain reaction (PCR) follow Prendini et al. (2005). The adjuvants bovine serum albumin, dimethyl sulphoxide and magnesium chloride were added when necessary to assist PCR amplifications.

Five phylogenetically informative gene loci were selected that evolve at different rates and would thus be expected to provide phylogenetic resolution at different, overlapping taxonomic levels (Giribet *et al.*, 2001; Prendini *et al.*, 2003, 2005). Two loci from the nuclear genome were included primarily to resolve relationships among the outgroup taxa. The complete sequence of the small-subunit ribosomal RNA gene (18S rRNA, or 18S) and a variable fragment (D3 region)

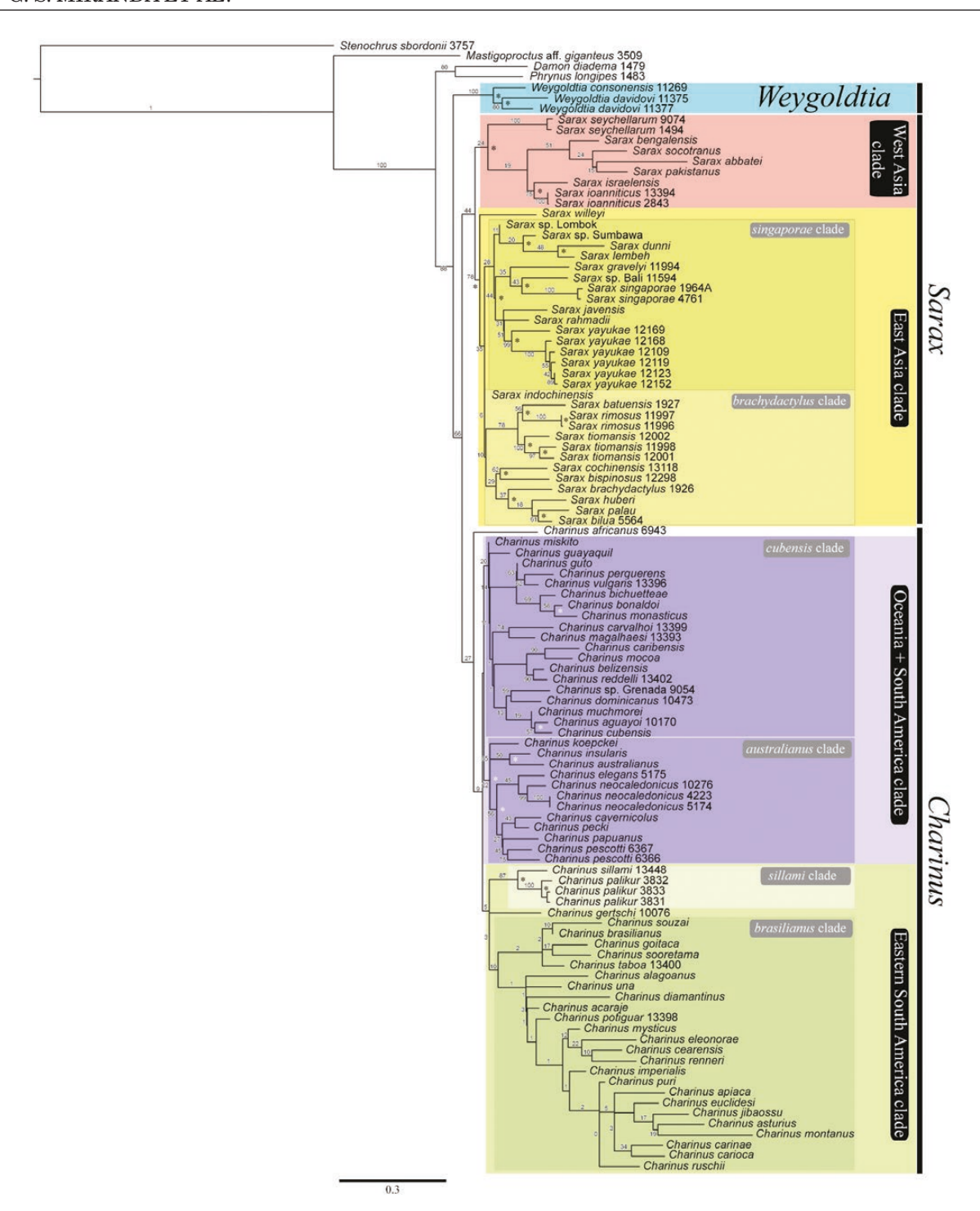


Figure 3. Phylogeny of the whip spider family Charinidae Quintero, 1986: maximum likelihood tree of 138 morphological characters and DNA sequences from two nuclear and three mitochondrial gene loci. Support values (bootstrap) are indicated on the branches. Asterisks indicate nodes with 100% posterior probability support in an analysis with Bayesian Inference.

of the large-subunit ribosomal RNA gene (28S rRNA, or 28S) were amplified. Three loci were selected from the mitochondrial (mt) genome, to provide resolution

among the ingroup taxa. Fragments of the mt homologs of the nuclear small-subunit ribosomal RNA gene (12S rRNA, or 12S) and the nuclear large-subunit ribosomal

RNA gene (16S rRNA, or 16S), both of which also contain conserved regions, were chosen, together with a more conserved fragment of the cytochrome c oxidase subunit I (COI) protein-coding gene. These fragments have been used effectively in studies of arachnid phylogeny at higher and lower levels, e.g. Giribet $et\ al.$ (2001), Prendini $et\ al.$ (2003, 2005), Gonzalez-Santillán & Prendini (2015) and references therein.

SEQUENCE ASSEMBLY AND ALIGNMENT

Sequences of the 52 terminals (34 taxa) were edited and assembled with SEQUENCHER v.5.0 (Gene Codes Corporation, Ann Arbor, MI, USA) and GENEIOUS v.9 (Biomatters Ltd., Auckland, New Zealand) and subsequently aligned with MAFFT v.7 (Kuraku *et al.*, 2013).

The ends of the alignments were trimmed to remove primers and marginal positions with poor coverage. The *COI* protein-coding gene was aligned using the L-INS-i method (Katoh et al., 2005). However, ribosomal RNA genes contain variable regions and structural constraints that affect the distribution of insertions and deletions in stem regions (Rix et al., 2008), so the rRNA secondary structure was also considered during alignment of the 18S, 28S, 12S and 16S rRNA gene loci, by using the Q-INS-i method (Katoh & Toh, 2008). After alignment, ambiguously aligned regions of the 12S and 16S rRNA loci were identified and removed with GBlocks (Talavera & Castresana, 2007).

A total of 250 sequences were generated for this study, with five sequences for *Damon diadema* (Simon, 1876) added from GenBank (Supporting Information, Appendix S2). Eight sequences were missing for the 16S locus and one each for the 18S and 28S loci. Seven 16S sequences, one 18S sequence and one *COI* sequence were incomplete.

After trimming ends and removing alignment-ambiguous regions, the remaining 241 sequences varied in length as follows: 18S, 1760–1764 basepairs (bp) (mean, mode: 1763); 28S, 503–524 bp (mean: 520; mode: 521); 12S, 196–201 bp (mean, mode: 201); 16S, 330–339 bp (mean: 338; mode: 339); *COI* 253–702 bp (mean: 693, mode: 702) (Supporting Information, Appendix S2). The concatenated, aligned dataset was 3535 bp, with 1889 bp variable and 729 parsimony informative. The nucleotide composition of the concatenated, aligned dataset was 26% A, 22% C, 25% G and 27% T.

Data partitions and models of evolution

The concatenated molecular dataset was partitioned into seven data blocks: three for each codon position of the protein-coding *COI* locus and four for the ribosomal loci. PartitionFinder v.2 (Guindon *et al.*, 2010; Lanfear *et al.*, 2016) and PhyML (Guindon *et al.*, 2010) were

used to identify the best-fitting models of evolution for the respective partitions.

The performance of the data under different parameters was tested with the GREEDY algorithm in PartitionFinder to assess the influence of ambiguously aligned regions on the models and how partition schemes affected the results. Matrices before and after trimming alignment-ambiguous regions with GBlocks were analysed with linked and unlinked branchlength estimations. Three information criteria (Akaike Information Criterion, AIC; AIC with small-sample correction, AICc; Bayesian Information Criterion, BIC) were tested for each analysis, using RAxML-HPC v.8 (Stamatakis, 2014) and MrBayes v.3.2.2 (Ronquist et al., 2012). The log-likelihood, information criteria, tree topology and branch support were then evaluated to identify which combination of parameters generated the best partitioning and model of evolution for the data. The unlinked branch-length estimation using AICc for the GBlocks-trimmed matrix retrieved the best branch support hence the trees generated under these parameters were selected.

PHYLOGENETIC ANALYSIS

The matrix used for the simultaneous analysis in the maximum likelihood (ML), Bayesian inference (BI) and parsimony analyses comprised 86 ingroup (82 described species plus four morphospecies) and four outgroup taxa represented by 107 terminals (103 ingroup and four outgroup terminals) and 3673 characters (3535 bp and 138 morphological characters). Sixty-two species and two morphospecies were represented only by morphological data. Fourteen morphological characters (41, 42, 47, 48, 55, 56, 77, 78, 79, 89, 96, 99, 108, 110) were uninformative and deactivated in the analysis.

Maximum likelihood was performed with RAxML-HPC v.8.2.0 (Stamatakis, 2014) on the USNM High-Performance Computer Cluster (Hydra). Branches were allowed independently selected gamma-shape parameters under a GTR model for the molecular data and a multistate model for the morphological characters (-m MULTIGAMMA -K MK), applied for each partition as selected by PartitionFinder (Lewis, 2001; Lanfear et al., 2012). Nodal support was assessed with the fast bootstrap algorithm (BS, 1000 replicates) (Stamatakis et al., 2008). Long branch lengths resulting from missing data introduced by taxa with incomplete molecular data were fixed using the branchlength stealing algorithm (-f k). Best-scoring ML trees were inferred for each gene locus to assess potential incongruence between the individual gene trees.

Bayesian inference was performed using MrBayes v.3.2.2 with two simultaneous and independent runs, consisting of four Metropolis-coupled Markov chain

Monte Carlo simulations (MCMCs), one cold and three incrementally heated, running for 100 million generations. The following models were selected by PartitionFinder (Lanfear et al., 2012) for each partition: GTR+I+G for the 12S, 16S, 18S, 28S and third-codon position of the COI; GTR+G for the firstcodon position of the COI: SYM+I+G for the secondcodon position of the COI; and the Mkv model for the morphological characters. Trees were sampled every 1000 generations to calculate posterior probabilities (PP). In order to assess the convergence of runs, the split frequencies and effective sample size (ESS) of all the parameters were evaluated and the loglikelihood of the samples plotted against the number of generations in TRACER v.1.6 (Rambaut et al., 2014). An ESS exceeding 200 was acknowledged as a good indicator of convergence. All trees sampled prior to reaching the log-likelihood plateau were discarded as burn-in and the remaining samples used to generate a 50% majority rule consensus tree.

Parsimony analyses were performed in TNT v.1.1 (Goloboff et~al., 2008), using new technology algorithms (Nixon, 1999). All characters were unordered and multistate characters treated as non-additive (Fitch, 1971). A batch file used in the TNT run is provided in Morphobank, project number 3538. Equal weighting (EW) and extended implied weighting (IW) with different values of the concavity constant, k (Goloboff, 2013), were applied to explore the sensitivity of the data. Extended implied weighting was used as it reduces the effect of missing data in the final calculations of character weights (Mirande, 2019).

Support for nodes was estimated for the EW tree using group frequencies under jackknifing with probability of alteration, P=0.33. Support in the implied weighting was measured as the absolute (non-GC) frequency from symmetric resampling, a jack-knifing method that accounts for character weights and the GC frequency from symmetric resampling (Goloboff *et al.*, 2003). Groups with no support or contradictory support in the most-parsimonious tree received zero (absolute frequency) or negative (GC frequency) values.

Morphological characters were optimized in the maximum likelihood tree to assess character homoplasy. Statistics such as consistency indices (CIs), retention indices (RIs) and fit were calculated using TNT and charts prepared using the R packages tidyverse (Wickham, 2019), hablar (Sjoberg, 2020), ggplot2 (Wickham, 2016) and egg (Auguie, 2019) (Fig. 5).

FOSSIL CALIBRATION AND DIVERGENCE DATING

Divergence times were estimated indirectly based on two node calibration points, one each for Amblypygi, Weygoldtina anglica (Pocock, 1911) and the outgroup Thelyphonida, *Parageralinura naufraga* (Brauckmann & Koch, 1983), constraining the minimum age of the internal node.

Weygoldtina anglica, from the British Middle Coal Measures of Coseley, near Dudley, Staffordshire, UK (Late Carboniferous, Westphalian B or Duckmantian), is the oldest fossil reliably identified as a whip spider. Dunlop et al. (2007) redescribed W. anglica and considered it a member of the Amblypygi crown group due to its similarity to the putatively basal whip spider, Paracharon Hansen, 1921 and, subsequently, Dunlop (2018) placed it sister to Paracharontidae Weygoldt, 1996. U-Pb dating of zircons constrains the upper boundary of the Duckmantian to 313.78 Mya ± 0.08 Myr, hence a minimum age for W. anglica is 313.7 Myr (Wolfe et al., 2016).

Parageralinura naufraga, from deposits of 'Ziegelei-Grube', Hagen-Vorhalle, near Ruhr, North Rhine-Westphalia, Germany (Late Carboniferous, Namurian B or Marsdenian), is the oldest known fossil of Tetrapulmonata and considered the plesion of extant Thelyphonidae Lucas, 1835 (Tetlie & Dunlop, 2008). The (Upper) Namurian—(Lower) Westphalian boundary lacks a precise isotopic date but an age of c. 319.9 Mya was estimated for the base of the Westphalian (top of the Namurian, only slightly younger than the Marsdenian) according to Milankovitch cycles of sedimentation, providing a minimum age for P. naufraga (Wolfe et al., 2016). Geological names and dates follow Cohen et al. (2013; updated)

Two independent runs of 100 million generations, with trees sampled every 5000 generations, were performed in BEAST v.1.8.0 (Drummond et al., 2012) on the CIPRES Science Gateway v.3.3 (https://www. phylo.org). Convergence was visualized in TRACER v.1.6 (Rambaut et al., 2014), ensuring all ESS values were above 200. The dataset was partitioned by genes and the clock and site partitions unlinked. A randomly generated starting tree was used together with an uncorrelated lognormal relaxed clock with a birth-death tree prior. Most priors were set at default values but the ucld.mean was set to a gamma distribution with shape value 0.001 and scale 1000.0 (Heath, 2012; Dimitrov et al., 2016). Postburn in trees were combined using LogCombiner and maximum clade credibility trees created using TreeAnnotator, with additional annotation in FigTree v.1.4.2 (http://tree.bio.ed.ac.uk/software/figtree) and Adobe Photoshop CS6.

Historical events that might have affected the evolution and diversification of Charinidae around the time of the median age estimates (with highest posterior probability) are hypothesized based on the literature. The highest posterior density (HPD) for each time age estimate is provided in parenthesis.

RESULTS

MAXIMUM LIKELIHOOD ANALYSIS

The ML tree recovered the monophyly of Charinidae (BS = 88%), with Weygoldtia (BS = 100%) placed sister to a clade comprising *Charinus* and Sarax (BS = 66%), neither of which was reciprocally monophyletic (Fig. 3). Charinus africanus Hansen, 1921 was placed sister to the rest of *Charinus* (BS = 27%), which formed two main clades, hereafter referred to as the 'Oceania + South America clade' (BS = 11%) and the 'eastern South America clade' (BS = 5%). The Oceania + South America clade, in turn, comprised two subclades: the first comprising 19 species from northern South America (mostly Amazonia) and the Caribbean (BS = 20%), hereafter referred to as the 'cubensis clade', and the second comprising nine species from Oceania (Papua New Guinea, Australia and New Caledonia) or the Pacific coast of South America (BS = 22%), hereafter referred to as the 'australianus clade'. Two species of the cubensis clade, Charinus guayaquil Miranda et al., 2021, and Charinus miskito Miranda et al., 2021, diverged prior to the rest, which also formed two subclades: the first comprising six species from the Brazilian Amazon (BP = 14%), including Charinus monasticus Miranda et al., 2021. probably a human introduction to a monastery in Rio de Janeiro, and the second comprising 11 species from the Amazon, the Caribbean and Central America (BS = 1%; Fig. 3). In the australianus clade, Charinus koepckei Weygoldt, 1972 from Peru was placed sister to a clade comprising Charinus insularis Banks, 1902 from the Galapagos Islands and Charinus australianus (L. Koch, 1867) (BS = 35%) from Samoa. This clade was in turn placed sister to a clade of six species, in which a clade comprising *Charinus elegans* Weygoldt, 2006 and Charinus neocaledonicus Kraepelin, 1895 (BP = 45%) was placed sister to a clade comprising Charinus cavernicolus Weygoldt, 2006, Charinus papuanus Weygoldt, 2006, Charinus pecki Weygoldt, 2006 and Charinus pescotti Dunn, 1949 (BP = 27%).

The eastern South America clade also comprised two subclades: the first, hereafter referred to as the 'sillami clade' (BS = 87%), comprising two species from French Guiana, and the second, hereafter referred to as the 'brasilianus clade' (BS = 3%), comprising 24 species from north-eastern Brazil, with Charinus gertschi Goodnight & Goodnight, 1946 sister to all the rest. The low branch support for the brasilianus clade may be due to the high amount of missing data (only two of the 24 terminals were represented by both morphological and molecular data).

Sarax was divided into two clades, hereafter referred to as the 'West Asia clade' (BS = 24%) and the 'East Asia clade' (BS = 78%). The West Asia clade comprised seven species previously assigned to

Charinus, which are transferred to Sarax (Miranda et al., 2021): Sarax abbatei (Delle Cave, 1986), Sarax bengalensis (Gravely, 1911), Sarax ioanniticus (Kritscher, 1959), Sarax israelensis (Miranda et al., 2016), Sarax pakistanus (Weygoldt, 2005), Sarax seychellarum (Kraepelin, 1898) and Sarax socotranus (Weygoldt et al., 2002). Sarax seychellarum was placed sister to two subclades: one comprising S. ioanniticus and S. israelensis (BS = 75%), the other comprising the four remaining species (BS = 19%). All of these species, except S. seychellarum, were previously part of the bengalensis species group, with finger-like female gonopods (Weygoldt, 2005; Miranda & Giupponi, 2011).

The East Asia Clade comprised *Sarax willeyi* Gravely, 1915, placed sister to two clades, hereafter referred to as the 'brachydactylus clade' and the 'singaporae clade'. In the ML tree, the brachydactylus clade (BS = 6%) included *Sarax indochinensis* Miranda et al., 2021, placed sister to two subclades: the first comprising three species from the Malay Peninsula and adjacent Tioman Island (subclade 6; BS = 78%) and the second comprising six species from India, Sri Lanka, the Philippines, Palau and the Solomon Islands (subclade 7; BS = 29%).

The singaporae clade (BS = 28%) comprised three subclades in the ML tree: the first (BS = 11%) comprising Sarax dunni Miranda et al., 2021, Sarax lembeh Miranda et al., 2021 and two undescribed morphospecies from Lombok and Sumbawa; the second (BS = 35%) comprising Sarax gravelyi Miranda et al., 2021, Sarax singaporae Gravely, 1911 and an undescribed morphospecies from Bali; and the third (BS = 31%) comprising Sarax javensis (Gravely, 1915), Sarax rahmadii Miranda et al., 2021, and Sarax yayukae Rahmadi et al., 2010.

BAYESIAN INFERENCE

As in the analysis with ML, BI recovered the monophyly of Charinidae (PP = 0.96), with Weygoldtia (PP = 1) placed sister to a clade comprising *Charinus* and Sarax (PP = 0.96), neither of which was reciprocally monophyletic. Charinus was divided into two main clades: the Oceania + South America clade and the eastern South America clade. The taxonomic composition of these clades closely resembled the corresponding clades in the tree obtained with ML. The primary differences concerned the placement of Charinus sooretama Miranda et al., 2021, from eastern Brazil, sister to all other *Charinus* (PP = 0.57), and Charinus guayaquil sister to a clade comprising C. africanus, S. abbatei, S. bengalensis, S. pakistanus and S. socotranus (PP = 0.68), all of which were placed in the *cubensis* clade.

The topology obtained with BI also separated the species of Sarax into two clades (PP = 0.93): the

West Asia clade (PP = 0.95) and the East Asia clade (PP = 0.99). However, four of the seven species assigned to the West Asia clade in the ML analysis ($S.\ abbatei$, $S.\ bengalensis$, $S.\ pakistanus$ and $S.\ socotranus$) were placed within the *cubensis* clade in the analysis with BI (PP = 0.68), leaving only $S.\ ioanniticus$, $S.\ israelensis$ and $S.\ seychellarum$ in the West Asia clade.

The East Asia clade was divided into two main clades: one comprising four species, Sarax batuensis Roewer, 1962, S. indochinensis, S. rimosus (Simon, 1901) and S. tiomanensis Miranda et al., 2021 (PP = 0.54), the other comprising 16 species (PP = 0.59). The first of these clades included some species assigned to the brachydactylus clade in the analysis with ML, the rest of which, i.e. Sarax bilua Miranda et al., 2021, Sarax bispinosus (Nair, 1934), Sarax brachydactylus Simon, 1892, Sarax cochinensis (Gravely, 1915), Sarax huberi Seiter et al., 2015 and Sarax palau Miranda et al., 2021, grouped sister to all other species of the singaporae clade (PP = 0.64). Other differences from the analysis with ML concerned the position of S. rahmadii, placed sister to S. gravelyi in the analysis with BI (PP = 0.92), rather than sister to S. yayukae, as in the ML analysis, and the position of Sarax willevi (Gravely, 1915), unresolved in the singaporae clade in the analysis with BI (PP = 0.59), unlike the analysis with ML, in which it grouped sister to all other East Asian species of *Sarax*.

PARSIMONY ANALYSIS

Parsimony analysis with equal weighting recovered 871 trees of 6945 steps, resulting in extensive polytomies, with low support, in the strict consensus (Fig. S2). In contrast, only two trees were obtained in all analyses with implied weighting and k values varying from six to 90. The CIs and RIs of the trees obtained with implied weighting are predictably higher than those of the trees obtained with equal weighting. Whereas the trees obtained with k values greater than 40 are identical in length (6946 steps) and topology, those obtained with lower k values differ topologically and are less parsimonious (Table 2).

Charinidae and *Weygoldtia* were monophyletic, whereas *Charinus* and *Sarax* were paraphyletic, in all parsimony analyses (Figs S2–S7; trees with branch support available in Morphobank, project number 3538). *Weygoldtia davidovi* was paraphyletic with low support (GC = 21) in the analyses with k = 6–30 but monophyletic with low support (GC = 28) in the analyses with k = 40–90. *Sarax abbatei*, *S. bengalensis*, *S. pakistanus* and *S. socotranus* were placed sister to a clade of *Charinus* in the implied weighting analyses with k = 6–30 (GC = 43, GF = 15) and nested within a clade of *Sarax* in the implied weighting analyses with k = 40–90 (GC = 13). *Sarax seychellarum* was placed

Table 2. Length (steps), Fit, consistency index (CI) and retention index (RI), of most parsimonious trees (MPTs) obtained with equal weighting (EW) and implied weighting (IW) using incremental values of the concavity constant, k, in simultaneous phylogenetic analysis of the whip spider family Charinidae Quintero, 1986

Weighting	Length	Fit	CI	RI	MPTs
EW	6945	553.57	0.163	0.167	871
IW $k = 6$	6979	438.79	0.257	0.532	2
$IW\ k=10$	6972	439.09	0.258	0.532	2
$\mathrm{IW}k=20$	6963	439.51	0.258	0.533	2
IWk=30	6955	440.05	0.258	0.534	2
$\mathrm{IW}k=40$	6946	440.84	0.259	0.535	2
IWk = 50	6946	440.84	0.259	0.535	2
$IW\ k = 60$	6946	440.84	0.259	0.535	2
$IW\ k = 70$	6946	440.84	0.259	0.535	2
IW $k = 80$	6946	440.84	0.259	0.535	2
$IW\ k = 90$	6946	440.84	0.259	0.535	2
IW k = 100	6946	440.84	0.259	0.535	2

sister to a clade comprising species of *Charinus* and *Sarax* in all parsimony analyses.

PREFERRED TREE

Branch support values for the trees recovered with ML, BI and parsimony were mostly low due to the absence of molecular data for over half the terminal taxa in the analysis. However, the tree obtained with ML was better resolved and received greater nodal support (Fig. 3) than the trees obtained with BI and parsimony (Figs S2–S8) and its topology was more congruent with the individual gene trees (Figs S9–S13). Additionally, the CIs and RIs of the morphological characters were generally greater in the ML tree than in the trees obtained with parsimony and BI (see Fig. 5 and Morphobank Project 3538). The ML tree is, therefore, presented as the preferred tree, on which the results and discussion are based.

DIVERGENCE TIME ESTIMATION

The phylogeny obtained by the divergence dating analysis (Fig. 4) was largely congruent with the preferred phylogeny obtained by the simultaneous analysis with ML (Fig. 3). The tree topology differed primarily in relationships among the species of *Charinus*, notably *C. africanus*, placed sister to *Charinus vulgaris* Miranda & Giupponi, 2011 (PP = 0.50), and *Charinus potiguar* Vasconcelos *et al.*, 2013, placed sister to *Charinus gertschi* (PP = 0.50). The

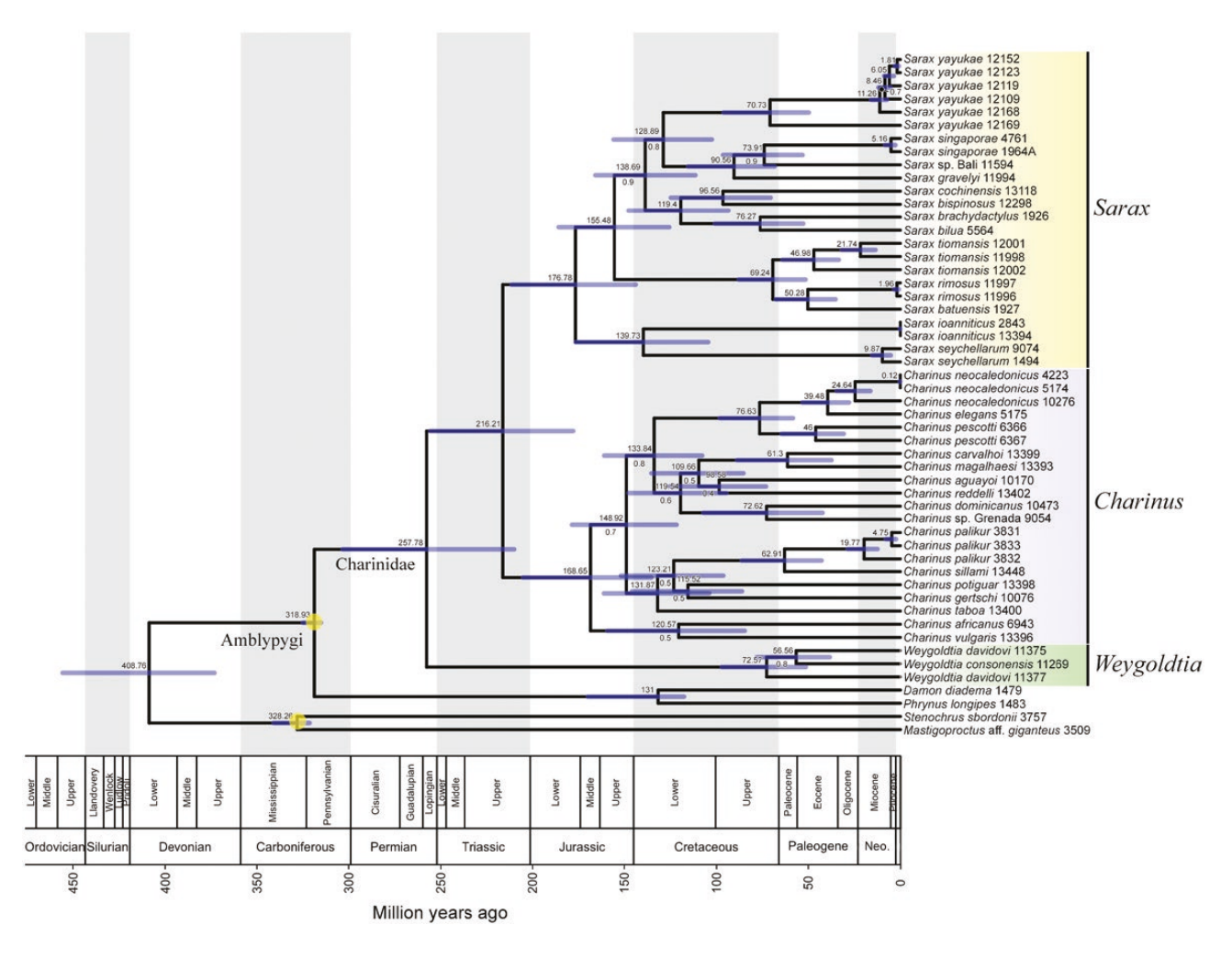


Figure 4. Phylogeny of the whip spider family Charinidae Quintero, 1986: maximum clade credibility tree obtained by analysis with BEAST. Calibration points for Uropygi and Amblypygi indicated with yellow circles at nodes. Median dates and posterior probabilities indicated above and below branches, respectively. Support values (PP) less than 1 indicated below branches. Neo: Neogene.

highest branch support values (PP = 1) were obtained for Charinidae, *Charinus*, *Sarax* and *Weygoldtia*.

The age estimate for the most recent common ancestor of extant Charinidae is 318.9 Mya (95% HPD interval: 315–325 Mya). The age estimate for the divergence between *Weygoldtia* and the clade comprising *Charinus* and *Sarax* is 257.8 Mya (95% HPD interval: 210–303 Mya) and for the divergence between *Charinus* and *Sarax*, 216.2 Mya (95% HPD interval: 178.0–255.8 Mya).

DISCUSSION

HOMOPLASY AND RELATIONSHIPS

The morphology of whip spiders is rather homogeneous (Weygoldt, 1998, 1999a; Miranda *et al.*, 2016a, 2018a, b). Diagnostic and phylogenetic characters

in the order are based on qualitative and meristic differences, resulting in a limited number of phylogenetically informative characters. A wellresolved topology may be obtained when a small taxon sample is used to reconstruct a morphological phylogeny within Amblypygi (Garwood et al., 2017; Miranda et al., 2018b). However, when the ingroup is densely sampled, and all variation within character states is accounted for, as in the present study, homoplasy negatively affects the resolution and support of clades. In the discussion that follows, some morphological synapomorphies and diagnostic characters historically used to define taxonomic groups of Charinidae are discussed, based on the simultaneous phylogenetic analysis of the morphological and molecular data with ML (Fig. 3). Diagnostic characters and details of the variation

within the genera and species of Charinidae are provided elsewhere (Miranda et al., 2021).

Among the different character systems (carapace, cheliceral basal segment, cheliceral claw, eyes, genital operculum, male gonopod, female gonopod, basitibia IV, tarsomere IV, opisthosoma, pedipalp coxae, pedipalp femur, pedipalp patella, pedipalp tarsus, pedipalp tibia, pedipalp trochanter, sternum, tarsi I and tibia I), the best CI and RI (mean/median) were obtained for characters of the carapace (CI = 0.78/0.90, RI = 0.93/0.95), pedipalp trochanter (CI = 0.75/0.75, RI = 0.75/0.75), tibia I (CI = 0.75/0.75, RI = 0.75/0.75) and pedipalp tibia (CI = 0.73/1, RI = 0.9/1) (Fig. 5). The best fit (mean/median) were obtained for the characters of the pedipalp trochanter (Fit = 1.5/1.5), tibia I (Fit = 1.5/1.5), opisthosoma (Fit = 2/2), carapace (Fit = 2/2.67), eyes (Fit = 2.5/3.17) and tarsomere IV (Fit = 1/3.6) (Fig. 5).

One seta posterior to the lateral ocular triad (character 13; CI = 0.50, RI = 0.97, Fit = 2; Figs 6A, 7N), a plesiomorphic state occurring in most Amblypygi analysed, is absent in the East Asian clade of Sarax, for which setae adjacent to the lateral eyes (character 14; CI = 1, RI = 1, Fit = 1) are synapomorphic (Figs 6B, 7B). A curved carina on the carapace (character 9; CI = 0.20, RI = 0.91, Fit = 5), diagnostic for most species of Sarax, as noted by Kraepelin (1899), is also homoplastic, occurring in Weygoldtia and some species of Charinus (Fig. 7). A straight carina, anterior to the lateral eyes (character 11; CI = 1, RI = 1, Fit = 1), is synapomorphic for Weygoldtia (Fig. 7C).

A long, projecting tooth on the retrolateral surface of the chelicera, adjacent to the bifid tooth (character 19; CI = 0.07, RI = 0.63, Fit = 14), widespread among Amblypygi, is variable within Charinidae; it is long in a few *Charinus* species but short in *W. davidovi* and some species of *Sarax* (character 20; CI = 1, RI = 1, Fit = 1; Fig. 8J). The number of teeth on the cheliceral fang is extremely variable among Charinidae (character 31; CI = 0.17, RI = 0.59, Fit = 29; Fig. 8C; Vasconcelos *et al.*, 2013). Although four or five teeth is the ancestral state, Charinidae possess three to 13.

The relative size of the cusps of the bifid tooth (character 23; Fig. 8G), a diagnostic character among Caribbean and Central American *Charinus* (Miranda *et al.*, 2016b), was not synapomorphic for any groups within the genus (CI = 0.29, RI = 0.44, Fit = 7). The ventral sac cover (character 35; Fig. 9) is known to be homoplastic in Amblypygi, occurring in *Charon* (Charontidae; Weygoldt, 1996), Sarax and, although reduced to a small exposed border, Weygoldtia (CI = 0.50, RI = 0.97, Fit = 2).

The primary diagnostic character for Sarax is the finger-like female gonopod (character 43; CI = 0.33, RI = 0.93, Fit = 6; Figs 6C, 10C), which occurs in all species of the genus and supported the transfer of eight species from Charinus to Sarax (below). One exception

is *S. seychellarum*, considered not to possess a gonopod (Weygoldt, 1999b), an autapomorphy for this species. A variation of the finger-like gonopod morphology is also present, i.e. the plunger-like gonopod, characterized by a stalk similar to the finger-like gonopod, but with a small terminal invagination and the apex sometimes broader than the base. *Charinus africanus*, the only species outside *Sarax* with a modified finger-like gonopod bearing small claws at the apex (see fig. 3 of Weygoldt, 2008), is nevertheless highly supported as a member of *Charinus* (Figs 3 and 5).

Whereas the number of articles on the tarsus of leg I (character 52; CI = 0.46, RI = 0.77, Fit = 13) varies among the species of Charinidae, the number of articles on the tibia of leg I (character 50; CI = 0.50, RI = 0.50, Fit = 2) is conserved, with 21–25 observed in most species of the family, except *Charinus montanus* Weygoldt, 1972, with 26–45.

A ventromedial apophysis anteriorly directed on the pedipalp trochanter (character 60; CI = 1, RI = 1, Fit = 1; Fig. 11A) is synapomorphic for Charinidae (Weygoldt, 1996). The number of spines on the pedipalp femur and patella is not synapomorphic, but two ventral spines on the patella is the ancestral state of *Charinus*, and three spines the ancestral state of *Sarax* (character 72; CI = 0.17, CI = 0.69, CI = 0.69

A row of setae at the base of the cleaning organ (pedipalp tarsus; character 88; CI = 1, RI = 1, Fit = 1) was considered synapomorphic for Charontidae by Weygoldt (1996). The charontid genera, *Charon* and *Catageus*, each possess a row of more than four setae near the proximal border of the cleaning organ. However, one or two setae also occur in the charinid genus, *Weygoldtia*. Therefore, the diagnostic character state for Charontidae is a row on more than two setae, rather than a row of setae.

A carina with a semicircular configuration, on the dorsal surface of the pedipalp coxae (character 93; CI=1, RI=1, Fit=1; Fig. 12), was synapomorphic for Charinidae, as first noted by Delle Cave (1986). This carina is also present in Charontidae, in which it has a triangular configuration. The anterior border of the carina often bears three prominent setae (character 94, state 1; CI=0.20, RI=0.59, Fit=25). Whereas these setae are markedly separated in *Charinus* (Fig. 12), the two largest setae on the anterior border are adjacent to one another in Sarax (character 95, state 1; CI=0.25, RI=0.92, Fit=4), a synapomorphy for the genus.

The number of articles on the basitibia of leg IV (character 121; CI = 0.20, RI = 0.66, Fit = 15), once used to diagnose the genera *Charinides* and *Tricharinus*, presently in synonymy with *Charinus*, was demonstrated to be homoplastic. Most species of *Charinus* possess three articles and several species of *Sarax* possess four, but no state is exclusive to a

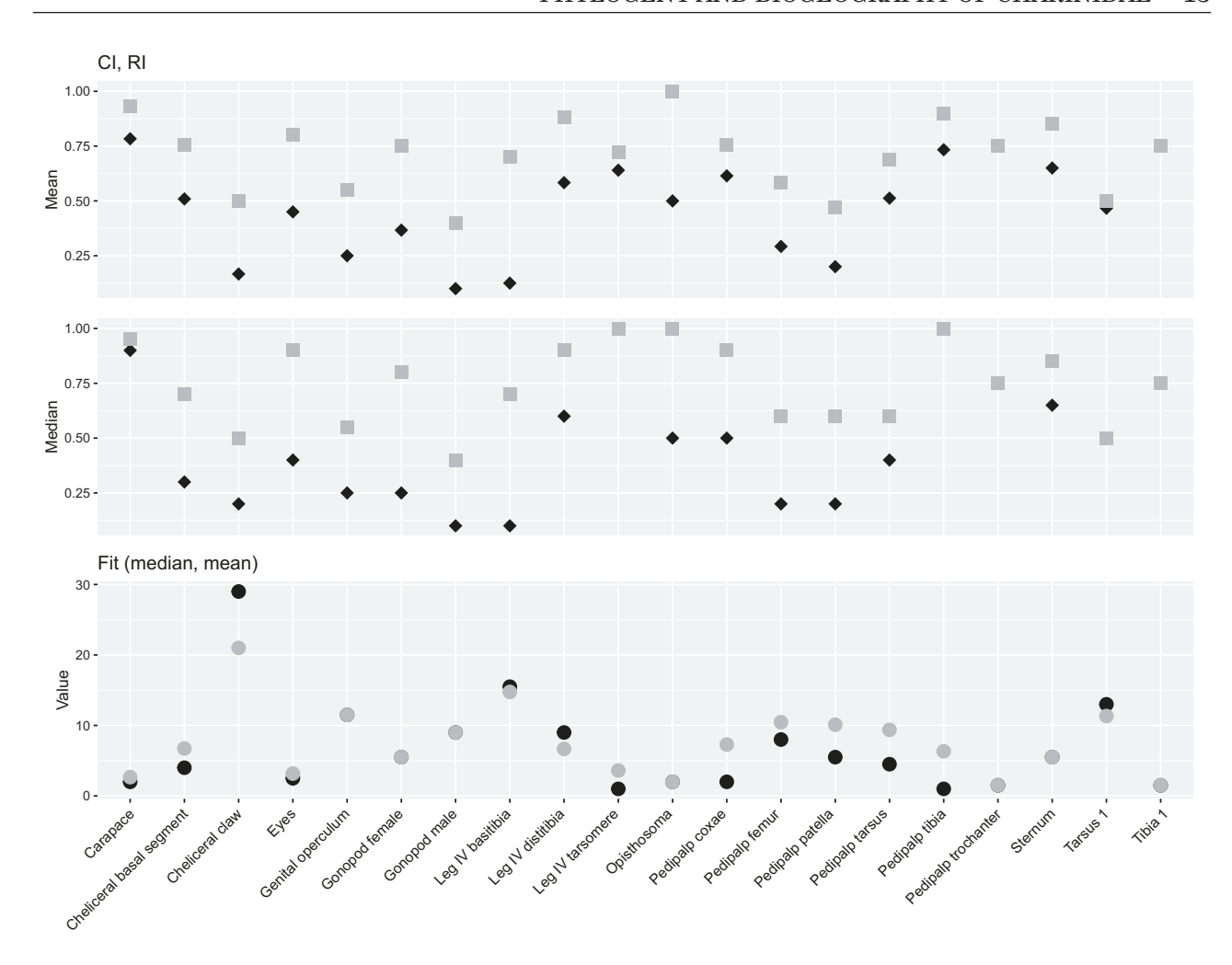


Figure 5. Mean and median homoplasy statistics, i.e. consistency index (CI, black diamond), retention index (RI, grey square) and Fit (mean, dark grey circles; median, black circles), for parsimony-informative morphological characters, arranged by character system (Appendix 2), on optimal phylogeny of the whip spider family Charinidae Quintero, 1986 (Fig. 3).

particular genus. A marked division of the distitibia of leg IV, distal to the triad of trichobothria (character 133; CI = 1, RI = 1, Fit = 1; Fig. 13), occurs in all Charinidae but also in Charontidae.

Charinus, Sarax and Weygoldtia exhibit equal numbers of trichobothria in the frontal and caudal series of leg VI [characters 130 (CI = 0.56, RI = 0.88, Fit = 9) and 131 (CI = 0.60, RI = 0.88, Fit = 10)], usually five, but sometimes six in Charinus and Sarax compared with six or nine in Weygoldtia. A pulvillus occurs in Paracharontidae, Charinidae and Charontidae (character 135; CI = 1, RI = 1, Fit = 1; Fig. 14), as noted by Quintero (1986) and Weygoldt (1996).

BIOGEOGRAPHY AND ORIGIN OF CHARINIDAE

According to the reconstruction presented here, the most recent common ancestor of Charinidae and Phrynoidea lived 318.9 Mya (95% HPD interval:

315-325 Mya), during the Late Carboniferous (Lower Pennsylvanian; Fig. 4), five million years older than the oldest known fossil of Amblypygi (Wolfe et al., 2016; Dunlop, 2018). During the Late Carboniferous, Pangaea was intact and present-day Europe and North America (Euamerica) were situated over the equator and covered by humid rainforest (Fig. 4) (Sahney et al., 2010). Based on what is known about the habitat of extant whip spiders in tropical rainforests, it may be assumed that the habitats of Palaeozoic species were similar to those of living species, which would explain the presence of Amblypygi fossils in the Coal Measures of Coseley, Staffordshire (UK), Mazon Creek, Illinois (USA) and Nova Scotia (Canada), all of which were tropical during the Palaeozoic. The oldest fossils of Uropygi, the sister-group of Amblypygi, also occur in eastern North America and Europe, which is hypothesized to be the ancestral area of the group (Clouse et al., 2017).

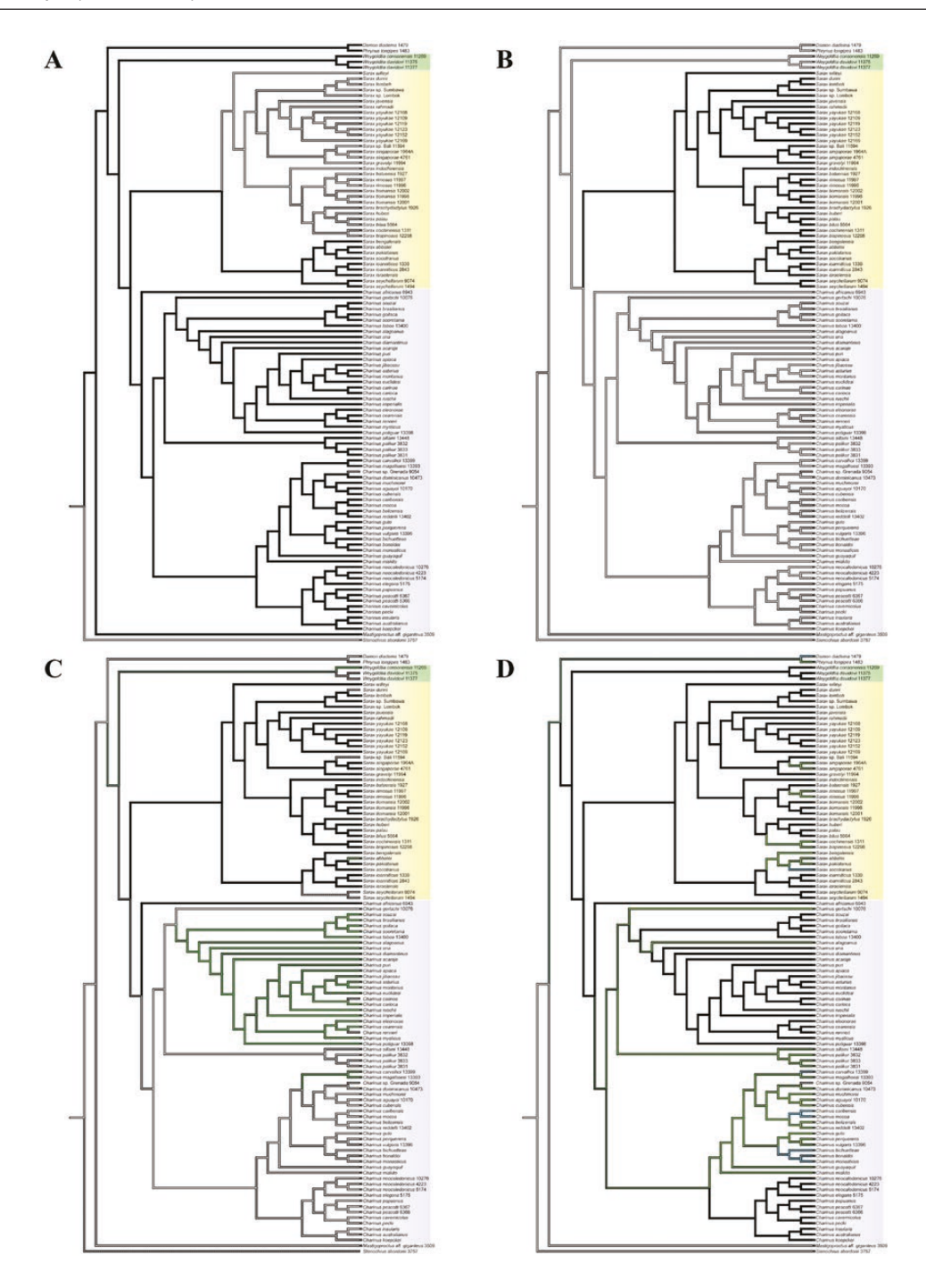


Figure 6. Ancestral state reconstruction of selected morphological characters on the phylogeny of the whip spider family Charinidae Quintero, 1986. A, character 13; presence of setae posterior to lateral ocular triad; dark lines, present; grey lines, absent. B, character 14, presence of setae lateral to ocular triad; dark lines, present; grey lines, absent. C, character 43; shape of female gonopod; white lines, cushion-like; green lines, sucker-like; black lines, finger-like (includes plunger-like gonopods). D, character 121, number of articles on basitibia IV; white, 1; blue, 2; green, 3; black, 4. *Charinus* Simon, 1892 represented in blue, *Sarax* Simon, 1892 in yellow, and *Weygoldtia* Miranda *et al.*, 2018 in green.



Figure 7. Whip spiders of the family Charinidae Quintero, 1986, carapace, sinistral margin, retrolateral view, illustrating curved or straight carina between lateral eyes and lateral carapace margin (arrows in A, B, C; characters 9–12), and setae posterior or adjacent to lateral ocular triad (arrows in B, N; characters 13, 14). A, Sarax brachydactylus Simon, 1892, \$\delta\$ (AMNH [LP 1926]). B, Sarax cochinensis (Gravely, 1915), \$\varphi\$ [AMNH (LP 13118)]. C, Weygoldtia davidovi (Fage, 1946), \$\delta\$ [AMNH (LP 11377)]. D, Sarax gravelyi Miranda et al., 2021, \$\varphi\$ [AMNH (LP 11995)]. E, Sarax willeyi Gravely, 1915, \$\varphi\$ (SMF 64589). F, Sarax yayukae Rahmadi et al., 2010, \$\delta\$ [AMNH (LP 12109)]. G, Charinus dominicanus Armas & González Perez, 2001, \$\delta\$ (AMNH). H, Sarax ioanniticus (Kritscher, 1959), \$\varphi\$ (NHMW 19137). I, Sarax seychellarum (Kraepelin, 1898), \$\varphi\$ [AMNH (LP 9075)]. J, Sarax pakistanus (Weygoldt, 2005), \$\delta\$ (MHNG). K, Sarax israelensis (Miranda et al., 2016), \$\varphi\$ (HUJ INVAMB 111). L, Sarax abbatei (Delle Cave, 1986), \$\varphi\$ (MZUF 1896–167). M, Charinus belizensis Miranda et al., 2016, \$\delta\$ (HUJ INVAMB 117). N, Charinus acosta (Quintero, 1983), \$\varphi\$ (USNM ENT 784407). O, Charinus montanus Weygoldt, 1972, \$\varphi\$ (MNRJ 9087). Scale bars: A, B, D–O, 0.2 mm; C, 0.5 mm.

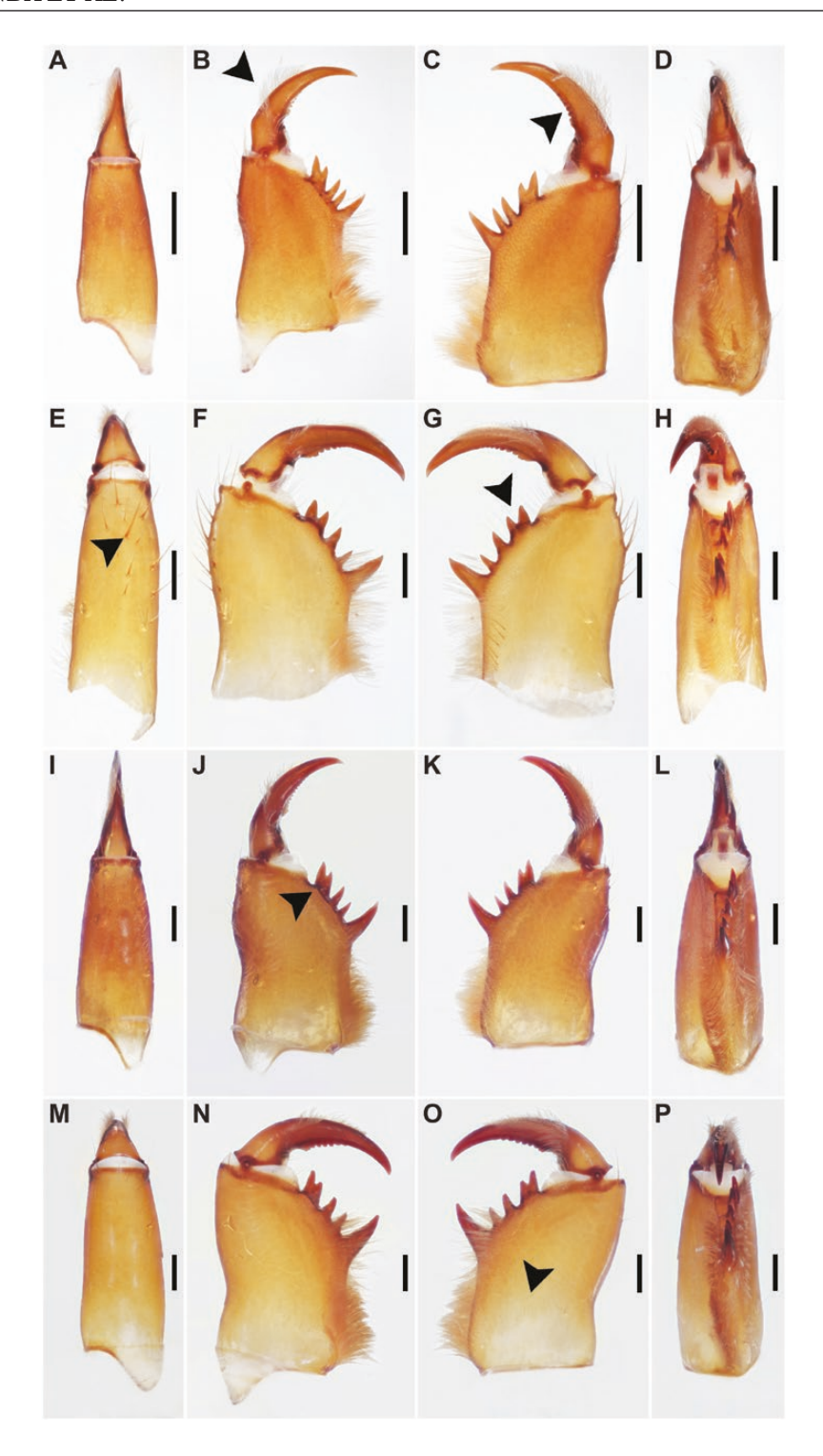


Figure 8. Whip spiders of the family Charinidae Quintero, 1986, chelicerae, dorsal, retrolateral, prolateral and ventral views, illustrating dentition and setation (characters 17–34; arrow in B, characters 32 and 33; arrow in C character 31; arrow in E, characters 27–30; arrow in G, characters 22–24; arrow in J, characters 18, 19; arrow in O characters 25–26). A–D, Charinus montanus Weygoldt, 1972, ♀ (MNRJ 9087). E–H, Charinus troglobius Baptista & Giupponi, 2002, ♂ (MNRJ 9069). I–L, Charinus mysticus Giupponi & Kury, 2002, ♀ (MNRJ 9022). M–P, Charinus diamantinus Miranda et al., 2021, ♂ (MNRJ 9189). Scale bars: 0.5 mm.

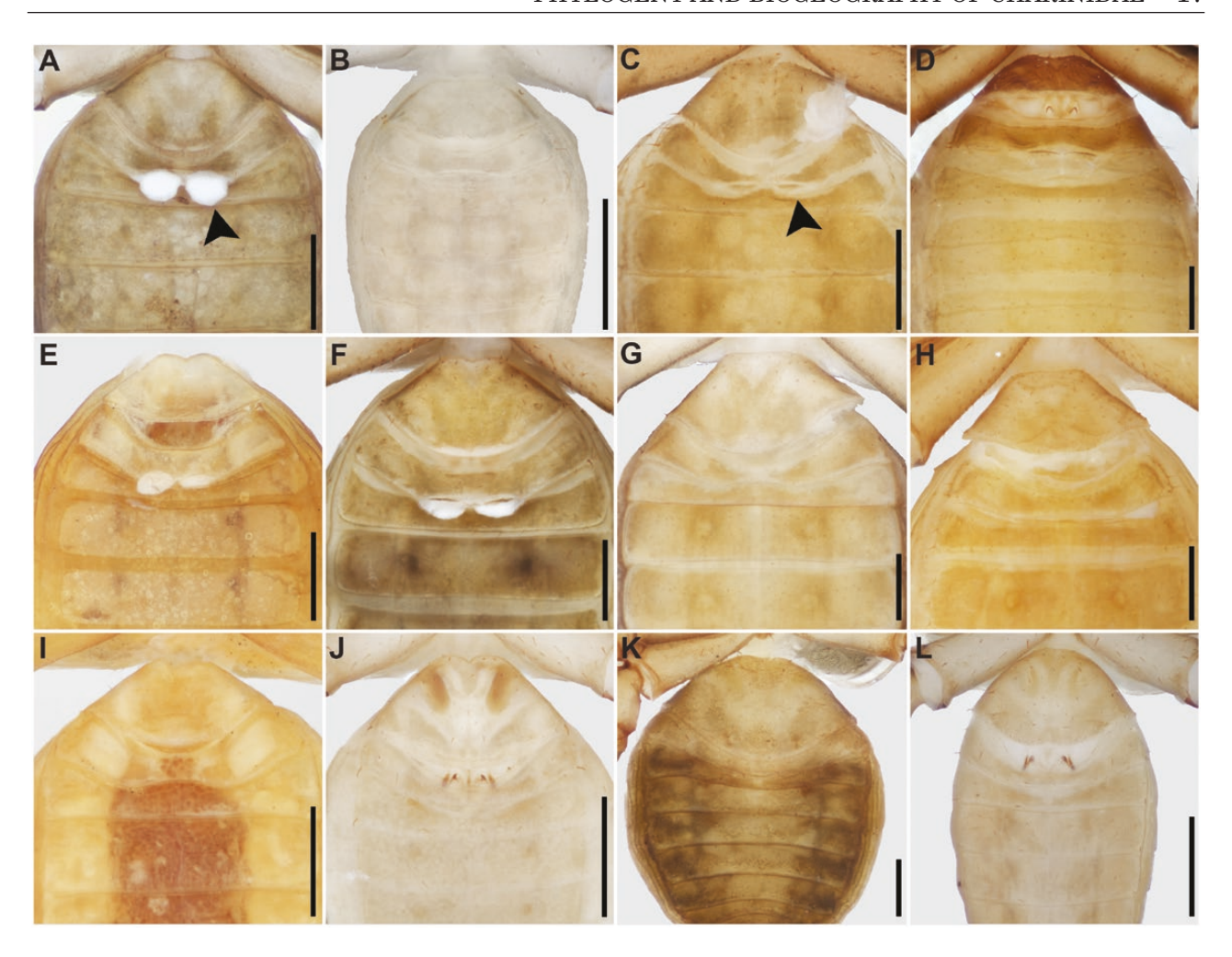


Figure 9. Whip spiders of the family Charinidae Quintero, 1986, opisthosoma, ventral view illustrating ventral sac and ventral sac cover (arrows in A, C; character 35). A, Sarax gravelyi Miranda et al., 2021, \Diamond [AMNH (LP 11995)]. B, Sarax bispinosus (Nair, 1934), \eth [AMNH (LP 12298)]. C, Sarax brachydactylus Simon, 1892, \eth [AMNH (LP 1926)]. D, Sarax sp. from Bali, \eth [AMNH (LP 11594)]. E, Sarax willeyi Gravely, 1915, \Diamond (SMF 64589). F, Sarax yayukae Rahmadi et al., 2010, \eth [AMNH (LP 12119)]. G, Weygoldtia davidovi Fage, 1946, \eth [AMNH (LP 11377)]. H, Charinus ruschii Miranda et al., 2016, \Diamond (MNRJ 9235). I, Sarax abbatei (Delle Cave, 1986), \Diamond (MZUF 1896–167). J, Charinus dominicanus Armas & González Perez, 2001, \eth (AMNH). K, Charinus palikur Miranda et al., 2021, \eth [AMNH (LP 3831)]. L, Charinus belizensis Miranda, Giupponi & Wizen, 2016, \eth (HUJ INVAMB 117). Scale bars: 1 mm.

The Late Carboniferous was marked by major changes in climate, with temperature shifts and atmospheric carbon dioxide fluctuations that led to aridification and a reduction and fragmentation of forest coverage in the tropics (DiMichele et al., 2009, 2010; Sahney et al., 2010; Hedge et al., 2019). Divergence between the Charinidae and other families of Amblypygi may have occurred in those fragmented forests (Fig. 4). Speciation associated with environmental change is among the limited evidence of climatic regionalization during the Palaeozoic. At this time, arthropods were highly diverse: arachnids, insects and myriapods formed sophisticated interconnected communities and a high abundance of rainforest leaf-litter arthropods

comprised elaborate food chains (Shear & Kukalova-Peck, 1990; Falcon-Lang *et al.*, 2006; Labandeira, 2006). Whip spiders were almost certainly part of the dynamic leaf-litter environment during the Palaeozoic.

Another 60 Myr passed before the ancestor of all living genera of Charinidae diverged into two lineages, Weygoldtia and the common ancestor of Charinus and Sarax. By the late Permian (Fig. 4), around 257.8 Mya (95% HPD interval: 210–303 Mya), terrestrial organismal diversity was rich with complex amphibian and reptile faunas, and numerous plant taxa providing new habitats (Benton, 2003). Some floras were endemic, indicating geographical differentiation associated with climatic zonation

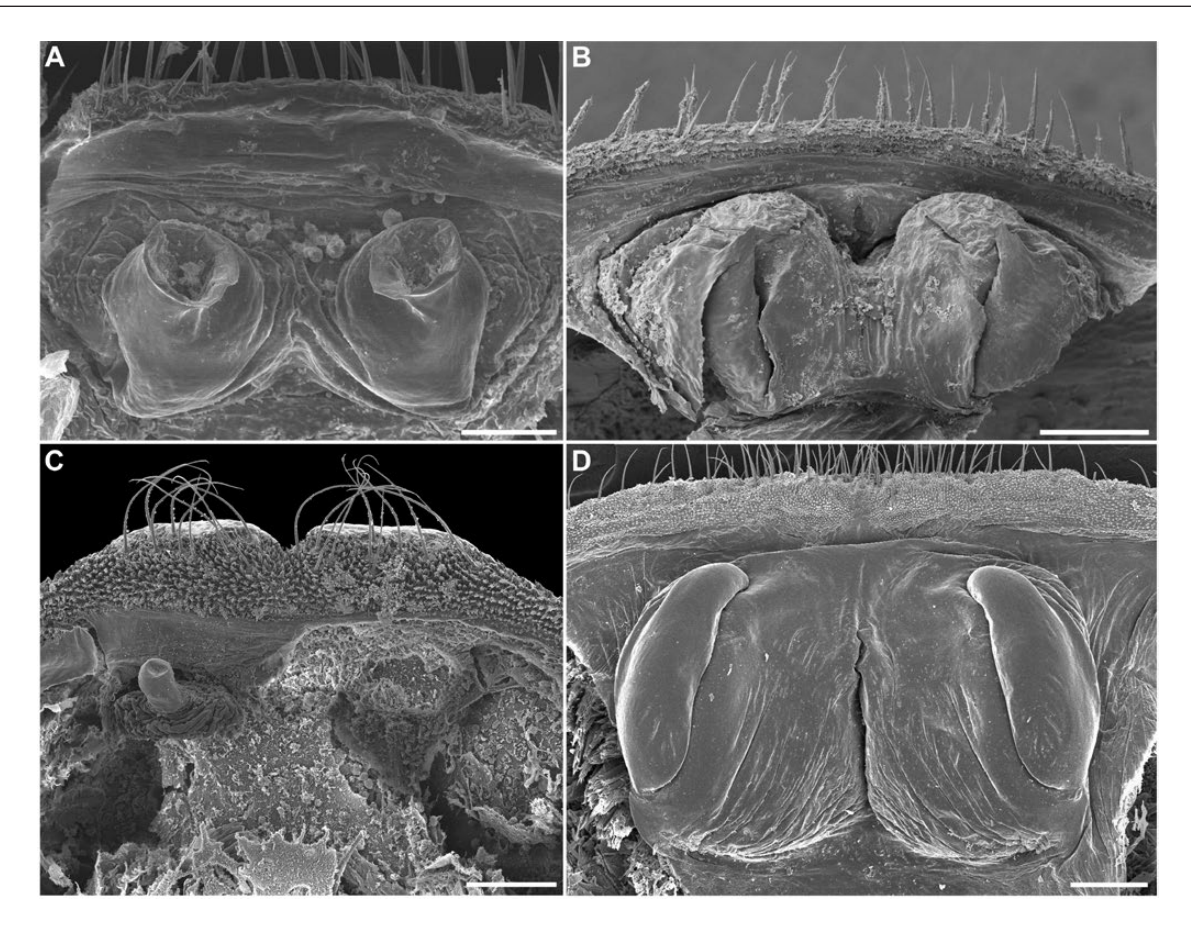


Figure 10. Whip spiders of the families Charinidae Quintero, 1986 and Phrynidae Blanchard, 1852, \$\varphi\$ gonopod, dorsal view illustrating diverse shapes (characters 37–43). A, Charinus ruschii Miranda et al., 2016, \$\varphi\$ (MNRJ 9237). B, Charinus belizensis Miranda et al., 2016, \$\varphi\$ (HUJ INVAMB 118). C, Sarax tiomanensis Miranda et al., 2021, \$\varphi\$ [AMNH (LP 11998)] D, Heterophrynus vesanicus Mello-Leitão, 1931, \$\varphi\$ (MNRJ 09026). Scale bars: A–C, 100 μm; D, 300 μm.

(Benton & Twitchett, 2002). However, by the end of the Permian, mass extinctions caused more than 90% of the organisms to vanish (Benton & Twitchett, 2002). The split between *Weygoldtia* and its sister-group occurred during that time, around the Guadalupian and Permian extinctions (Raup & Sepkoski, 1982; Jin et al., 1994; Stanley & Yang, 1994). Both events had severe effects on marine and terrestrial life, purging 58% of all marine invertebrate genera during the Guadalupian extinction (Knoll et al., 1996) and 70% of the remainder during the Permian extinction (Benton & Twitchett, 2002; Clapham et al., 2009).

According to the reconstruction presented here, *Charinus* and *Sarax* diverged around 216 Mya (95% HPD interval: 178.0–255.8 Mya; Fig. 4). This was a time of recovery from the Permian extinctions, reappearance of new vegetation cover and, consequently, the availability of new niches for terrestrial arthropods (Grauvogel-Stamm & Ash, 2005). Pangaea had moved northwards, northern South America and central Africa were situated across the equator, large parts

of North America were still tropical and whip spiders could presumably occupy much of the Americas and Africa. The divergence between *Charinus* and *Sarax* probably resulted from vicariance events following continental drift.

EARLY EVOLUTION OF THE CHARINID GENERA

Weygoldtia diverged from its closest relatives early in the evolution of Charinidae (257.8 Mya; Fig. 4), but the separation of its two species, Weygoldtia consonensis Miranda et al., 2021 and W. davidovi (Fage 1946) occurred much later, around 72.6 Mya (95% HPD interval: 51.4–97.1 Mya; Campanian, Late Cretaceous). Today, W. davidovi occurs in southern Vietnam, whereas W. consonensis is endemic to the Con Dao Islands in the South China Sea, c. 90 km south of the mainland. The time of emergence of the Con Dao Islands is unknown, but the archipelago is situated on the broad, shallow continental shelf of the South China Sea, strongly influenced by the East

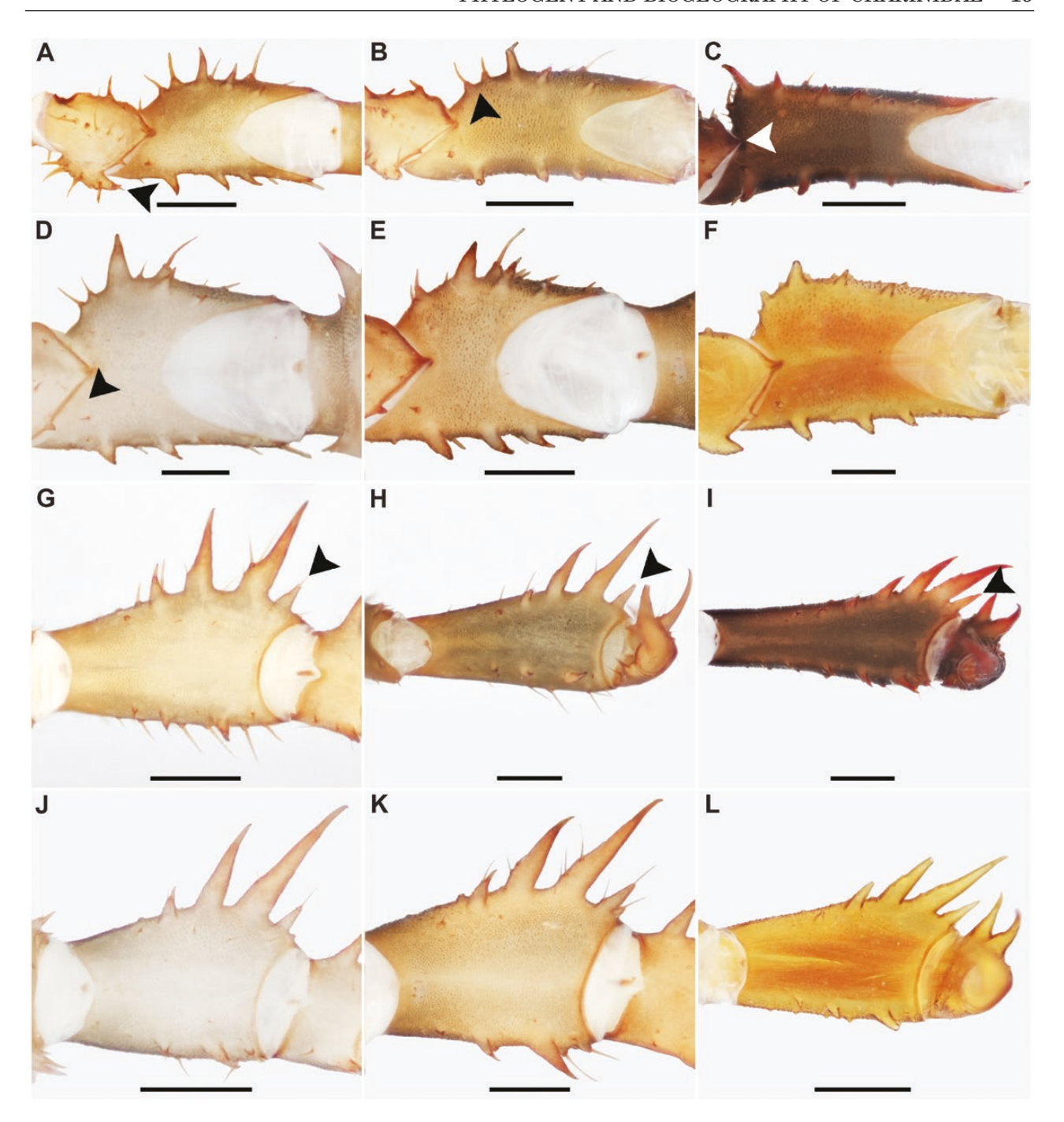


Figure 11. Whip spiders of the family Charinidae Quintero, 1986, pedipalp trochanter, femur and patella, prolateral view illustrating dorsal articulation (hinge) between trochanter and femur (arrow in C; character 56), trochanter with anteriorly directed ventromedian apophysis; arrow-shaped apophysis (arrow in A; character 58), spine or conspicuous setiferous tubercle adjacent to proximal margin or parallel to spine 1 on pedipalp femur (arrow in D; characters 62–64) and projection between spine 1 and distal margin of patella (arrow in G–I; characters 107–112). A, G, *Charinus sillami* Réveillion & Maquart, 2015, ♀ [AMNH (LP 13448)]. B, H, *Charinus palikur* Miranda *et al.*, 2021, ♂ [AMNH (LP 3831)]. C, I, *Charinus gertschi* Goodnight & Goodnight, 1946, ♂ [AMNH (LP 10076)]. D, J, *Sarax bispinosus* (Nair, 1934), ♂ [AMNH (LP 12298)]. E, K, *Sarax cochinensis* (Gravely, 1915), ♀ [AMNH (LP 13118)]. F, L, *Sarax willeyi* Gravely, 1915, ♀ (SMF 64589). Scale bars: 0.5 mm.

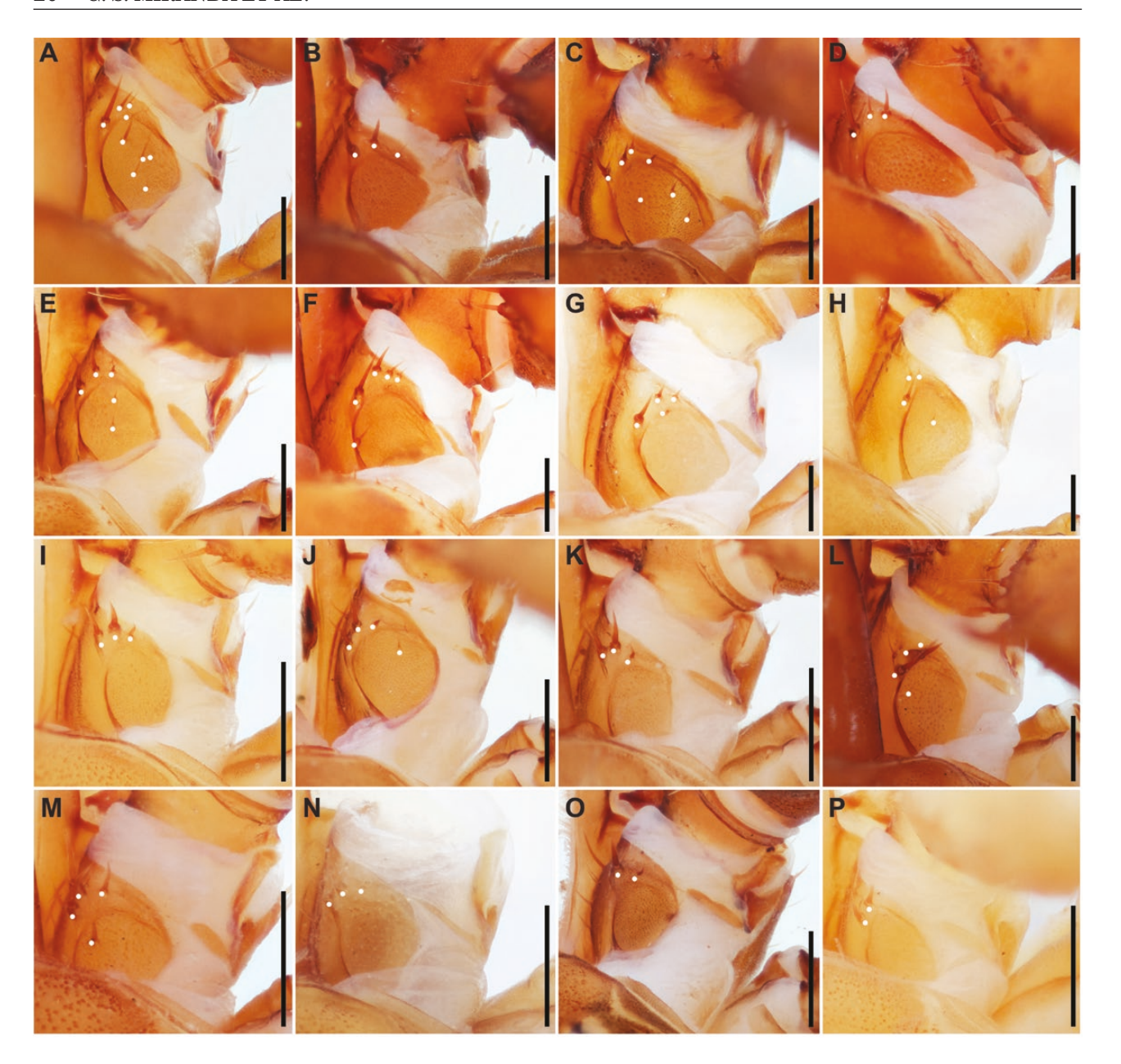


Figure 12. Whip spiders of the family Charinidae Quintero, 1986, pedipalp coxae, dorsal view illustrating semicircular carina (characters 91–97); setae indicated with white dots. A, Charinus ruschii Miranda et al., 2016, ♀ (MNRJ 9237). B, Charinus montanus Weygoldt, 1972, ♂ (MNRJ 9242). C, Charinus australianus (L. Koch, 1867), ♂ (SMF). D, Charinus koepckei Weygoldt, 1972, ♀ (SMF 25762). E, Charinus cavernicolus Weygoldt, 2006, ♀ (MNHN AM 2). F, Charinus elegans Weygoldt, 2006, ♀ (MNHN AM 4). G, Charinus longipes Weygoldt, 2006, ♀ (MNHN AM 5). H, Charinus fagei Weygoldt, 1972, ♀ (MNHN). I, K, Sarax indochinensis Miranda et al., 2021, ♀ (MNHN AM 15). J, Sarax pakistanus Weygoldt, 2005, ♂ (SMF 40168). L, Sarax batuensis (Roewer, 1962), ♂ (SMF 13906). M, Sarax rimosus (Simon, 1901), ♀ (SMF 35614). N, Sarax willeyi (Gravely, 1915), ♀ (SMF 64592). O, Sarax gravelyi Miranda et al., 2021, ♀ (SMF 62287). P, Sarax cochinensis (Gravely, 1915), ♀ (SMF 64592). Scale bars: 0.5 mm.

Asian monsoon, as well as discharges from the Mekong River (Dang *et al.*, 2004), suggesting some, if not all, the biota of the archipelago may have dispersed from the South-East Asian mainland.

Among the species of *Sarax*, the most recent common ancestor of the East Asia clade and the clade comprising *S. ioanniticus* and *S. seychellarum*, separated into two distinct lineages around 177 Mya (95% HPD interval:

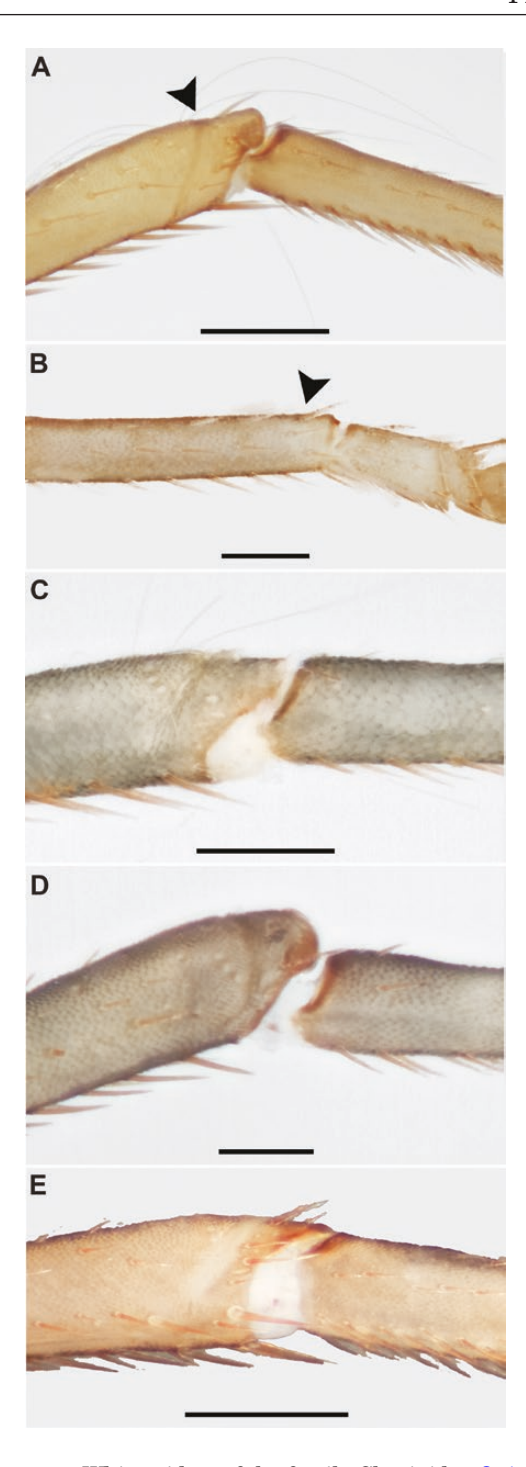


Figure 13. Whip spiders of the family Charinidae Quintero, 1986, leg IV distitibia, lateral view illustrating marked division distal to trichobothria (arrows in A, B; character 131, 137). A, *Charinus insularis* Banks, 1902, ♀ (KBIN). B, *Charinus palikur* Miranda *et al.*, 2021, ♂ [AMNH (LP 3831)]. C, *Sarax bispinosus* (Gravely, 1915), ♂ [AMNH (LP 12298)]. D, *Weygoldtia davidovi* Fage, 1946, ♀ [AMNH (LP 11377)]. Scale bars: A, B, E, 0.5 mm; C, D, 0.3 mm.

143.9-211.4 Mya; Toarcian, Early Jurassic). During the Early Jurassic, Pangaea began to fragment, with the landmass comprising the precursors of South America and Africa (West Gondwana) separating from the landmass comprising the precursors of Antarctica, Australia, India, Madagascar and Seychelles (East Gondwana) (Ali & Aitchison, 2008). The divergence between the East Asia clade and the clade comprising S. ioanniticus and S. seychellarum followed the separation of those supercontinents. Species of the East Asia clade currently occur in South-East Asia and part of Oceania and Melanesia, whereas the clade comprising S. ioanniticus and S. seychellarum, including the species transferred from *Charinus* to Sarax, occur in the eastern Mediterranean, East Africa, the Arabian Peninsula, the Seychelles and Pakistan (Miranda et al., 2021).

The species in the clade comprising *S. ioanniticus* and *S. seychellarum* drifted with Africa and the Arabian Peninsula during the Cretaceous before attaining their current distributions. During Late Miocene (c. 10 Mya), the Afro-Arabian plate reached the Eurasian plate and the *Sarax* species dispersed from the Arabian Peninsula to mainland Asia, eventually attaining their current distribution (Zhang et al., 2014). The presently arid climate of the Middle East and the Arabian Peninsula restricts living species of *Sarax* almost exclusively to caves, e.g. *Sarax dhofarensis* (Weygoldt et al., 2002), *Sarax israelensis* (Miranda et al., 2016), and *Sarax stygochthobius* (Weygoldt & Van Damme, 2004).

The ancestor of the species in the East Asia clade probably reached South-East Asia and Melanesia by rafting from Australia, as no Indonesian islands existed at that time (Hall, 2012), or by rafting on landmasses detached from Gondwana, such as the Western Burma Block (Poinar, 2018). This hypothesis is supported by evidence that the peak of *Sarax* diversification occurred during the Cretaceous, a prolific time for life on Earth (Shear & Kukalova-Peck, 1990).

The timing of divergence between the clades comprising Sarax brachydactylus Simon, 1872 and Sarax bilua Miranda et al., 2021, from the Philippines and the Solomon Islands, respectively, and the clade comprising Sarax cochinensis (Gravely, 1915) and Sarax bispinosus (Nair, 1934), from India and Sri Lanka, respectively, occurred during the Lower Cretaceous, before India reached Asia. The presence of this clade in South Asia can only be explained by dispersal after the Indian continent reached Asia during the Eocene (c. 40 Mya) (Ali & Aitchison, 2008), a pattern demonstrated by some other terrestrial invertebrates (e.g. Köhler & Glaubrecht (2007)). Further evidence of an early Gondwanan origin for Sarax is the presence

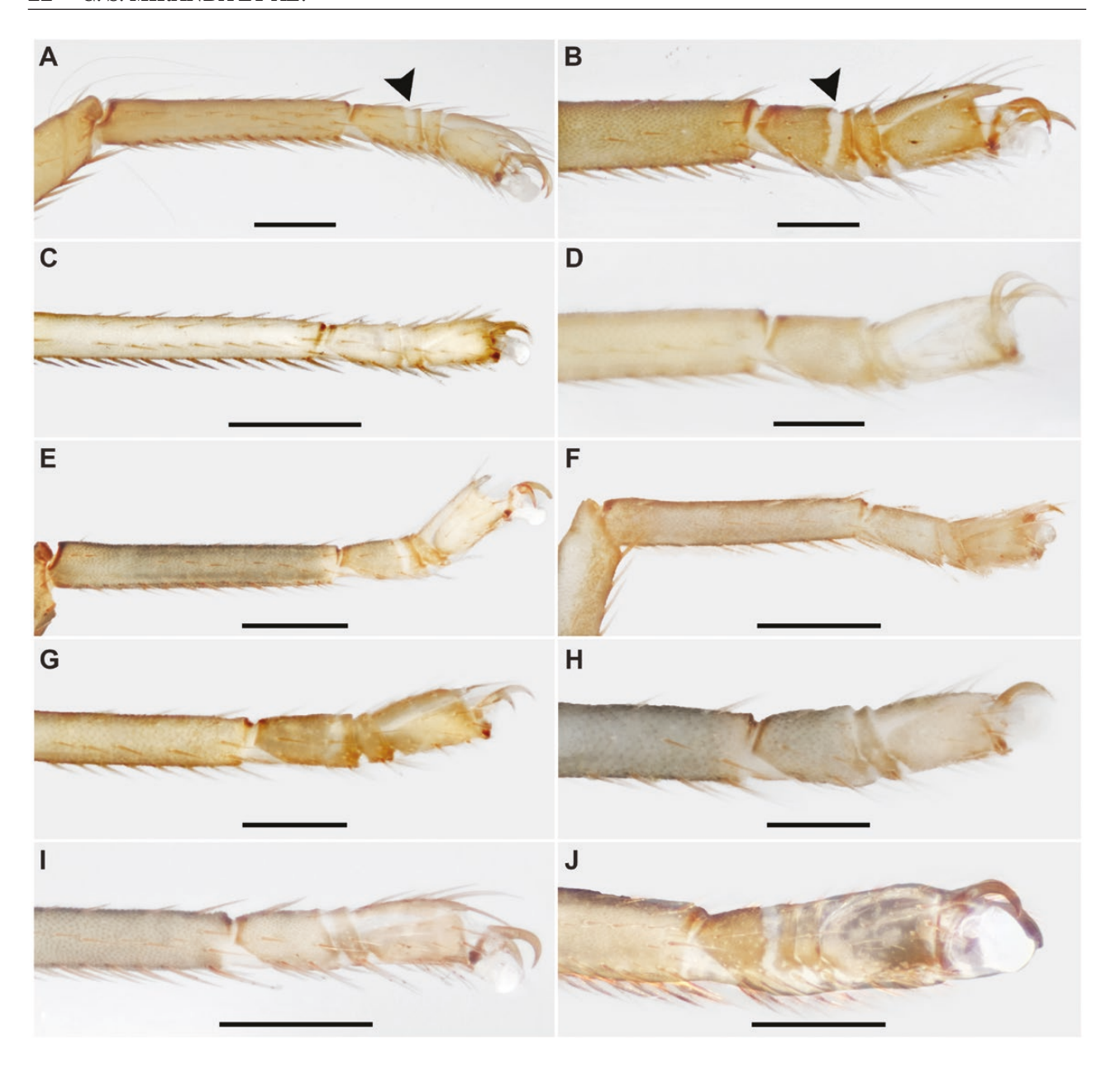


Figure 14. Whip spiders of the family Charinidae Quintero, 1986, leg IV second tarsal segment, lateral view illustrating presence and extent of weakly sclerotized area (arrows in A, B; characters 135, 136). A, Charinus insularis Banks, 1902, ♀ (KBIN). B, Charinus pescotti Dunn, 1949, ♂ [AMNH (LP 6367)]. C, Charinus belizensis Miranda et al., 2016, ♂ (HUJ INV AMB 117). D, Sarax pakistanus (Weygoldt, 2005), ♂ (MHNG). E, Sarax seychellarum (Kraepelin, 1898), ♀ [AMNH (LP 9075)]. F, Charinus palikur Miranda et al., 2021, ♂ (AMNH LP 3831). G, Charinus sillami Réveillion & Maquart, 2015, ♀ [AMNH (LP 13448)]. H. Sarax bispinosus (Nair, 1934), ♂ [AMNH (LP 12298)]. I, Sarax cochinensis Gravely, 1915, ♀ [AMNH (LP 13118)]. J, Weygoldtia davidovi (Fage, 1946), ♂ [AMNH (LP 11377)]. Scale bars: A, B, C, E, F, I, J, 0.5mm; D, 0.25 mm; G, 0.4 mm; H, 0.3 mm.

of the genus on the Sahul Shelf, the continental shelf uniting the Australian continent and New Guinea, which is of Gondwanan origin (Atkins *et al.*, 2001). The early divergence between *Sarax willeyi* Gravely, 1915, from New Guinea, and all other species of the East Asia clade, adds additional evidence for the hypothesis

that species of Sarax dispersed northwards from Gondwanaland.

How *Sarax* came to occupy the islands of the Indo-Pacific is difficult to answer with the current dataset due to a shortage of records from those islands and samples for molecular divergence dating. The

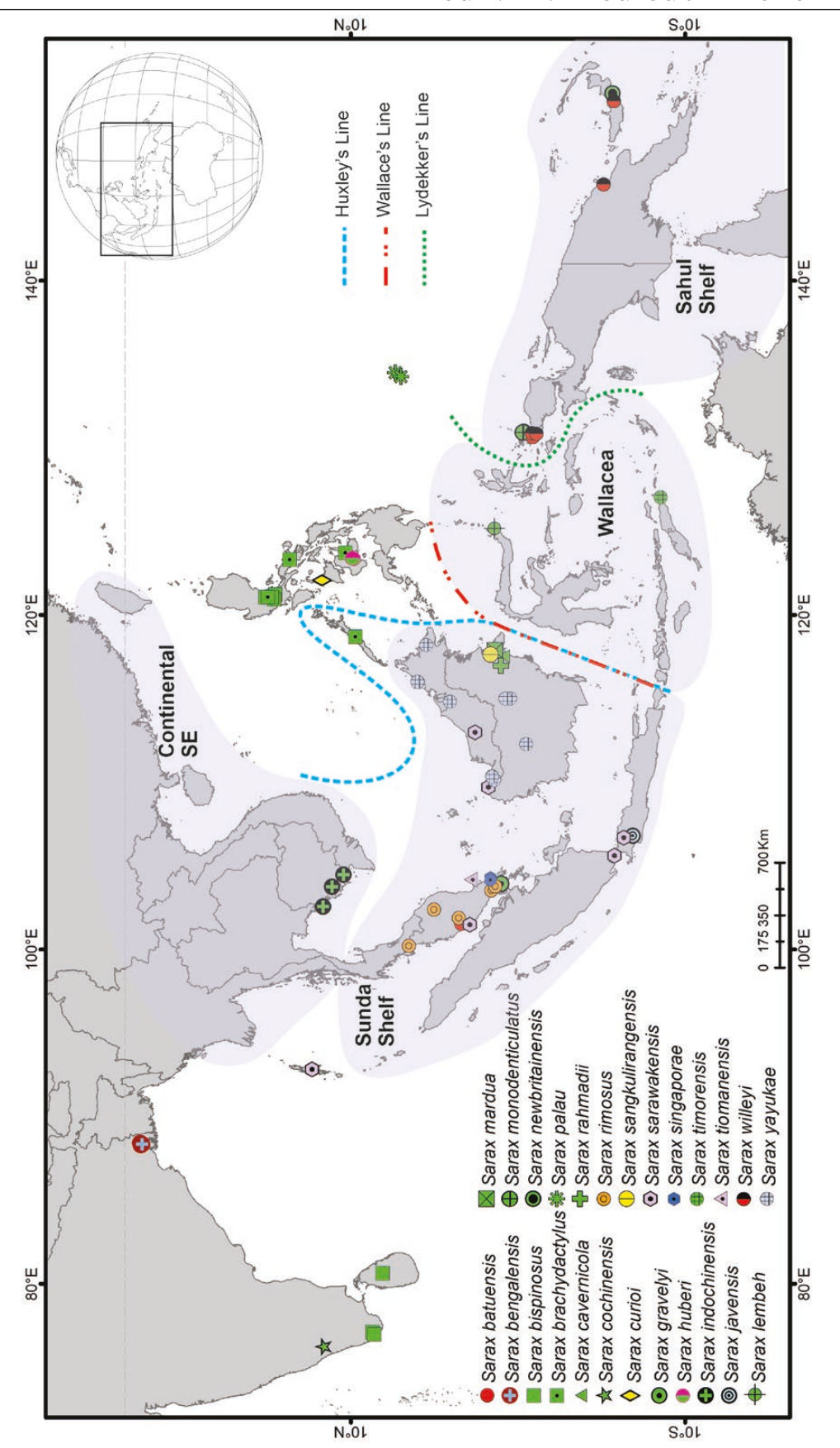


Figure 15. Contemporary islands and biogeographical divisions of the Indo-Pacific Archipelago, modified from Lohman et al. (2011), illustrating distributions of Sarax Simon, 1872 whip spiders in the region. Map includes all species known from the region, including those excluded from the study due to absence of samples for analysis, such as S. cavernicola Rahmadi et al., 2010, S. curioi Giupponi & Miranda, 2012, S. mardua Rahmadi et al., 2010, S. monodenticulatus Rahmadi & Kojima, 2010, S. newbritainensis Rahmadi & Kojima, 2010, S. sangkulirangensis Rahmadi et al., 2010, S timorensis Miranda & Reboleira, 2019.

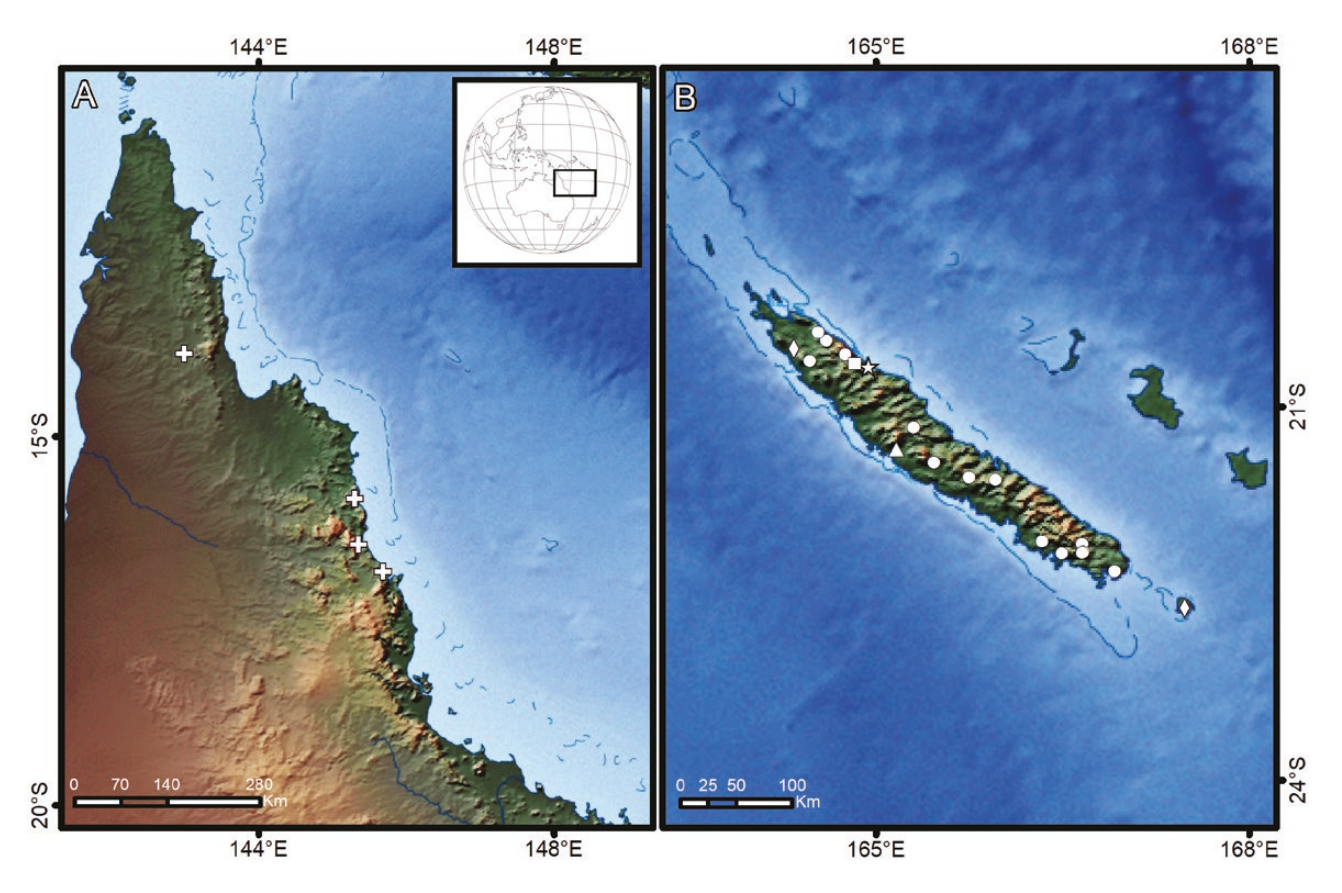


Figure 16. Distributions of the Australian (A) and New Caledonian (B) species of Charinus Simon, 1892 whip spiders: Charinus cavernicolus Weygoldt, 2006 (diamond); Charinus elegans L. Koch, 1867 (triangle); Charinus longipes Weygoldt, 2006 (star); Charinus neocaledonicus Simon in Kraepelin, 1895 (circles); Charinus pecki Weygoldt, 2006 (square); Charinus pescotti Dunn, 1949 (cross).

Indonesian Archipelago, for example, comprises more than 20 000 islands and is among the most geographically complex tropical regions on Earth (Lohman et al., 2011; Tänzler et al., 2014). The archipelago has undergone many geological changes over the past million years (Lohman et al., 2011) and the changes that resulted in its present configuration occurred over the last 60 Mya, a time frame younger than most branches on the Sarax tree. However, one interpretation is offered for the current distribution of the species in the next section.

DISTRIBUTION AND BIOGEOGRAPHY OF ASIAN **CHARINIDAE**

The study of faunal changes in South-East Asia dates to the earliest zoogeographical investigations by Müller (1846), Sclater (1858) and Wallace (1860, 1869). Several zoogeographical 'lines' have been proposed to demarcate the limits between faunas with Laurasian and Gondwanan origins in South-East Asia (Simpson, 1977; Atkins et al., 2001), but the most widely accepted are Wallace's Line, Huxley's Line and Lydekker's Line (Fig. 13) (Lohman et al., 2011). Wallace's Line (Huxley, 1868) separates Asia and a transitional zone between Asia and Australia (Wallace, 1860). Species occurring to the west of the line are usually more closely related to Asiatic species, whereas species to the east are a mix of Asian and Australasian species (Tänzler et al., 2014).

In accordance with Wallace's Line, two clades of Sarax occur on the Sunda shelf: the brachydactylus clade, comprising species on the Malay Peninsula, which is sister to S. indochinensis from Continental South-East Asia; and the *singaporae* clade, comprising species mostly present on the Sunda shelf and sister to a clade comprising species found in Wallacea (Fig. 15). Another pattern is illustrated by the *Sarax* species from Bali, which is most closely related to the species from Borneo and Malaysia, again in accordance with Wallace's Line. On the other hand, the two species occurring west of Wallace's Line, S. bilua and S. brachydactylus, are more closely related to the South Asian taxa, S. bispinosus and S. cochinensis. Also ignoring biogeographical lines, S. brachydactylus

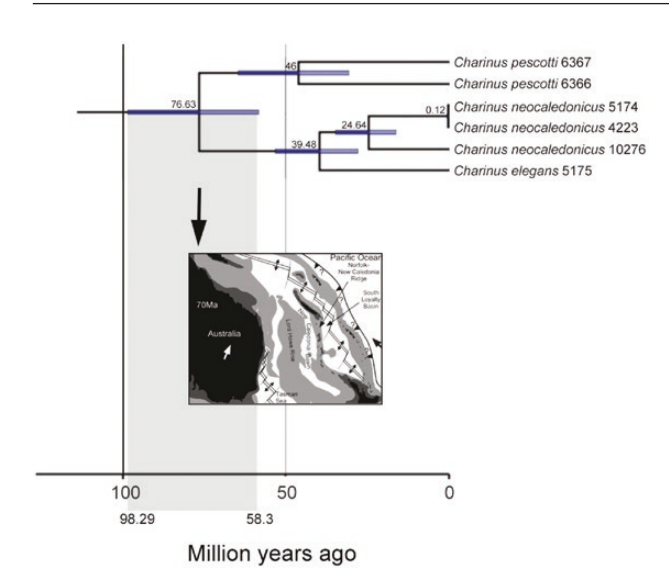


Figure 17. Phylogeny of the whip spider genus *Charinus* Simon, 1892: excerpt of tree obtained by analysis with BEAST, showing divergence between clades of Australian *Charinus pescotti* Dunn, 1949 and Neocaledonian *Charinus neocaledonicus* Kraepelin, 1895 and *Charinus elegans* Weygoldt, 2006. Paleomap of part of Oceania at 70 Mya, modified from Crawford *et al.* (2003).

occurs on either side of Huxley's Line, on Palawan as well as on the main islands of the Philippines.

Sarax sarawakensis (Thorell, 1888) was the first species to be described in the genus (Thorell, 1888) and, for many years, all Sarax species from South-East Asia were assigned to it (Fage, 1929; Weygoldt, 1994). As currently defined, S. sarawakensis is restricted to the Sunda Shelf, extending from the Andaman Islands to Java. Its wide distribution may be explained by dispersal, as it is an epigaean species (Rahmadi et al., 2010), but might also be an artefact of the poor understanding of its taxonomy. For example, records of S. sarawakensis from the Andaman Islands, Peninsular Malaysia and Java (Rahmadi et al., 2010), may prove to be different species upon closer examination.

Despite occurring in New Guinea, species of *Charinus* have not been recorded from the Indonesian Archipelago (Fig 2). *Charinus* has only been recorded on the Sahul Shelf and there are no records west of Wallace's Line. This does not appear to be a sampling artefact, as the amblypygid fauna of South-East Asia is fairly well known. The absence of *Charinus* from the Indonesian Archipelago suggests they never got there.

Diversification events linked to divergence dates among the basal clades of *Charinus* are difficult to estimate due to the limited data available for the genus in the present study (c. 13% of the described species diversity). Therefore, the remaining discussion

focuses on the *Charinus* of New Caledonia, a clade with comprehensive taxonomic and geographical sampling.

NEW CALEDONIAN CHARINUS AS GONDWANAN RELICTS

New Caledonia is a tropical island in the south-western Pacific with a remarkably diverse and largely endemic fauna and flora (Grandcolas et al., 2008). Despite being connected to the western part of Australia until 80 Mya as part of an old Gondwana tectonic plate, much of the biota of the island is thought to be the product of recent diversification after colonization during the Pliocene–Pleistocene (Murienne et al., 2005). Stratigraphical and fossil evidence strongly support the hypothesis that New Caledonia was completely submerged during the Palaeocene–Eocene, suggesting the biota on this island is the result of recolonization after the island re-emerged during the Oligocene, consistent with studies of molecular dating (Grandcolas et al., 2008).

However, exceptions to this hypothesis exist (Giribet & Baker, 2019). For example, Mathews & Donoghue (1999) placed Amborella trichopoda Baill. (Amborellaceae), an angiosperm endemic to New Caledonia, as the sister-group of all flowering plants, a position supported to this day (Drew et al., 2014; APG, 2016). The near-flightless kagu bird, Rhynochetos jubatus Verreaux & DesMurs, 1860, is also endemic to New Caledonia, with its closest relatives occurring in New Zealand and South America (Cracraft, 2001). Boyer et al. (2007) discovered a lineage of endemic harvestmen, Troglosironidae Shear, 1993, in New Caledonia with sister-lineages in South America and West Africa. The most parsimonious explanation for the presence of these endemic taxa in New Caledonia would appear to be as Gondwanan relicts (Giribet & Baker, 2019). However, Grandcolas et al. (2008) argue that the absence of sister-taxa on nearby landmasses, such as Australia or New Zealand, requires the assumption of many extinction events, while not providing much biogeographical and temporal information.

Whip spiders of the genus *Charinus* provide a unique model system for understanding the biogeographical history of New Caledonia. Five species are endemic to the island: *Charinus neocaledonicus* Simon in Kraepelin, 1895 is widespread and can be considered a regional endemic, whereas the other four, *Charinus cavernicolus* Weygoldt, 2006, *Charinus elegans* L. Koch, 1867, *Charinus longipes* Weygoldt, 2006 and *Charinus pecki* Weygoldt, 2006, are local endemics restricted to caves (Fig. 16) (Weygoldt, 2006).

In the phylogeny presented here, *Charinus pescotti* Dunn, 1949, from Queensland, Australia, groups with *Charinus papuanus* Weygoldt, 2006, from Papua New Guinea. This clade is in turn placed sister to



Figure 18. Whip spiders of the family Charinidae Quintero, 1986, sternum, ventral view (characters 15, 16) A. *Sarax tiomanensis* Miranda *et al.*, 2021, ♂ (AMCC [LP 12001]), B. *Charinus acosta* (Quintero, 1983), ♀ (USNM 784407), C. *Charinus montanus* Weygoldt, 1972, ♀ (MNRJ 9087). Scale bars: 1 mm.

C. cavernicolus and *C. pecki*, both from New Caledonia. All four species are placed sister to another clade, comprising *C. elegans* and *C. neocaledonicus*.

Only three species of this clade, C. elegans, C. neocaledonicus and C. pescotti, are included in the molecular dating analysis (Fig. 17). The suggested divergence date between the Australian and New Caledonian clades is c. 76 Mya, slightly more recent than the separation of the two landmasses (Fig. 17). The recent divergence date could be attributed to the conservative approach used in the analysis for the oldest calibration point for Amblypygi, which shares several similarities with extant taxa, implying that the Amblypygi stem lineage is probably older. The time interval estimated by the BEAST analysis is between 98.3 and 58.3 Mya (Fig. 17), hence the only possible explanation for the presence of *Charinus* in New Caledonia is that these taxa are Gondwanan relicts. The divergence date for two of the species endemic to New Caledonia, i.e. C. elegans and C. neocaledonicus, is estimated at c. 37 Mya (95% HPD interval: 27.9-53.0 Mya), during the Oligocene, the period in which New Caledonia re-emerged (Cluzel et al., 2001, 2012).

The absence of *Charinus* or any other Amblypygi from New Zealand might be attributed to extinction, after the temperate climate of that island became unsuitable for continued survival. The only charinid known to occur south of the Tropic of Capricorn is *Charinus asturius* Pinto-da-Rocha *et al.*, 2002, occurring at 23°44'S 45°19'W, in the Brazilian Atlantic rainforest, a region with a stable, tropical climate, different from New Zealand. Another possibility is that *Charinus* species never occurred in New Zealand, which has a unique terrestrial invertebrate fauna composed of relictual temperate taxa (Giribet & Boyer, 2010).

Charinus australianus, another Melanesian species, was not included in the dated analysis but was placed sister to *C. insularis* from the Galapagos Islands. Most of the taxa occurring on the Galapagos Islands, a young oceanic and volcanic archipelago, are closely related to the taxa of Central and South America (Parent et al., 2008). This unexpected relationship could be an artefact of the lack of knowledge about whip spiders in that part of South America or additional evidence for an eastward trans-Pacific dispersal event involving a terrestrial invertebrate, as observed in the landsnail genus Tornatellides Pilsbry, 1910 and the spider genus Desis Walckenaer, 1837 (Carlquist, 1965; Grehan, 2001). Such a dispersal event might have happened if an ancestral population of Charinus was carried from Melanesia to the Pacific Coast of South America by the eastward flowing Pacific Equatorial Countercurrent, but such events are rare (Dennis & Gunn, 1971).

WHY ARE THERE SO FEW SPECIES OF AMBLYPYGI?

Despite the recent increase in described species, Amblypygi remains a low-diversity arachnid order (Harvey, 2003). The small number of living and fossil species suggests Amblypygi was never diverse. The close resemblance between the oldest fossil taxon, Weygoldtina anglica, and the living Paracharon caecus Hansen, 1921, implies a conservative groundplan (Weygoldt, 1999c). Unlike their close relatives, the spiders, for which the evolution of silk facilitated diversification into new habitats and adaptation to a broader range of prey (Fernández et al., 2018), few novelties appeared in the evolution of whip spiders. Whip spiders appear to have always occupied the same niche as ambush predators on rock surfaces and tree trunks, among the leaf litter or

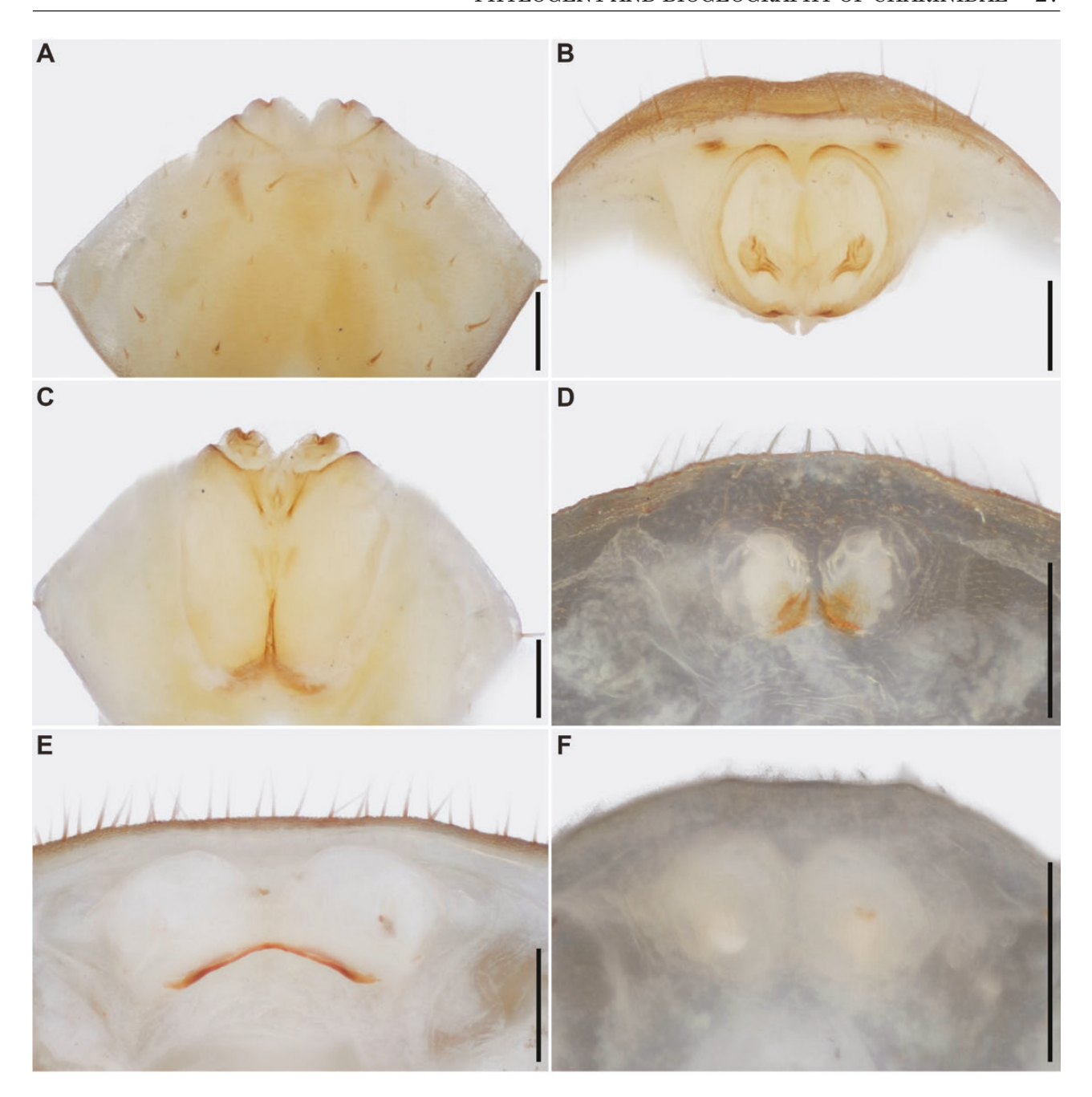


Figure 19. Whip spiders of the family Charinidae Quintero, 1986, male and female gonopods, ventral view (characters 36–46). A–C, *Sarax pakistanus* (Weygoldt, 2005), & (MHNG). D, *Charinus brasilianus* Weygoldt, 1972, \$\rightarrow\$ (MNRJ 9232). E, *Charinus gertschi* Goodnight & Goodnight, 1946, \$\rightarrow\$ (AMNH [LP 10076]). F, *Charinus acosta* (Quintero, 1983), \$\rightarrow\$ (USNM ENT 784407). Scale bars: 0.25 mm.

inside caves, not exploring three-dimensional habitats in the vegetation, like web-building spiders, for example. Even extant whip spiders inhabiting vastly different habitats, such as the Amazon rainforest (*Charinus*) and the Namib Desert (*Xerophrynus* Weygoldt, 1996), share most characters besides differences in their physiological tolerance for temperature and humidity.

Stabilizing selection, when slightly deleterious, and advantageous mutations (i.e. neutral variations) reach fixation at a similar rate by the process of genetic drift (Kimura, 1981), has been suggested to explain the low diversity of Amblypygi (Weygoldt, 2000). Amblypygi appear to have developed the required physiological and morphological adaptations early in

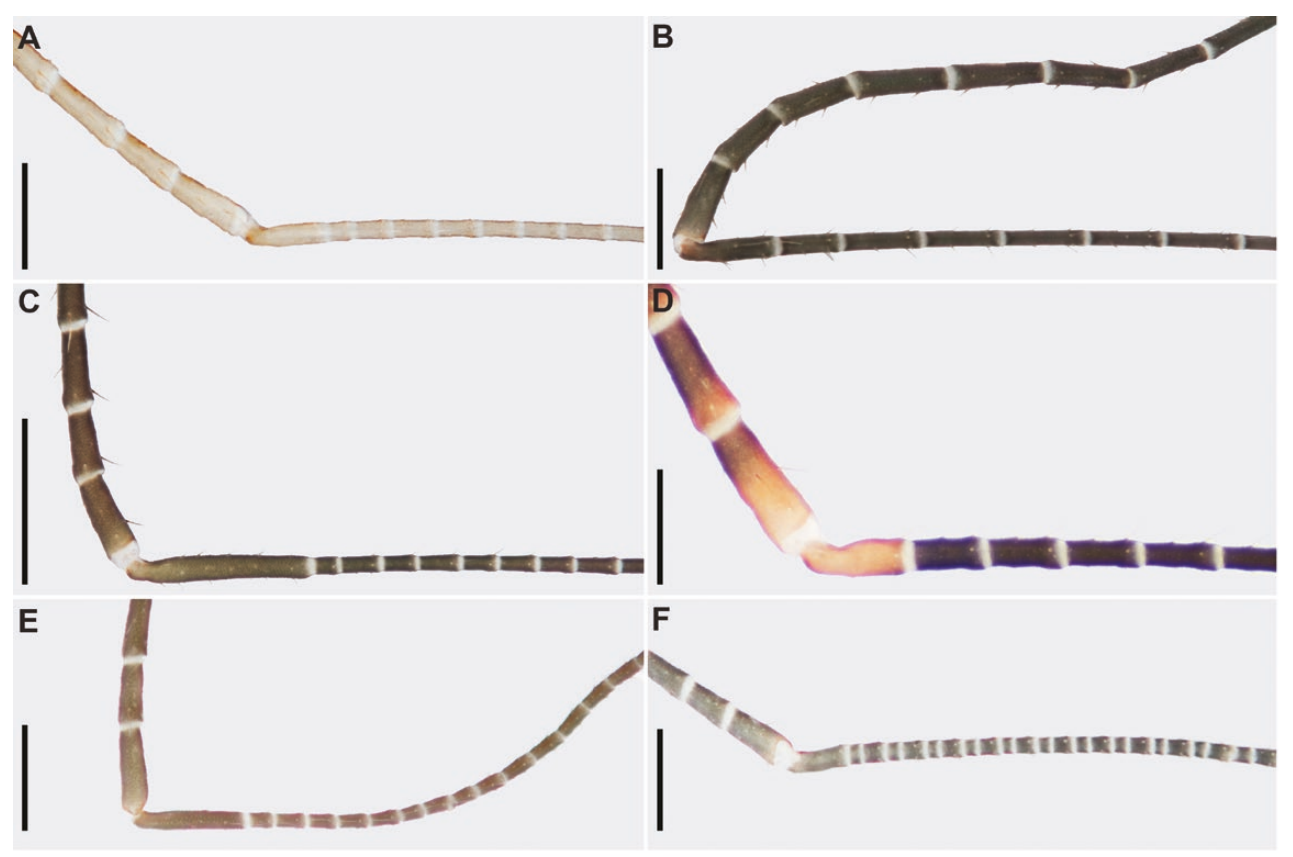


Figure 20. Whip spiders of the family Charinidae Quintero, 1986, tarsus I, lateral view illustrating size of first (proximal) article (character 53); note regenerated leg in (F), where total number of articles is augmented compared to 'normal' leg. A, Charinus belizensis Miranda et al., 2016, & (HUJ INVAMB 117). B, Sarax seychellarum (Kraepelin, 1898), Q [AMNH (LP 9075)]. C, Charinus pescotti Dunn, 194[AMNH (LP 10076)]. E, Charinus palikur Miranda et al., 2021, & [AMNH (LP 3831)]. F, Sarax bispinosus (Nair, 1934), & [AMNH (LP 12298)]. Scale bars: 0.5 mm.

their evolution and, despite past changes in global climate, managed to surpass major extinction events by finding stable habitats in refugia such as forest remnants and caves, thereby avoiding the selection pressures that would have induced evolutionary novelty.

The relatively long generation times of whip spiders may perhaps also explain why most families of Amblypygi are not diverse. Among Charontidae, Phrynichidae and Phrynidae, embryonic development takes about three months and time to sexually maturity about one to two years (Weygoldt, 2000). The family Charinidae includes smaller species with faster generation times and some parthenogenetic species produce eggs even as small juveniles (Armas, 2000; Weygoldt, 2007; Seiter & Wolff, 2014). Perhaps because of their faster generation times, Charinidae is the most speciose family in the order.

CONCLUSIONS

The phylogenetic analysis of Charinidae presented here provides the first estimate of relationships among the genera and species of the family, divergence dates for its major clades, and a framework for its classification, on the basis of which nine species possessing a finger-like female gonopod, formerly assigned to *Charinus*, are transferred to *Sarax* (Miranda *et al.*, 2021). Multilocus DNA sequence data and morphology greatly assisted the phylogenetic reconstruction. The efficacy of the molecular data suggests that the collection of more tissue samples, both for Sanger-dideoxy DNA sequencing and phylogenomics, should be prioritized in future.

Most currently known species of Amblypygi were described based on characters of the somatic and genitalic morphology. As in many other taxa, research based on DNA sequence data has revealed cryptic

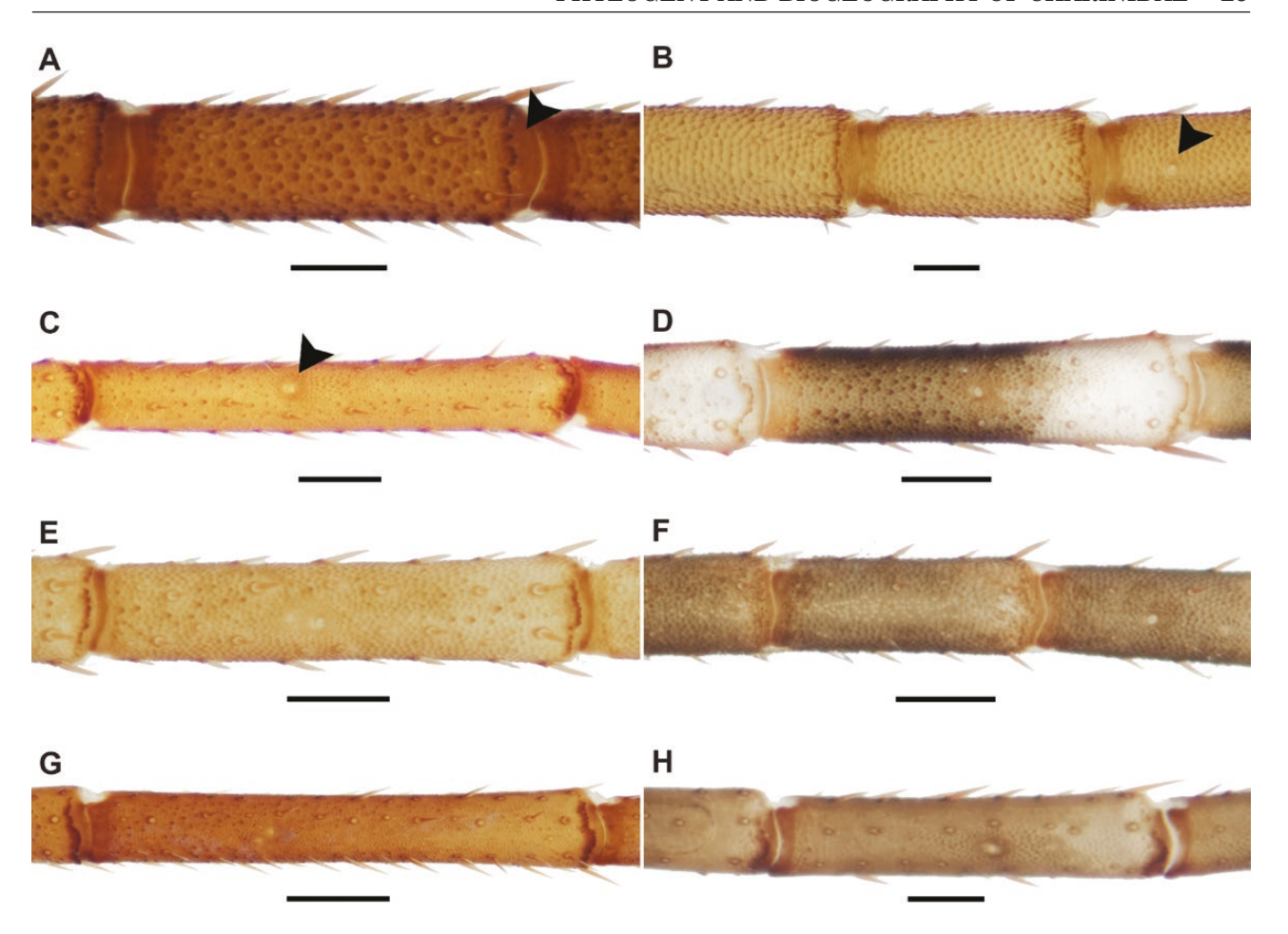


Figure 21. Whip spiders of the family Charinidae Quintero, 1986, leg IV basitibia, dorsal view illustrating strongly sclerotized denticulate border, projecting (or not) from distal apex (arrow in A; characters 121–124), and position of trichobothria bt on distal article (arrows in B, C; character 120). A, Charinus insularis Banks, 1902, \(\rho\$ (KBIN). B, Sarax pakistanus (Weygoldt, 2005), \(\rho\$ (MHNG). C, Charinus carioca Miranda et al., 2021, \(\rho\$ (MNRJ 9201). D, Charinus gertschi Goodnight, 1946, \(\rho\$ [AMNH (LP 10076)]. E, Charinus souzai Miranda et al., 2021, \(\rho\$ (MNRJ 9090). F, Charinus pescotti Dunn, 1949, \(\rho\$ [AMNH (LP 6367)]. G, Charinus goitaca Miranda et al., 2021, \(\rho\$ (MNRJ 9224). H, Sarax yayukae Rahmadi et al., 2010, \(\rho\$ [AMNH (LP 12109)]. Scale bars: A, D, E, F, H, 0.25 mm; B, 0.3 mm; C, G, 0.5 mm.

diversity (Prendini et al., 2005; Esposito et al., 2015). Whip spider species, with broad distributions and variation in pedipalp spine number and female genitalia shape, such as Charon grayi (Gervais, 1842) (Charontidae), Damon variegatus C. L. Koch, 1850, Phrynichus orientalis Weygoldt, 1998 (Phrynichidae), Heterophrynus longicornis (Butler, 1873) (Phrynidae) and Sarax yayukae (Charinidae), may comprise more species than presently recognized (Prendini et al., 2005; Rahmadi et al., 2010; Miranda et al., 2018b; Miranda & Zamani, 2018). Continued research into the molecular systematics of Amblypygi will likely provide a more accurate assessment of the ordinal diversity.

Nevertheless, there remains room for the development of morphological characters that, in combination with molecular data, may help to resolve clades while providing diagnostic characters at higher and lower levels in the taxonomic hierarchy. The morphological characters revised and newly generated in the present study, together with new microstructural data from the integument (Wolff *et al.*, 2015b, 2016, 2017), provide phylogenetically informative data that should be further explored. Scanning electron microscopy has scarcely been applied in studies of Amblypygi morphology, hence a substantial amount of new phylogenetic data can be expected from this technique.

ACKNOWLEDGEMENTS

GSM acknowledges the Coordenação de Aperfeiçoamento de Pessoal de Nível Superior (CAPES, http://www.capes. gov.br/) for a Science Without Borders Ph.D. grant

(process number 8922-13-6). GSM is currently funded by a GGI Peter Buck Postdoctoral Fellowship (Smithsonian Institution). This research was also supported by the SYNTHESYS Project (http://www.synthesys.info). which is financed by European Community Research Infrastructure Action under the FP7 'Capacities' Program (DE-TAF-6158 and FR-TAF-5129). NS and GSM acknowledge the Danish National Research Foundation for support to the Center for Macroecology, Evolution and Climate (grant DNRF96). Field collections involving AMNH staff and students, and DNA sequencing conducted at the AMNH, were supported by the following awards to LP: U.S. National Science Foundation grants DEB 0413453, DEB 0640219, DEB 1655050, DEC 0910091, DEC 0910147, DEC 1310855 and EAR 0228699, a grant from the Richard Lounsbery Foundation and three Constantine S. Niarchos Expedition grants from the Stavros Niarchos Foundation. We acknowledge the following friends and colleagues for assistance with fieldwork and/or donations of material used in the study: A. Ang, S. Basi, E. F. Bezerra Lima, L. A. Esposito, O. Francke, E. Gavish-Regev, A. Gluesenkamp, E. González, P. Horsley, S. Huber, J. H. Huff, K. B. Kunt, A. Kury, J. Lazell, S. F. Loria, H. T. Luu, W. Maddison, C. Magalhães, Y. M. Marusik, L. Monod, J. Murienne, J. A. Ochoa, F. Réveillon, C. Savvas, S. Schoenbrun, P. Schwendinger, M. Seiter, L. Sousa de Carvalho, P. Sprouse, P. & S. Weygoldt, R. Wickramarachchi, G. Wizen, H. Yamaguti; the following curators and collections managers for loaning material from the collections in their care and/or assistance during our visits: I. Agnarsson (UVM), L. Baert (KBIN), J. Beccaloni (BMNH), E. F. Bezerra Lima (CNHUFPI), A. Brescovit (IBSP), J. Dunlop (ZMB), E. Gavish-Regev (HUJ), G. Giribet (MCZ), M. Glaubrecht (ZMH), M. Harvey (WAM), J. Holstein (SMNS), C. Hörweg (NHMW), P. Jäger (SMF), M. Judson (MNHN), A. Kury (MNRJ), M. Lowe (CUMZ), C. Magalhães (INPA), R. Pintoda-Rocha (MZSP), R. Raven (QM), P. Schwendinger (MHNG), P. Sierwald (FMNH), P. Sirvid (NMNZ), C. Whitehill (FSCA), S. Whitman (MZUF), H. Wood (USNM); P. A. Colmenares, O. Delgado, P. Horsley, J. H. Huff, M. M. Locke and L. Sorkin for logistical support with collections at AMNH; D. Casellato (funded by the Brazil Scientific Mobility Program of the Institute for International Education), D. Pietri, P. Rubi and T. Sharma for assisting with lab work at the AMNH and/or generating DNA sequence data used in the study: L. Sousa de Carvalho and R. L. Ferreira for providing live habitus photos.

REFERENCES

Ali JR, Aitchison JC. 2008. Gondwana to Asia: plate tectonics, paleogeography and the biological connectivity of the Indian

- sub-continent from the Middle Jurassic through latest Eocene (166–35 Ma). Earth Science Reviews 88: 145–166.
- APG. 2016. An update of the Angiosperm Phylogeny Group classification for the orders and families of flowering plants: APG IV. Botanical Journal of the Linnean Society 181: 1–20.
- **Armas LF de. 2000.** Parthenogenesis in Amblypygi (Arachnida). *Avicennia* **12/13:** 133-134.
- Armas LF de, Palomino-Cárdenas AC, de Castillo-Espinoza M. 2016. Amblipigios de los Departamentos Cusco y Madre de Dios, Perú, con la descripción de un nuevo Charinus (Amblypygi: Charinidae, Phrynidae). Revista Iberica de Aracnologia 28: 45–50.
- Atkins H, Preston J, Cronk QCB. 2001. A molecular test of Huxley's Line: Cyrtandra (Gesneriaceae) in Borneo and the Philippines. Biological Journal of the Linnean Society 72: 143–159.
- Auguie B. 2019. Egg: extensions for 'ggplot2': custom geom, custom themes, plot alignment, labelled panels, symmetric scales, and fixed panel size. R package v.0.4.5. Available at: https://rdrr.io/cran/egg/.
- Benton MJ. 2003. When life nearly died: the greatest mass extinction of all time. London: Thames & Hudson.
- Benton MJ, Twitchett RJ. 2002. How to kill (almost) all life: the end-Permian extinction event. *Trends in Ecology and Evolution* 18: 358–365.
- Boyer SL, Clouse RM, Benavides LR, Sharma P, Schwendinger PJ, Karunarathna I, Giribet G. 2007. Biogeography of the world: a case study from cyphophthalmid Opiliones, a globally distributed group of arachnids. *Journal of Biogeography* 34: 2070–2085.
- Carlquist S. 1965. Island life. Garden City: The Natural History Press.
- Clapham ME, Shen S, Bottjer DJ. 2009. The double mass extinction revisited: reassessing the severity, selectivity, and causes of the end-Guadalupian biotic crisis (Late Permian). *Paleobiology* **35:** 32–50.
- Cluzel D, Aitchison JC, Picard C. 2001. Tectonic accretion and underplating of mafic terranes in the Late Eocene intraoceanic fore-arc of New Caledonia (southwest Pacific): geodynamic implications. *Tectonophysics* 340: 23–59.
- Cluzel D, Maurizot P, Collot J, Sevin B. 2012. An outline of the geology of New Caledonia; from Permian–Mesozoic South-East Gondwanaland active margin to Cenozoic obduction and supergene evolution. *Episodes* 35: 72–86.
- Cohen KN, Finney SC, Gibbard PL, Fan J-X. 2013 updated. The ICS International Chronostratigraphic Chart. *Episodes* 36: 199–204.
- Cracraft J. 2001. Avian evolution, Gondwana biogeography and the Cretaceous-Tertiary mass extinction event. Proceedings of the Royal Society of London, Ser. B: Biological Sciences 268: 459–469.
- Dang PX, Mitsuguchi T, Kitagawa H, Shibata Y, Kobayashi T. 2004. Marine reservoir correction in the south of Vietnam estimated from an annually-banded coral. Radiocarbon 46: 657-660.
- **Delle Cave L. 1986.** Biospeleology of the Somaliland Amblypygi (Arachnida, Chelicerata) of the caves of the Showli Berdi and Mugdile (Bardera, Somaliland). *Redia* **69:** 143–170.

- **Dennis JV**, **Gunn CR. 1971.** Case against trans-Pacific dispersal of the coconut by ocean currents. *Economic Botany* **25:** 407–413.
- DiMichele WA, Montanez IP, Poulsen CJ, Tabor N. 2009. Climate and vegetational regime shifts in the Late Paleozoic Ice Age Earth. *Geobiology* 7: 200–226.
- DiMichele WA, Cecil B, Montanez IP, Falcon-Lang HJ. 2010. Cyclic changes in Pennsylvanian paleoclimate and its effects on floristic dynamics in tropical Pangaea. *International Journal of Coal Geology* 83: 329–344.
- Dimitrov D, Benavides LR, Arnedo MA, Giribet G, Griswold CE, Scharff N, Hormiga G. 2016. Rounding up the usual suspects: a standard target-gene approach for resolving the interfamilial phylogenetic relationships of ecribellate orb-weaving spiders with a new family-rank classification (Araneae, Araneoidea). Cladistics 33: 221–250.
- Drew BT, Ruhfel BR, Smith SA, Moore MJ, Briggs BG, Gitzendanner MA, Soltis PS, Soltis DE. 2014. Another look at the root of the angiosperms reveals a familiar tale. Systematic Biology 63: 368–382.
- Drummond AJ, Suchard MA, Xie D, Rambaut A. 2012.
 Bayesian phylogenetics with BEAUti and the BEAST 1.7.
 Molecular Biology and Evolution 29: 1969–1973.
- **Dunlop JA. 2018.** Systematics of the Coal Measures whip spiders (Arachnida: Amblypygi). Zoologischer Anzeiger 273: 14–22.
- Dunlop JA, Zhou GRS, Braddy SJ. 2007. The affinities of the Carboniferous whip spider Graeophonus anglicus Pocock, 1911 (Arachnida: Amblypygi). Transactions of the Royal Society of Edinburgh, Earth and Environmental Science 98: 165–178.
- Esposito LA, Bloom T, Caicedo-Quiroga L, Alicea-Serrano AM, Sánchez-Ruíz JA, May-Collado LJ, Binford GJ, Agnarsson I. 2015. Islands within islands: Diversification of tailless whip spiders (Amblypygi, *Phrynus*) in Caribbean caves. *Molecular Phylogenetics and Evolution* 93: 107–117.
- Fage L. 1929. Fauna of the Batu Caves, Selangor. X. Arachnida: Pedipalpi (part) & Araneae. Journal of the Federated Malay States Museums 14: 356–364.
- Fage L. 1939. Les pédipalpes africains du genre Charinus à propos d'une espèce nouvelle du Fouta-Djalon: Charinus milloti, n. sp. Bulletin de la Société Entomologique de France 44: 153–160.
- Fage L. 1954. Remarques sur la distribution géographique des pédipalpes amblypyges africains, accompagnées de la description d'une espèce nouvelle de Madagascar: Charinus madagascariensis, nov. sp. Annales du Musée du Congo Belge, Sciences Zoologiques 1: 180–184.
- Falcon-Lang HJ, Benton MJ, Braddy SJ, Davies SJ. 2006. The Pennsylvanian tropical biome reconstructed from the Joggins Formation of Canada. *Geological Society of London* 163: 561–576.
- Farris JS. 1989. Hennig86: a PC-DOS program for phylogenetic analysis. Cladistics 5: 163.
- Fernández R, Kallal RJ, Dimitrov D, Ballesteros JA, Arnedo MA, Giribet G, Hormiga G. 2018. Phylogenomics,

- diversification dynamics, and comparative transcriptomics across the spider Tree of Life. Current Biology 28: 1489–1497.
- Fitch WM. 1971. Toward defining the course of evolution—minimum change for a specific tree topology. Systematic Zoology 20: 406–416.
- Garwood RJ, Dunlop JA, Knecht BJ, Hegna TA. 2017. The phylogeny of fossil whip spiders. BMC Evolutionary Biology 17: 105.
- Giribet G, Baker C. 2019. Further discussion on the Eocene drowning of New Caledonia: discordances from the point of view of zoology. *Journal of Biogeography* 46: 1912–1918.
- Giribet G, Boyer SL. 2010. 'Moa's Ark' or 'Goodbye Gondwana': is the origin of New Zealand's terrestrial invertebrate fauna ancient, recent, or both? *Invertebrate Systematics* 24: 1–8.
- Giribet G, Edgecombe GD, Wheeler WC. 2001. Arthropod phylogeny based on eight molecular loci and morphology. Nature 413: 157–161.
- **Giupponi APL**, **Kury AB**. **2013**. Two new species of *Heterophrynus* Pocock, 1894 from Colombia with distribution notes and a new synonymy (Arachnida: Amblypygi: Phrynidae). *Zootaxa* **3647**: 329–342.
- Giupponi APL, Miranda GS. 2016. Eight new species of *Charinus* Simon, 1892 (Arachnida: Amblypygi: Charinidae) endemic for the Brazilian Amazon, with notes on their conservational status. *PLoS One* 11: e0148277.
- **Goloboff PA. 2013.** Extended implied weighting. *Cladistics* **30:** 260–272.
- Goloboff PA, Farris JS, Källersjö M, Oxelman B, Ramírez MJ, Szumik CA. 2003. Improvements to resampling measures of group support. *Cladistics* 19: 324–332.
- **Goloboff PA, Farris JS, Nixon KC. 2008.** TNT, a free program for phylogenetic analysis. *Cladistics* **24:** 774–786.
- González-Santillán E, Prendini L. 2015. Phylogeny of the North American vaejovid scorpion subfamily Syntropinae Kraepelin, 1905, based on morphology, mitochondrial and nuclear DNA. *Cladistics* 31: 341–405.
- Grandcolas P, Murienne J, Robillard T, Desutter-Grandcolas L, Jourdan H, Guilbert E, Deharveng L. 2008. New Caledonia: a very old Darwinian island? Philosophical Transactions of the Royal Society of London, Ser. B: Biological Sciences 363: 3309–3317.
- Grant T, Frost DR, Caldwell JP, Gagliardo R, Haddad CFB, Kok PJR, Means DB, Noonan BP, Schargel WE, Wheeler WC. 2006. Phylogenetic systematics of dartpoison frogs and their relatives (Amphibia: Athesphatanura: Dendrobatidae). Bulletin of the American Museum of Natural History 299: 1–262.
- Grauvogel-Stamm L, Ash SR. 2005. Recovery of the Triassic land flora from the end-Permian life crisis. *General Palaeontology* 4: 593-608.
- Gravely FH. 1911. Notes on Pedipalpi in the collection of the Indian Museum. I. New Pedipalpi from Ceylon. Records of the Indian Museum 6: 36–38.
- Gravely FH. 1915. A revision of the Oriental subfamilies of Tarantulidae (Order Pedipalpi). Records of the Indian Museum 11: 433–455.

- Grehan J. 2001. Biogeography and evolution of the Galapagos: integration of the biological and geological evidence. Biological Journal of the Linnean Society 74: 267–287.
- Guindon S, Dufayard JF, Lefort V, Anisimova M, Hordijk W, Gascuel O. 2010. New algorithms and methods to estimate maximum-likelihood phylogenies: assessing the performance of PhyML 3.0. Systematic Biology 59: 307–321.
- Hall R. 2012. Late Jurassic-Cenozoic reconstructions of the Indonesian region and the Indian Ocean. *Tectonophysics* 570-571: 1-41.
- Harms D. 2018. A new species of *Charinus* (Amblypygi: Charinidae) from Ghana, with notes on West African whip spiders. *Evolutionary Systematics* 2: 45–53.
- Harvey MS. 2003. Catalogue of the smaller arachnid orders of the world. Amblypygi, Uropygi, Schizomida, Palpigradi, Ricinulei and Solifugae. Collingwood: CSIRO Publishing, 385 pp.
- Harvey MS, West PLJ. 1998. New species of *Charon* (Amblypygi, Charontidae) from Northern Australia and Christmas Island. *Journal of Arachnology* 26: 273–284.
- Heath TA. 2012. A hierarchical Bayesian model for calibrating estimates of species divergence times. Systematic Biology 61: 793–809.
- Hedge J, Shillito AP, Davies NS, Butler RJ, Sansom IJ. 2019. Invertebrate trace fossils from the Alveley Member, Salop Formation (Pennsylvanian, Carboniferous), Shropshire, UK. Proceedings of the Geologists' Association 130: 103–111.
- Hirst S. 1913. Second report on the Arachnida the scorpions, Pedipalpi, and supplementary notes on the Opiliones & pseudoscorpions. Transactions of the Linnean Society of London, Zoology 2: 31–37.
- **Huxley TH. 1868.** On the classification and distribution of the Alectoromorphae and Heteromorphae. *Proceedings of the Zoological Society of London* **1868:** 214–319.
- Jin YG, Zhang J, Shang QH. 1994. Two phases of end-Permian mass extinction. Canadian Society of Petroleum Geologists Memoir 17: 813-822.
- Katoh K, Toh H. 2008. Improved accuracy of multiple ncRNA alignment by incorporating structural information into a MAFFT-based framework. BMC Bioinformatics 9: 212.
- Katoh K, Kuma K-I, Toh H, Miyata T. 2005. MAFFT v.5: improvement in accuracy of multiple sequence alignment. Nucleic Acids Research 33: 511–518.
- Kimura M. 1981. Possibility of extensive neutral evolution under stabilizing selection with special reference to nonrandom usage of synonymous codons. Proceedings of the National Academy of Sciences of the USA 78: 5773–5777.
- Knoll AH, Bambach RK, Canfield DE, Grotzinger JP. 1996. Comparative Earth history and Late Permian mass extinction. Science 273: 452–457.
- Köhler F, Glaubrecht M. 2007. Out of Asia and into India: on the molecular phylogeny and biogeography of the endemic freshwater gastropod *Paracrostoma* Cossmann, 1900 (Caenogastropoda: Pachychilidae). *Biological Journal of the Linnean Society* 91: 627–651.
- Kraepelin K. 1898. Neue Pedipalpen und Scorpione des Hamburger Museums. Mitteilungen aus dem Naturhistorischen Museum in Hamburg 15: 1-6.

- Kraepelin K. 1899. Scorpiones und Pedipalpi. Das Tierreich 8, (Arachnoidea). Berlin: R. Friedländer und Sohn Verlag, i–xviii. 1–265.
- Kritscher E. 1959. Ergebnisse der von Dr. O. Paget und Dr. E. Kritscher auf Rhodos durchgeführten zoologischen Exkursionen. II. Pedipalpi (Amblypygi). Annalen des Naturhistorischen Museums in Wien 63: 453–457.
- Kuraku S, Zmasek CM, Nishimura O, Katoh K. 2013. aLeaves facilitates on-demand exploration of metazoan gene family trees on MAFFT sequence alignment server with enhanced interactivity. *Nucleic Acids Research* 41: W22–W28.
- **Labandeira CC. 2006.** The four phases of plant-arthropod associations in deep time. *Geologica* **4:** 409–439.
- Lanfear R, Calcott B, Ho SYW, Guindon S. 2012. PartitionFinder: combined selection of partitioning schemes and substitution models for phylogenetic analyses. *Molecular Biology and Evolution* 29: 1695–1701.
- Lanfear R, Frandsen PB, Wright AM, Senfeld T, Calcott B. 2016. PartitionFinder 2: new methods for selecting partitioned models of evolution for molecular and morphological phylogenetic analyses. *Molecular Biology and Evolution* 34: 772–773.
- **Lewis PO. 2001.** A likelihood approach to estimating phylogeny from discrete morphological character data. *Systematic Biology* **50:** 913–925.
- Lohman DJ, de Bruyn M, Page T, von Rintelen K, Hall R, Ng P, Shih H-T, Carvalho G, Von Rintelen T. 2011. Biogeography of the Indo-Australian Archipelago. Annual Review of Ecology, Evolution, and Systematics 42: 205–226.
- Maddison W, Maddison DR. 2017. Mesquite: a modular system for evolutionary analysis, v.3.2. Available at: http://mesquiteproject.org. Accessed 20 September 2017.
- Mathews S, Donoghue MJ. 1999. The root of angiosperm phylogeny inferred from duplicate phytochrome genes. *Science* 286: 947–950.
- Mello-Leitão C. 1931. Pedipalpos do Brasil e algumas notas sobre a ordem. *Archivos do Museu Nacional* 33: 7–72.
- Miranda GS, Giupponi APL. 2011. A new synanthropic species of *Charinus* Simon, 1892 from Brazilian Amazonia and notes on the genus (Arachnida: Amblypygi: Charinidae). *Zootaxa* 2980: 61–68.
- Miranda GS, Zamani A. 2018. Filling the gap of whip spider distribution in Asia: *Phrynichus persicus* sp.n. (Arachnida, Amblypygi), a new Phrynichidae from Iran. *Zootaxa* 4413: 339–350.
- Miranda GS, Aharon S, Gavish-Regev E, Giupponi APL, Wizen G. 2016a. A new species of *Charinus* Simon, 1892 (Arachnida: Amblypygi: Charinidae) from Israel and new records of *C. ioanniticus* (Kritscher, 1959). *European Journal of Taxonomy* 234: 1–17.
- Miranda GS, Giupponi APL, Wizen G. 2016b. Two new species of whip spider (Amblypygi): an epigean and a cave dwelling *Charinus* Simon, 1892 from Belize. *Zootaxa* 4098: 545–559.
- Miranda GS, Giupponi AP, Prendini L, Scharff N. 2018a. Weygoldtia, a new genus of Charinidae Quintero, 1986 (Arachnida, Amblypygi) with a reappraisal of the genera in the family. Zoologischer Anzeiger 273: 23–32.

- Miranda GS, Kury AB, Giupponi APL. 2018b. Review of Trichodamon Mello-Leitão 1935 and phylogenetic placement of the genus in Phrynichidae (Arachnida, Amblypygi). Zoologischer Anzeiger 273: 33–55.
- Miranda GS, Giupponi AP, Prendini L, Scharff N. 2021. Systematic revision of the pantropical whip spider family Charinidae Quintero, 1986 (Arachnida, Amblypygi). European Journal of Taxonomy:1–409.
- Mirande JM. 2019. Morphology, molecules and the phylogeny of Characidae (Teleostei, Characiformes). *Cladistics* 35: 282–300.
- Müller S. 1846. Über den Charakter der Thierwelt auf den Inseln des indischen Archipels. Archiv für Naturgeschichte
- Murienne J, Grandcolas P, Piulachs MD, Bellés X, D'Haese C, Legendre F, Pellens R, Guilbert E. 2005. Evolution on a shaky piece of Gondwana: is local endemism recent in New Caledonia? *Cladistics* 21: 2–7.
- Nishiguchi MK, Doukakis P, Egan M, Goldstein PZ, Kizirian D, Phillips A, Prendini L, Rosenbaum HC, Torres E, Wyner Y, DeSalle R, Giribet G. 2002. DNA isolation procedures. In: DeSalle R, Giribet G, Wheeler WC, eds. Methods and tools in biosciences and medicine. Techniques in molecular evolution and systematics. Basel: Birkhäuser Verlag AG, 249–287.
- **Nixon K. 1999.** The parsimony ratchet, a new method for rapid parsimony analysis. *Cladistics* **414**: 407–414.
- Parent CE, Caccone A, Petren K. 2008. Colonization and diversification of Galápagos terrestrial fauna: a phylogenetic and biogeographical synthesis. *Philosophical Transactions of the Royal Society of London, Ser. B: Biological Sciences* 363: 3347–3361.
- Poinar G. 2018. Burmese amber: evidence of Gondwanan origin and Cretaceous dispersion. *Historical Biology* 31: 1304, 1309.
- Prendini L, Crowe TM, Wheeler WC. 2003. Systematics and biogeography of the family Scorpionidae Latreille, with a discussion on phylogenetic methods. *Invertebrate Systematics* 17: 185–259.
- Prendini L, Weygoldt P, Wheeler WC. 2005. Systematics of the *Damon variegatus* group of African whip spiders (Chelicerata: Amblypygi): evidence from behaviour, morphology and DNA. *Organisms, Diversity and Evolution* 5: 203–236.
- Quintero DJ. 1986. Revision de la clasificacion de amblypygidos pulvinados: creacion de subordenes, una nueva familia y un nuevo genero con tres nuevas especies (Arachnida: Amblypygi). In: Eberhard WG, Lubin YD, Robinson BC, eds. Proceedings of the Ninth International Congress of Arachnology, Panama. Washington, DC. Panama: Smithsonian Institution Press, 203–212.
- Rahmadi C, Harvey MS, Kojima J-I. 2010. Whip spiders of the genus *Sarax* Simon 1892 (Amblypygi: Charinidae) from Borneo Island. *Zootaxa* 2612: 1–21.
- Rambaut A, Suchard MA, Xie D, Drummond AJ. 2014. Tracer v.1.6. Available at: http://beast.bio.ed.ac.uk/Tracer. Accessed 15 April 2016.
- Raup DM, Sepkoski JJJ. 1982. Mass extinctions in the marine fossil record. *Science* 215: 1501–1503.

- Rix MG, Harvey MS, Roberts JD. 2008. Molecular phylogenetics of the spider family Micropholcommatidae (Arachnida: Araneae) using nuclear rRNA genes (18S and 28S). Molecular Phylogenetics and Evolution 46: 1031–1048.
- Ronquist F, Teslenko M, Mark PVD, Ayres DL, Darling A, Höhna S, Larget B, Liu L, Suchard MA, Huelsenbeck JP. 2012. MrBayes 3.2: efficient Bayesian phylogenetic inference and model choice across a large model space. Systematic Biology 61: 539–542.
- Sahney S, Benton MJ, Falcon-Lang HJ. 2010. Rainforest collapse triggered Carboniferous tetrapod diversification in Euramerica. Geology 38: 1079–1082.
- Sclater PL. 1858. On the general geographical distribution of the class Aves. Zoological Journal of the Linnean Society 2: 130–145.
- Seiter M, Wolff J. 2014. Description of Sarax buxtoni (Gravely 1915) (Arachnida: Amblypygi: Charinidae) and a new case of parthenogenesis in Amblypygi from Singapore. Journal of Arachnology 42: 233–239.
- Seiter M, Schramm FD, Schwaha T. 2018. Description of a new *Charinus* species (Amblypygi: Charinidae) from the Monseñor Nouel Province, Dominican Republic. *Zootaxa* 4438: 349–361.
- **Sereno PC. 2007.** Logical basis for morphological characters in phylogenetics. *Cladistics* **23:** 565–587.
- Shear WA, Kukalova-Peck J. 1990. The ecology of Paleozoic terrestrial arthropods: the fossil evidence. Canadian Journal of Zoology 68: 1807–1834.
- **Shultz JW. 2007.** A phylogenetic analysis of the arachnid orders based on morphological characters. *Zoological Journal of the Linnean Society* **150:** 221–265.
- Simpson GG. 1977. Too many lines; the limits of the Oriental and Australian zoogeographic regions. *Proceedings of the American Philosophical Society* 121: 107–120.
- Sjoberg D. 2020. Hablar: non-astonishing results in R. R package v.0.3.0. Available at: https://rdrr.io/cran/hablar/.
- **Stamatakis A. 2014.** RAxML v.8: a tool for phylogenetic analysis and post-analysis of large phylogenies. *Bioinformatics* **30:** 1312–1313.
- Stamatakis A, Hoover P, Rougemont J. 2008. A fast bootstrapping algorithm for the RAxML web-servers. Systematic Biology 57: 758-771.
- Stanley SM, Yang X. 1994. A double mass extinction at the end of the Paleozoic Era. *Science* 266: 1340–1344.
- **Talavera G, Castresana J. 2007.** Improvement of phylogenies after removing divergent and ambiguously aligned blocks from protein sequence alignments. *Systematic Biology* **56:** 564–577.
- Tänzler R, Toussaint EFA, Suhardjono YR, Balke M, Riedel A. 2014. Multiple transgressions of Wallace's Line explain diversity of flightless *Trigonopterus* weevils on Bali. *Proceedings of the Royal Society of London, Ser. B: Biological Sciences* 281: 2013–2528.
- Teruel R. 2016. The genus *Charinus* Simon, 1892 (Amblypygi: Charinidae) on the Island of Hispaniola, Greater Antilles. *Revista Ibérica de Aracnología* 28: 3–12.
- Tetlie OE, Dunlop JA. 2008. Geralinura carbonaria (Arachnida; Uropygi) from Mazon Creek, Illinois, USA, and

- the origin of subchelate pedipalps in whip scorpions. *Journal* of Paleontology **82:** 299–312.
- Thorell T. 1888. Pedipalpi e scorpioni dell'Arcipelago Malese conservati nel Museo Civico di Storia Naturale di Genova. Annali del Museo Civico di Storia Naturale di Genova 26: 327–428.
- Vasconcelos ACO, Ferreira RL. 2016. Description of two new species of *Charinus* Simon, 1892 from Brazilian caves with remarks on conservation (Arachnida: Amblypygi: Charinidae). *Zootaxa* 4072: 185–202.
- Vasconcelos ACO, Ferreira RL. 2017. Two new species of cave-dwelling *Charinus* Simon, 1892 from Brazil (Arachnida: Amblypygi: Charinidae). *Zootaxa* 4312: 277–292.
- Vasconcelos ACO, Giupponi APL, Ferreira RL. 2013. A new species of *Charinus* Simon, 1892 from northeastern Brazil with comments on the potential distribution of the genus in Central and South Americas (Arachnida: Amblypygi: Charinidae). *Zootaxa* 3737: 488–500.
- Vasconcelos ACO, Giupponi APL, Ferreira RL. 2016. Description of a new troglomorphic species of *Charinus* Simon, 1892 from Brazil (Arachnida, Amblypygi, Charinidae). *ZooKeys* 600: 35–52.
- Wallace AR. 1860. On the zoological geography of the Malay Archipelago. Zoological Journal of the Linnean Society 4: 172–184.
- Wallace AR. 1869. The Malay Archipelago. London: Macmillan.
 Weygoldt P. 1972. Charontidae (Amblypygi) aus Brasilien.
 Zoologische Jahrbücher, Abteilung für Systematik, Ökologie und Geographie der Tiere 99: 107–132.
- Weygoldt P. 1994. Amblypygi. In: Juberthie C, Decu V, eds. Encyclopaedia biospeologica. France and Romania: Moulis & Bucarest: Société de Biospéologie, 241–247.
- Weygoldt P. 1996. Evolutionary morphology of whip spiders: towards a phylogenetic system (Chelicerata: Arachnida: Amblypygi). *Journal of Zoological Systematics and Evolution Research* 34: 185–202.
- Weygoldt P. 1998. Revision of the species of *Phrynichus* Karsch, 1879 and *Euphrynichus* Weygoldt, 1995 (Chelicerata, Amblypygi). *Zoologica, Stuttgart* 147: 1–65.
- Weygoldt P. 1999a. Revision of the genus *Damon* C. L Koch, 1850 (Chelicerata: Amblypygi: Phrynichidae). *Zoologica*, *Stuttgart* 150: 1–45.
- Weygoldt P. 1999b. Sperm transfer, spermatophore morphology, and female genitalia of three species of whip spiders: Charinus seychellarum Kraepelin, 1898, Damon medius (Herbst, 1797), and Phrynichus scaber (Gervais, 1844) (Chelicerata, Amblypygi). Zoologica, Stuttgart 150: 47–64.
- Weygoldt P. 1999c. Spermatophores and the evolution of female genitalia in whip spiders (Chelicerata, Amblypygi). Journal of Arachnology 27: 103-116.
- **Weygoldt P. 2000.** Whip spiders (Chelicerata: Amblypygi).

 Their biology, morphology and systematics. Stenstrup: Apollo Books
- Weygoldt P. 2002. Chelicerata, Spinnentiere. In: Rieger R, ed. Spezielle Zoologie. Heidelberg, Berlin: Springer Verlag. 449–497.

- Weygoldt P. 2005. Biogeography, systematic position, and reproduction of *Charinus ioanniticus* (Kritscher, 1959) with the description of a new species from Pakistan (Chelicerata, Amblypygi, Charinidae). *Senckenbergiana Biologica* 85: 1–14.
- Weygoldt P. 2006. New Caledonian whip spiders: notes on Charinus australianus, Charinus neocaledonicus and other south-western Pacific species of the Charinus australianus species group (Chelicerata, Amblypygi, Charinidae). Verhandlungen des Naturwissenschaftlichen Vereins in Hamburg 42: 5–37.
- Weygoldt P. 2007. Parthenogenesis and reproduction in Charinus ioanniticus (Kritscher, 1959) (Chelicerata, Amblypygi, Charinidae). Bulletin of the British Arachnological Society 14: 81-82.
- Weygoldt P. 2008. Spermatophores, female genitalia, and courtship behaviour of two whip spider species, *Charinus africanus* and *Damon tibialis* (Chelicerata: Amblypygi). Zoologischer Anzeiger 247: 223–232.
- Weygoldt P, Hoffmann P. 1995. Reproductive behavior, spermatophores, and female genitalia in the whip spiders *Damon diadema* (Simon, 1876), *Phrynichus* cf. ceylonicus (C.L. Koch, 1843) and *Euphrynichus alluaudi* (Simon, 1936) (Chelicerata: Amblypygi). *Zoologischer Anzeiger* 234: 1–18.
- Weygoldt P, Van Damme K. 2004. A new troglomorphic whip spider of the genus *Charinus* (Amblypygi: Charinidae) from Socotra Island. *Fauna of Arabia* 20: 327–334.
- Weygoldt P, Hans P, Polak S. 2002. Arabian whip spiders: Four new species of the genera Charinus and Phrynichus (Chelicerata: Amblypygi) from Oman and Socotra. Fauna of Arabia 19: 289–309.
- Wickham H. 2016. *Ggplot2: elegant graphics for data analysis*. New York: Springer-Verlag.
- Wickham H. 2019. Welcome to the tidyverse. Journal of Open Source Software 4: 1686.
- Wilkinson M. 1995. A comparison of two methods of character construction. Cladistics 11: 297–308.
- Wolfe JM, Daley AC, Legg DA, Edgecombe GD. 2016. Fossil calibrations for the arthropod Tree of Life. *Earth Science Reviews* 160: 43–110.
- Wolff J, Huber SJ, Gorb S. 2015a. How to stay on mummy's back: morphological and functional changes of the pretarsus in arachnid postembryonic stages. Arthropod Structure and Development 44: 301–312.
- Wolff J, Seiter M, Gorb SN. 2015b. Functional anatomy of the pretarsus in whip spiders (Arachnida, Amblypygi). *Arthropod Structure and Development* 44: 524–540.
- Wolff JO, Schwaha T, Seiter M, Gorb SN. 2016. Whip spiders (Amblypygi) become water-repellent by a colloidal secretion that self-assembles into hierarchical microstructures. Zoological Letters 2: 23.
- Wolff JO, Seiter M, Gorb SN. 2017. The water-repellent cerotegument of whip-spiders (Arachnida: Amblypygi). Arthropod Structure and Development 46: 116–129.
- Zhang Z, Ramstein G, Schuster M, Li C, Contoux C, Yan Q. 2014. Aridification of the Sahara Desert caused by Tethys Sea shrinkage during the Late Miocene. *Nature* 513: 401–404.

SUPPORTING INFORMATION

Additional Supporting Information may be found in the online version of this article at the publisher's web-site:

Appendix S1. List of material examined.

Appendix S2. List of GenBank accession codes.

Appendix S3. Supplemental figures.

Figure S1. Phylogeny of the whip spider family Charinidae Quintero, 1986 reconstructed with maximum likelihood. Matrix pruned to include only taxa with both molecular and morphological data. Green, *Weygoldtia* Miranda *et al.*, 2018; yellow, *Sarax* Simon 1892; blue, *Charinus* Simon 1892.

Figure S2. Phylogeny of the whip spider family Charinidae Quintero, 1986 reconstructed with parsimony and equal weighting.

Figure S3. Phylogeny of the whip spider family Charinidae Quintero, 1986 reconstructed with parsimony and implied weighting with k = 6.

Figure S4. Phylogeny of the whip spider family Charinidae Quintero, 1986 reconstructed with parsimony and implied weighting with k = 10.

Figure S5. Phylogeny of the whip spider family Charinidae Quintero, 1986 reconstructed with parsimony and implied weighting with k = 20.

Figure S6. Phylogeny of the whip spider family Charinidae Quintero, 1986 reconstructed with parsimony and implied weighting with k = 30.

Figure S7. Phylogeny of the whip spider family Charinidae Quintero, 1986 reconstructed with parsimony and implied weighting with k = 40-90.

Figure S8. Phylogeny of the whip spider family Charinidae Quintero, 1986 reconstructed with Bayesian inference. Green, *Weygoldtia* Miranda *et al.*, 2018; yellow, *Sarax* Simon 1892; blue, *Charinus* Simon 1892.

Figure S9. Phylogeny of the whip spider family Charinidae Quintero, 1986 reconstructed with maximum likelihood. Tree based on morphological characters analysed with Mkv model. Green, *Weygoldtia Miranda et al.*, 2018; yellow, *Sarax* Simon 1892; blue, *Charinus* Simon 1892.

Figure S10. Phylogeny of the whip spider family Charinidae Quintero, 1986 reconstructed with maximum likelihood. Gene tree of fragments 12S and 16S (partition 1). Green, *Weygoldtia* Miranda *et al.*, 2018; yellow, *Sarax* Simon 1892; blue, *Charinus* Simon 1892.

Figure S11. Phylogeny of the whip spider family Charinidae Quintero, 1986 reconstructed with maximum likelihood. Gene tree of 18S, 28S and *COI* third-codon position (partition 2). Green, *Weygoldtia Miranda et al.*, 2018; yellow, *Sarax* Simon 1892; blue, *Charinus* Simon 1892.

Figure S12. Phylogeny of the whip spider family Charinidae Quintero, 1986 reconstructed with maximum likelihood. Gene tree of *COI* first-codon position (partition 3). Green, *Weygoldtia* Miranda *et al.*, 2018; yellow, *Sarax* Simon 1892; blue, *Charinus* Simon 1892.

Figure S13. Phylogeny of the whip spider family Charinidae Quintero, 1986 reconstructed with maximum likelihood. Gene tree of *COI* second-codon position (partition 4). Green, *Weygoldtia Miranda et al.*, 2018; yellow, *Sarax* Simon 1892; blue, *Charinus* Simon 1892.

APPENDIX 1

Morphological matrix of four outgroup taxa and 92 ingroup taxa (plus three morphospecies of Sarax) used for phylogenetic analysis of the whip spider family Charinidae Quintero, 1986. Numbers following some taxon names refer to samples in Ambrose Monell Cryocollection at the American Museum of Natural History, from which DNA sequences were generated. Character states scored numerically from 0 to 7, polymorphic states indicated within [], inapplicable states are denoted with -, and unknown/missing

entries with question marks. Character descriptions provided in Appendix 2. Material examined provided in Supplementary material (Appendix S1).

OUTGROUP

Stenochrus Sbordonii 3757

10--0--00- 0-00000--- 50--10010-?0--0000-----0????0- 001-??1000 --0--00-- ------- --0-00---0-0------ 0-000---- --1000-

Mastigoproctus aff. giganteus 3509

110411010- 0010000--- 00--0-040- 0130002010 --00????0- 000-??1001 0710--000-?0------ 100-10--1 0-0----- 10001-0--- -----1 0-000---- ---1000-

DAMON DIADEMA 1479

PHRYNUS LONGIPES 1483

 $\begin{array}{c} 011411110 -\ 00101011111\ 0110111211\ 21[12]00020??\\ 1?-1011112\ 070?2?0001\ 0110--0050\ 0211111013\\ -010011--11105-----23010401122--2-0---112100100105\\ 61000110 \end{array}$

INGROUP

CHARINUS ACARAJE

Charinus Africanus 6943

010111110- 0010101100 1100100210 3120004001 0-21000011 0402??0001 1101000020 010000---0 11110110-0 111201001- 20002110-- 0011112110 3111100101 11101010

CHARINUS AGUAYOI 10170

010110110- 00101111100 1100100210 2110002000 --0011??11 0312??0001 1101010020 010-00---0 11100110-0 111200-01- 20002110-- 0011112310 2000100101 11101010

CHARINUS ALAGOANUS

01011111110 0010101100 1100110210 3120002000 --11????11 0412??0001 11011110020?20000---0 11100110-0 111201[01]02- 20003010-- 0011111210 2011100110 01101011

CHARINUS APIACA

CHARINUS ASTURIUS

010111110- 00101000-0 1101100311 3100001000 --1101??11 0412100001 1101100031 030000---0 11100110-0 111400-01- 40004010-- 0011110010 3010100102 21101010

CHARINUS AUSTRALIANUS

0101111110- 00101111100 1100100311 3130002000 --01??0011 0403??0001 1101110031?20000---0 11100110-0 111201101- 30014010-- 0011111210 3000100101 11101010

CHARINUS BELIZENSIS

010100110- 0010101100 1120100210 2130002001 0-0111??11 0422??0001 1101010020 010-00---0 11100120-0 111201101- 20002010-- 0011112310 2000100101 11101010

CHARINUS BICHUETTEAE

CHARINUS BONALDOI

010100110- 0010101100 1100100210 20-0000000 --00????11 0302??0001 1101000020?10-00---0 11110120-0 111301401- 20002010-- 0011112310 1000100111 11101010

CHARINUS BRASILIANUS

010111110- 0010101100 1101100210 3100002000 --1111??11 0402??0001 1101110030 0[34]0000--0 11100110-0 111[23]01001- [34]001[45]010--0011111[01]10 3011100101 11101010

Charinus brescoviti

010111110- 0010101100 1100100210 2110002001 0-00????11 030???0001 1101110030?10-00---0 11100110-0 111301001- 30002110-- 0011112110 1000100101 11101011

CHARINUS CARAJAS

0101111110 0010101110 1100100211 30-0002000 --0111??11 0402??0001 1101110030 020000---0 11100110-0 111201001- 30003010-- 0011112310 2000100111 11101010

CHARINUS CARIBENSIS

CHARINUS CARINAE

010111110- 0010101100 1101100311 51000??00? ????00??11 0402??0001 110110104? 140000---0 11100110-0 111401602- 40??5010-- 0011120010 3011100102 21101010

CHARINUS CARIOCA

CHARINUS CARVALHOI 13399

CHARINUS CAVERNICOLUS

CHARINUS CEARENSIS

CHARINUS CUBENSIS

010110110- 00101111100 1100100211 2110002000 --00????11 0332??0001 1101010020?10-00---0 11100110-0 111200-01- 20002110-- 0011112310 2000100101 11101010

CHARINUS DIAMANTINUS

CHARINUS DOMINICANUS 13399

CHARINUS ELEGANS 5175

CHARINUS ELEONORAE

Charinus euclidesi

010111110- 0010101100 1101100311 4100002000 --1000??11 0402??0001 1101110041 130000---0 11100110-0 111301002- 40004010-- 0011121010 3011100101 11101010

CHARINUS FAGEI

010111110- 0010101100 1100100311 41000????? ????11??11 0?0???0001 1101010030 120000---0 11100100-0 111201101- 30014010-- 0011112210 3011100111 11101010

Charinus Gertschi 10076

$CHARINUS\ GOITACA$

CHARINUS GUAYAQUIL

010110110- 00101111100 1110100210 3120002000 --00????11 0402??0001 1101000020?10-00---0 11100110-0 111201001- 20002110-- 0011112310 2000100211 11101010

CHARINUS GUTO

CHARINUS IMPERIALIS

CHARINUS INSULARIS

010111110- 00101111100 1100100311 2120002001 0-01????11 0403??0001 1101110030?20000---0 11100110-0 11120[01]001- 20004010-- 0011111110 3010100101 11101010

Charinus jibaossu

Charinus koepckei

CHARINUS LOKO

$Charinus\ longipes$

CHARINUS MADAGASCARIENSIS

CHARINUS MAGALHAESI 13393

010100010- 0010111100 1100100210 20-0002000 --10????11 0302??0001 1101000020?10-00---0 11100110-0 111101201- 20002110-- 0011112310 2000100111 1110100-

CHARINUS MILLOTI

010111110- 0010101110 1100100310 2100004000 --0101??11 0302??0001 1101110031 121101---0 11110110-0 1110-1501- 30002110-- 0011121310 3211100011 11101010

CHARINUS MISKITO

010111110- 0010111100 1110100310 2100002000 --0111??11 0302??0001 1101000020 010-00--0 11100110-0 111200-01- 20002010-- 0011112310 2000100111 11101010

CHARINUS MOCOA

010000110- 0010111100 1110100210 2130002000 --01????1? 0?????0001 1101010030?10-00---0 11110110-0 111201101- 20002010-- 0011112210 1000100111 11101010

CHARINUS MONASTICUS

010100110- 0010101100 1100100210 2110002000 --00????11 0302??0001 1101010020?10-00---0 11110120-0 111301401- 20002010-- 0011112310 1011100111 11101010

CHARINUS MONTANUS

010111110- 0010121100 1101100311 3130002000 --1100??12 0232??0001 1101100020 030000---0 11100110-0 111311002- 30004010-- 0111111110 3100100102 21101011

$CHARINUS\ MUCHMOREI$

010100110- 0010111100 1100100210 2130002000 --0011??11 0302??0001 1101010020 010-00---0 11100110-0 111201001- 20002110-- 0011112310 2000100101 11101010

CHARINUS MYSTICUS

01011111110 0010101100 1101100311 2100002000 --10????11 0402??0001 1101110031 020000---0 11110110-0 111301101- 30014010-- 0011121110 3011100102 21101010

Charinus neocaledonicus 4223 5174 10276

CHARINUS ORIENTALIS

Charinus Palikur 3831–3833

CHARINUS PAPUANUS

010111110- 0010121100 1100100311 2110000000 --00110011 0432??0001 110100003? 010000---0 11100110-0 111300-01- 40??2110-- 0011112310 3100100101 11101010

CHARINUS PECKI

CHARINUS PERQUERENS

CHARINUS PESCOTTI 6366 6367

0101111110- 0010131100 1100100311 2110002000 --00110011 0432??0001 1101000030 010000---0 11100110-0 11130[01]001- 30002110-- 0011111210 3200100101 11101010

CHARINUS POTIGUAR 13398

0101111110 0010101100 1101110311 5100002000 --1111??11 0402??0001 1101110030 010-00--0 11110110-0 111301401- 30002110-- 0011111310 3011100102 21101010

CHARINUS PURI

Charinus reddelli 13402

010100110- 0010101100 1120100210 2130002001 0-0111??11 0402??0001 1101010020 010-00---0 11100120-0 111201101- 30002110-- 0011112310 2010100101 11101010

CHARINUS RENNERI

0101101110 0010101100 1100100310 410000?00? ????11??11 0402??0001 1101100121 120000---0 11110110-0 111200-01- 30003010-- 0011111110 3011100102 21101010

CHARINUS RUSCHII

0101111110 0010101100 1101110311 5100000000 --11????11 0402??0001 1101100040?30000---0 11110120-0 111301402- 40015010-- 0011121010 3011100102 21101010

CHARINUS SILLAMI 13448

010111110- 0010101100 1100100210 2130002000 --00????11 0312??0001 1101100020?10-00---0 11100110-0 111101001- 200-2110-- 0011111310 2010100101 11101011

CHARINUS SOORETAMA

CHARINUS SOUZAI

CHARINUS SUSUWA

010110110- 0000101100 1100100310 2100001?00 --10????1? ??????0001 1101110020?2001-0100 11100110-0 111111201- 20113010-- 0011102-10 3000100101 11101010

CHARINUS TABOA 13400

010111110- 001010---- 1101--0--- 4---00200- --111--11 04--??0001 1101100031 03110----0 111001--- 111211011- 40004000-- 0011110010 3---100101
111010--

CHARINUS TROGLOBIUS

CHARINUS UNA

Charinus vulgaris 13396

010100010- 0010101100 1100110210 20-0002001 0-01????11 0302??0001 1101000020?10-00---0 11100110-0 111[12]01101- 20002010-- 0011112310 2000100111 11101010

SARAX ABBATEI

010111110- 0111101110 1120100310 3100000100 --101???11 03????0001 1101110030?10000---0 11110110-0 111101002- 30002110-- 0011110010 2100100212 21101010

SARAX BATUENSIS 1927

$Sarax\ bengalensis$

SARAX BILUA 5564

0101111112 0?01101100 1100100311 2100100100 --20????11 0402??0001 1101100030?10001---0 11110110-0 111211002- 30002110-- 0011102-10 3210100101 11101010

SARAX BISPINOSUS 12298

0101111112 0101101110 1100110210 2130112100 --2011??11 0302??0001 1101000040 020001---0 11100110-0 111310-02- 40004010-- 1011112310 2110100101 1110100-

Sarax Brachydactylus 1926

0101111112 0001101110 1100110211 1100104?00 --20010011 0503??0001 1101110030 020[01]00---0 11110110-0 1111111002- 40[01]14010-- 1011110010 310[01]100101 1110101[01]

SARAX COCHINENSIS 13118

0101111112 0101101110 1100110210 1120102100 --2000??11 040???0001 1101100030?20000---0 11100110-0 111210-01- 20004010-- 1011102-10 2???100????11010??

SARAX DUNNI

0101111112 0?01111110 1100110210 21301????? ???????????????0001 110111003? 030000---0 11100110-0 111210-02- 40?0401101 --11101-10 3210100002 21101010

SARAX GRAVELYI 11994

0101111112 0?01101110 1100110210 1100112?00 --20????11 0402??0001 1101110131?30100---0 11110110-0 111210-02- 3001401101 --11112210 3111100102 21101010

SARAX HUBERI

0101111112 0?01101110 1100110311 1130104?00 --2000??11 0402??0001 1101100030 020000---0 11110100-0 111210-02- 3000401101 --11111010 3210100001 11101010

SARAX INDOCHINENSIS

0101111112 0101101110 1100100210 1100112100 --2001??11 0402??0001 1101100030 020000---0 11100110-0 111210-02- 30004010-- 0011110010 3011100101 11101010

SARAX IOANNITICUS 2843 13394

010111110- 0111101100 1110100210 4100002100 --2010??11 0302??0001 1101010030 020000---0 11100110-0 111410-01- 30014010-- 1011111210 3000100211 11101011

SARAX ISRAELENSIS

SARAX JAVENSIS

SARAX LEMBEH

SARAX PAKISTANUS

SARAX PALAU

SARAX RAHMADII

$SARAX\ RIMOSUS\ 11996\ 11997$

 $\begin{array}{c} 01011111112\ 0001101110\ 1100110210\ 1100112?00\\ --20010011\ 0402110001\ 1101110031\ 0[23]0000---0\\ 11100110-0\ 111[23]10-02-\ [23]0004010--\ 1011110010\\ 2211100101\ 1110100- \end{array}$

SARAX SEYCHELLARUM 1494 9074

 $\begin{array}{c} 010111110-\ 0111101100\ 1100100310\ 410000200???-\\ -100011\ 0302010001\ 1101110140\ 14011-0210\\ 11100110-0\ 111410-01-\ 31004010--\ 0011111110\\ 3011100011\ 11101010 \end{array}$

SARAX SINGAPORAE 1964A 4761

SARAX SOCOTRANUS

SARAX TIOMANENSIS 11998 12001 12002

SARAX WILLEYI

0101111112 0101101100 1100100210 1110102?00 --2010??11 040???0001 1101110030?20000---0 11110110-0 111310-01- 3000211101 --11110010 3101100011 11101010

SARAX YAYUKAE 12109 12119 12123 12152 12168 12169

01011111112 0001101110 1100110310 1100112100 --2011??11 0402??0001 1101100141 13111-1000 11110110-0 111210-02- 3001401100 --11120010 3211100012 21101010

SARAX SP. BALI 11594

0101111111 0001101100 1100100210 21001????0
--??11??11 0402??0001 110110003? 120000---0
11110110-0 111310-02- 40??5010-- 0111110010
3101100002 21101010

SARAX SP. LOMBOK

0101111112 0?01101110 1100100210 1100112?00 --20??0011 0402??0001 1101100030?20000---0 11110110-0 111210-02- 3000401100 --11110010 3100100102 21101010

SARAX SP. SUMBAWA

0101111112 0?01101100 1100100210 2100112?00 --20????1? 0?????0001 1101110030?20000---0 11100110-0 111210-01- 30003010-- 0011120010 3100100102 21101010

Weygoldtia consonensis 11269

0101111112 1110101110 1101110211 3100104000 --1111??11 0502110001 1101110131 12111-0200 1110011100 1110-0-1-1 3000401100 --11120010 3211100005 51101010

Weygoldtia davidovi 11375 11377

APPENDIX 2

Morphological characters and character states used in phylogenetic analysis of the whip spider family Charinidae Quintero, 1986. Characters corresponding to previous matrices of Quintero (1986), Weygoldt & Hoffmann (1995), Weygoldt (1996), Shultz (2007), Garwood *et al.* (2017) and Miranda *et al.* (2018b) denoted, respectively, by abbreviations DQ, W&H, PW, JS, GEA and MEA, followed by the corresponding number. New characters indicated with asterisks.

CARAPACE

- 1. Tegument division: (0) absent; (1) present. | [JS 2]
- 2. Anterior margin, setae: (0) absent; (1) present. *
- 3. Anterior margin, position of setal sockets: (0) carapace; (1) spines. | [MEA 1]
- 4. Anterior margin, number of setae or spines/setae: (0) 4; (1) 6; (2) 8; (3) 10; (4) > 10. | [MEA 2]
- 5. Median eyes: (0) absent; (1) present. | [PW 29 (part)]
- 6. Median ocular tubercle: (0) absent; (1) present. | [PW 29 (part)]
- 7. Median ocular tubercle, pair of setae on/close to tubercle, or in corresponding position if tubercle absent: (0) absent; (1) present. | [MEA 5]
- 8. Lateral eyes: (0) absent; (1) present. *
- 9. Curved carina between lateral eyes and carapace lateral margin (Fig. 7 A, B, D, E): (0) absent; (1) present. | [MEA 6].
- 10. Distance from carina to lateral eyes (Fig. 7): (0)
 > four times one eye diameter; (1) ≤ twice one eye diameter; (2) smaller than one eye diameter, carina adjacent to lateral eyes. *
- 11. Straight carina anterior to lateral eyes, projecting from lateral ocular triad (Fig. 7C): (0) absent; (1) present. *
- 12. Distance from lateral eyes to carapace lateral margin if carina absent (Fig. 7): $(0) \le$ twice one eye diameter; (1) > twice one eye diameter. *

- 13. Setae posterior to lateral ocular triad (Fig. 7N): (0) absent; (1) present. | [MEA 7]
- 14. Setae adjacent to lateral ocular triad: (0) absent; (1) present. *

STERNUM

- 15. Tritosternum development: (0) short; (1) long, projecting anteriorly. | [MEA 8]
- 16. Number of medial and posterior sternum sclerites (Fig. 18): (0) one narrow sclerite only; (1) pair of narrow sclerites; (2) one flat, broad plaque; (3) two flat, broad plaques. | [MEA 9]

CHELICERAE

- 17. Basal segment, number of rows of teeth: (0) one; (1) two. *
- 18. Basal segment, tooth adjacent to bifid tooth (tooth 1) (Fig. 8J): (0) absent; (1) present. | [MEA 10]
- 19. Basal segment, size of tooth adjacent to bifid tooth (Fig. 8J): (0) small (sclerotized bump); (1) large (marked projection). | [MEA 11]
- 20. Basal segment, additional tooth adjacent to second tooth (tooth 2): (0) absent; (1) present. | [MEA 12]
- 21. Basal segment, number of teeth in prolateral row (Fig. 8C, G, K, O): (0) 3; (1) 4; (2) 5; (3) 6; (4) 7; (5) 8. | [DQ 2; PW 1; GEA 38; MEA 13]
- 22. Basal segment, number of cusps on distal tooth (Fig. 8G): (0) 1; (1) 2; (2) 3. | [PW 2; GEA 39; MEA 14]
- 23. Basal segment, relative size of cusps on bifid tooth (Fig. 8G): (0) distal (dorsal) larger than proximal; (1) proximal (ventral) larger than distal; (2) subequal. | [PW 3; MEA 15]
- 24. Basal segment, shape of distal (dorsal) cusp of bifid tooth (Fig. 8G): (0) straight; (1) with curved apex and concavity on retrolateral surface. *
- 25. Basal segment, prolateral surface, clavate or long, fine setae (Fig. 8O): (0) absent; (1) present. *
- 26. Basal segment, prolateral surface, number of rows of clavate or long, fine setae (additional row/s from base to apex) (Fig. 8O): (0) one; (1) > two. | [MEA 16]
- 27. Basal segment, dorsal setae, setiferous tubercle (Fig. 8E): (0) not projecting; (1) projecting. | [MEA 17]
- 28. Basal segment, number of dorsal setae (Fig. 8E):
 (0) 1; (1) 2; (2) 5–10; (3) 11–20; (4) > 20. |
 [MEA 18]
- 29. Basal segment, anterior retrolateral margin, setae (Fig. 8E): (0) absent; (1) present. | [MEA 19]
- 30. Basal segment, anterior retrolateral margin, number of setae (Fig. 8E): (0) 1; (1) 2. | [MEA 20]

- 31. Cheliceral claw, number of teeth (Fig. 8C): (0) 1; (1) 3; (2) 4 or 5; (3) 6 or 7; (4) 8 or 9; (5) 10–13. | [MEA 21].
- 32. Cheliceral claw, retrolateral surface, row of setae (Fig. 8B): (0) absent; (1) present. | [MEA 22]
- 33. Cheliceral claw, retrolateral surface, position of row of setae (Fig. 8B): (0) extending from base to dorsal side of fang (almost reaching row of setae on prolateral surface); (1) restricted to base of fang; (2) restricted to dorsal surface of fang; (3) extending from base to middle of fang. *
- 34. Cheliceral claw, dorsal surface, rows of setae between prolateral and retrolateral rows (Fig. 8): (0) absent; (1) present. *

OPISTHOSOMA AND GENITALIA

- 35. Opisthosoma, ventral sac cover (Fig. 9): (0) absent; (1) present. | [DQ 15; PW 26; GEA 124; MEA 23].
- 36. Genital operculum (Q), distal margin, shape and color of surface (Fig. 9): (0) flat, same color as rest of operculum; (1) with two medial convexities, paler, whitish ventrally. *
- 37. Genital operculum (Q), curvature of distal margin (Figs. 9, 10, 19): (0) concave; (1) straight; (2) convex; (3) with broad projection; (4) with small projection. | [MEA 24]
- 38. Gonopod (Q) (dorsal view), size of posterior border (Fig. 10): (0) short (thin layer; gonopods usually close to border); (1) long (longer than or equal to length of base of gonopod/gonopods far from border) | [PW 25 (part)]
- 39. Gonopod (♀), shape (Fig. 10): (0) circular or oval (1) rectangular (wider than long). | [PW 25 (part); MEA 25]
- 40. Gonopod (Q), claw-like projection (Fig. 10): (0) absent (1) present. | [DQ 4; PW 25 (part); MEA 26]
- 41. Gonopod (Q), tegument of claw-like projection (Fig. 10): (0) soft (1) sclerotized. | [W&H 8; PW 25 (part); MEA 27]
- 42. Gonopod (Q), tegument of claw-like projection, extent of sclerotization (Fig. 10): (0) restricted to apex; (1) extending from base to apex. | [PW 25 (part); MEA 28]
- 43. Gonopod (Q), shape of medial surface (Fig. 10): (0) cushion-like; (1) sucker-like; (2) finger-like (includes plunger-like gonopods). | [PW 25 (part); MEA 29]
- 44. Gonopod (Q), basal sclerotization: (0) absent (unsclerotized) (1) present (sclerotized). | [MEA 30]
- 45. Gonopod (3), sclerotizations at distal margin of fistula (Fig. 19): (0) absent (unsclerotized) (1) present (sclerotized). | [MEA 31]
- 46. Gonopod (3), sclerotizations at base of LoL1 (Fig. 19): (0) absent (unsclerotized) (1) present (sclerotized). | [MEA 32]

- 47. Spermatophore, position of sperm sac: (0) superficial (1) obscured. | [PW 27]
- 48. Spermatophore, shape: (0) simple; (1) complex sculpturing (with bars and levers). | [PW 27]

LEG I

- 49. Tibia, divided into pseudoarticles (Fig. 20): (0) absent (undivided); (1) present (divided). *
- 50. Tibia, number of pseudoarticles: (0) 16; (1) 21–25; (2) 26–45; (3) > 43. | [PW 18; MEA 33]
- 51. Tarsus, leaf-like setae on articles: (0) absent; (1) present. | [PW 20; MEA 34]
- 52. Tarsus, number of pseudoarticles: (0) 6–8; (1) 23; (2) 26–28; (3) 33–39; (4) 41–43; (5) 44–47; (6) 51–59; (7) 60–79; (8) 90–110. | [MEA 35]
- 53. Tarsus, size of first (proximal) article (Fig. 20): (0) subequal to others; (1) equal to sum of two articles; (2) equal to sum of three articles; (3) equal to sum of four articles.*
- 54. Tarsus, number of articles with slit sense organ (article has small elongation at distal margin): (0) 11–13; (1) 17; (2) 18; (3) 20; (4) 21; (5) 22; (6) 25. | [PW 19; MEA 36]
- 55. Tarsus, shape of rod sensilla: (0) rounded; (1) elliptical; (2) longilineal. | [MEA 37]
- 56. Tarsus, position of setae on rod sensilla: (0) on surface; (1) depressed into tegument. *

PEDIPALP

- 57. Coxae fused ventrally, forming posterior wall of pre-oral chamber: (0) absent (free); (1) present (fused). | [JS 30]
- 58. Dorsal articulation (hinge) of trochanter and femur, position: (0) anterior surface of femur; (1) dorsal surface of femur. | [PW 6; MEA 38]
- 59. Trochanter, posteriorly directed clavate apophysis: (0) absent; (1) present. | [PW 4, 5 (part)]
- 60. Trochanter, ventral surface, anteriorly directed ventromedial apophysis (Fig. 11): (0) absent; (1) present. | [PW 4, 5 (part)]
- 61. Trochanter, ventral surface, shape of anteriorly directed ventromedial apophysis (Fig. 11): (0) spine; (1) seta (broad projection with acute apex). [PW 4 (part); GEA 65 (part); MEA 39]
- 62. Trochanter, ventral surface, number of spines (excluding anteriorly directed ventromedial apophysis, if spine-like) (Fig. 11): (0) 1; (1) 2; (2) 3; (3) 4; (4) 5; (5) 6; (6) 7; (7) > 7. | [MEA 40]
- 63. Trochanter, dorsal surface, spines: (0) absent; (1) present. | [MEA 41]
- 64. Femur, ventral surface, spine or conspicuous setiferous tubercle proximal to spine 1 (Fig. 11): (0) absent; (1) present. | [MEA 42]

- 65. Femur, ventral surface, shape of projection proximal to spine 1 (Fig. 11): (0) setiferous tubercle; (1) spine. | [MEA 43]
- 66. Femur, ventral surface, position of spine/tubercle proximal to spine 1 (Fig. 11): (0) parallel to spine 1, prolateral; (1) adjacent to spine 1, in same row; (2) ventral to spine 1. | [MEA 44]
- 67. Femur, ventral surface, small spine close to articulation of femur and trochanter (Fig. 11): (0) absent; (1) present. *
- 68. Femur, ventral surface, spine parallel to spine 1 (in addition to aforementioned spine) (Fig. 11): (0) absent; (1) present. | [MEA 45]
- 69. Femur, ventral surface, number of spines (Fig. 11): (0) 1; (1) 2; (2) 3; (3) 4; (4) 5; (5) 6. | [MEA 46]
- 70. Femur, ventral surface (Q), small spine between spines 1 and 2 (dorsal to main row) (Fig. 11): (0) absent; (1) present. | [MEA 47]
- 71. Femur, ventral surface (3), small spine between spines 2 and 3 (dorsal to main row) (Fig. 11): (0) absent; (1) present. | [MEA 48]
- 72. Patella, ventral surface, number of spines (Fig. 11): (0) 1; (1) 2; (2) 3; (3) 4; (4) 5. | [MEA 49]
- 73. Patella, ventral surface, small spine between spines 1 and 2 (Fig. 11): (0) absent; (1) present. | [MEA 50]
- 74. Patella, ventral surface, small spine between spines 2 and 3 (Fig. 11): (0) absent; (1) present. *
- 75. Patella, ventral surface, shape of projection between spine 1 and distal margin (Fig. 11): (0) setiferous tubercle; (1) spine. | [MEA 52]
- 76.Patella, ventral surface, size of setiferous tubercle between spine 1 and distal margin (Fig. 11): (0) short, equal to other setiferous tubercle; (1) long, one-third the length of spine 1; (2) very long, half the length of spine 1.*
- 77. Patella, ventral surface, number of spines between spine 1 and distal margin (Fig. 11): (0) 1; (1) 2; (2) 3; (3) 4. | [MEA 53]
- 78. Patella, ventral surface, size of apical or largest (if more than one) spine between spine 1 and distal margin (Fig. 11): (0) short, one-third the length of spine 1; (1) long, half the length of spine 1; (2) very long, two-thirds the length of spine 1; (3) longer than spine 1. | [MEA 54]
- 79. Patella, ventral surface, shape of apical or largest (if more than one) spine between spine 1 and distal margin (Fig. 11): (0) straight; (1) curved, anteriorly directed. | [MEA 55]
- 80. Tibia, ventral surface, number of spines (Fig. 11): (0) 1; (1) 2; (2) 3; (3) 4. | [MEA 56]
- 81. Tibia, ventral surface, position of spine (if only one): (0) near proximal margin of basitarsus; (1) near distal margin of basitarsus; (2) medial. | [MEA 57]
- 82. Tibia, ventral surface, setiferous tubercle with long setae between spine 1 and distal margin of segment: (0) absent; (1) present. | [MEA 58]

- 83. Tibia, ventral surface, row of long, thin setae near distal margin: (0) absent; (1) present. | [MEA 59]
- 84. Tibia, ventral surface, number of setae in row near distal margin: (0) 1 or 2; (1) 3 or 4; (2) 5; (3) > 5. | [MEA 60]
- 85. Tarsus, ventral surface, spine: (0) absent; (1) present. | [DQ 16; PW 15, 16 (part); MEA 61]
- 86. Tarsus, ventral surface, cleaning organ: (0) absent: (1) present. | [JS 40]
- 87. Tarsus, ventral surface, number of setae in ventral row of cleaning organ: (0) 18–24; (1) 25–34; (2) 35–40. | [MEA 62]
- 88. Tarsus, row of setae at base of cleaning organ: (0) absent; (1) present. | [DQ 10; PW 17; MEA 63]
- 89. Tarsus, number of setae proximal to cleaning organ: (0) 1; (1) > 1. *
- 90. Coxae, position in relation to carapace (Fig. 12): (0) exposed; (1) obscured below carapace. *
- 91. Coxae, shape of sclerite (Fig. 12): (0) forming ring; (1) separated into small sclerites. *
- 92. Coxae, relative positions of plaques (sclerites) (Fig. 12): (0) adjacent to each other; (1) separated from each other. | [MEA 64]
- 93. Coxae, dorsal surface, sclerotized rounded or oval carina (Fig. 12): (0) absent; (1) present. | [MEA 65]
- 94. Coxae, dorsal surface, number of setae on anterior margin of rounded protuberance (Fig. 12): (0) 1; (1) 2; (2) 3; (3) 4; (4) 5; (5) 6. *
- 95. Coxae, dorsal surface, relative positions of two proximal large setae/tubercles on anterior margin of rounded protuberance (Fig. 12): (0) separated from each other; (1) adjacent to each other. *
- 96. Coxae, dorsal surface, setae on rounded protuberance (Fig. 12): (0) absent; (1) present. *
- 97. Coxae, dorsal surface, number of setae on rounded protuberance (Fig. 12): (0) 1; (1) 2; (2) 3; (3) 4; (4) 5; (5) 6; (6) 7. *
- 98. Femur, dorsal surface, shape of proximal series of spines/tubercles (Fig. 11): (0) setiferous tubercle; (1) spines. | [MEA 66]
- 99. Femur, dorsal surface, number of setiferous tubercles proximal to spine 1, situated in same row as primary series of spines (Fig. 11): (0) 1; (1) 2; (2) 3. *
- 100. Femur, dorsal, proximal series, number of spines (Fig. 11): (0) 1; (1) 2; (2) 3; (3) 4. \mid [MEA 67]
- 101. Femur, dorsal surface, number of spines (Fig. 11): (0) 1; (1) 2; (2) 3; (3) 4; (4) 5; (5) 6. | [MEA 68]
- 102. Femur, dorsal surface, small spine adjacent to spine 1 (Fig. 11): (0) absent; (1) present. *
- 103. Femur, dorsal surface (Q), small spine between spines 1 and 2 (Fig. 11): (0) absent; (1) present. | [MEA 69]

- 104. Femur, dorsal surface (Q), small spine between spines 2 and 3 (Fig. 11): (0) absent; (1) present. | [MEA 70]
- 105. Patella, dorsal surface, number of spines (Fig. 11): (0) 1; (1) 2; (2) 3; (3) 4; (4) 5; (5) 6. | [GEA 71 (part); MEA 71]
- 106. Patella, dorsal surface, long setiferous tubercle proximal to spine 3 (Fig. 11): (0) absent; (1) present. *
- 107. Patella, dorsal surface, long setiferous tubercle or spine between spine 1 and distal margin (Fig. 11): (0) absence; (1) presence. | [MEA 76]
- 108. Patella, dorsal surface, shape of projections between spine 1 and distal margin (Fig. 11): (0) setiferous tubercle; (1) spine. *
- 109. Patella, dorsal surface, number of spines between spine 1 and distal margin (Fig. 11): (0) 1; (1) 2; (2) 3; (3) 4; (4) 5. *
- 110. Patella, dorsal surface, length of proximal spine between spine 1 and distal margin (Fig. 11): (0) one-third the length of spine 1; (1) half the length of spine 1; (2) two-thirds the length of spine 1. *
- 111. Patella, dorsal surface, number of long setiferous tubercles between spine 1 and distal margin (refers only to setiferous tubercles that are broad basally and become acuminate apically; excludes tubercles of similar width from base to apex) (Fig. 11): (0) 1; (1) 2; (2) 3.*
- 112. Patella, dorsal surface, long setiferous tubercle between spine 1 and distal margin, size of proximal tubercle (Fig. 11): (0) one-third the length of spine 1; (1) half the length of spine 1; (2) two-thirds the length of spine 1.*
- 113. Tibia, number of dorsal spines: (0) 1; (1) 2; (2) 3; (3) > 3. | [DQ 12; MEA 77]
- 114. Tibia, relative size of dorsal spines (when two spines present): (0) proximal spine larger than distal; (1) distal spine larger than proximal. | [DQ 17; MEA 78]
- 115. Tarsus, dorsal surface, spine dorsal to cleaning organ: (0) absent; (1) present. | [GEA 76; MEA 79]
- 116. Tarsus, dorsal surface, number of spines: (0) 1; (1) 2; (2) 3; (3) > 3. | [PW 15, 16 (part); MEA 80]
- 117. Tarsus, dorsal surface, length of distal spine (or of single spine if only one present): (0) short (slightly longer than setiferous tubercle); (1) medium (one-third the length of distitarsus); (2) long (approximately half the length of distitarsus).
- 118. Tarsus, dorsal surface, relative size of two spines (or two distal spines, if more than two present): (0) proximal spine subequal to distal; (1) proximal spine two-thirds the length of distal; (2) proximal spine half the length of distal; (3) proximal spine one-third the length of distal. | [MEA 82]
- 119. Tarsus, dorsal surface, dorsal row of setae on cleaning organ: (0) absent; (1) present. | [MEA 83]

120. Tarsus and claw, fusion: (0) separate; (1) fused. | [DQ 11; PW 14; MEA 84]

LEG IV

- 121. Basitibia, number of articles: (0) 1; (1) 2; (2) 3; (3) 4. | [DQ 14; PW 23; MEA 85]
- 122. Basitibia, position of trichobothrium *bt* (Fig. 21): (0) proximal third; (1) medial third; (2) distal third. | [MEA 86]
- 123. Basitibia, markedly sclerotized denticulate border at distal apex of article (Fig. 21): (0) absent; (1) present. | [MEA 87]
- 124. Basitibia, markedly sclerotized denticulate border projection medially (Fig. 21): (0) absent; (1) present. | [MEA 88]
- 125. Distitibia, trichobothria *bc*: (0) absent; (1) present. | [MEA 89]
- 126. Distitibia, trichobothrium *nbf*: (0) absent; (1) present. | [PW 24 (part); MEA 90]
- 127. Distitibia, trichobothrium series *sbc*: (0) absent; (1) present. | [PW 24 (part); MEA 91]
- 128. Distitibia, relative positions of two most proximal trichobothria of *sf* and *sc*: (0) far apart (> 0.2 mm); (1) close to each other (0.05–0.1 mm, ratio of distance to length of distitibia between 0.01 and 0.09); (2) parallel or subparallel to each other (< 0.025 mm). | [MEA 92]
- 129. Distitibia, position of proximal trichobothria of *sf* and *sc*: (0) similar distance to the other trichobothria in the series; (1) distinctly displaced from series. | [MEA 93]
- 130. Distitibia, number of trichobothria on sf:(0) 4; (1) 5; (2) 6; (3) 7; (4) 8; (5) 9; (6) 10–12; (7) 20 (8) 26. | [MEA 94]
- 131. Distitibia, number of trichobothria on *sc*: (0) 3; (1) 5; (2) 6; (3) 7; (4) 8; (5) 9; (6) 10 or 11; (7) 12; (8) 13; (9) 19–21. | [MEA 95]
- 133. Distitibia, trichobothrium tm (tip of triad): (0) absent; (1) present. | MEA 96.
- 133. Distitibia, marked division distal to all trichobothria (Fig. 13): (0) absent; (1) present. | MEA 97.
- 134. Tarsomere, empodial claw: (0) absent; (1) present. *
- 135. Tarsomere, pulvillus: (0) absent; (1) present. | [DQ 1; MEA 98]
- 136. Tarsomere, oblique slit: (0) absent; (1) present. | [PW 21; MEA 99]
- 137. Tarsomere, weakly sclerotized area of second tarsal segment (Fig. 14): (0) absent; (1) present. | [MEA 100]
- 138. Tarsomere, extent of weakly sclerotized area of second tarsal segment (Fig. 14): (0) reaching ventrolateral setal row (1); not reaching ventrolateral setal row; (2) surpassing ventrolateral setal row (divides the article).*